THESIS

This is to certify that the

dissertation entitled

MODELS IN ELECTRON TRANSFER IN PHOTOSYSTEM II

presented by

Demetrios F. Ghanotakis

has been accepted towards fulfillment
of the requirements for

Ph.D. degree in Chemistry

Gerald T. Babcock
Major professor
Gerald T. Babcock

Date 8/15/84

0-12771

MODELS FOR ELECTRON TRANSFER IN PHOTOSYSTEM II

By

Demetrios F. Ghanotakis

A DISSERTATION

Submitted to
Michigan State University
in partial fulfillment of the requirements
for the degree of

DOCTOR OF PHILOSOPHY

Department of Chemistry

1984

ABSTRACT

MODELS FOR ELECTRON TRANSFER IN PHOTOSYSTEM II

By

Demetrios F. Ghanotakis

By using EPR spectroscopy we have studied the kinetic behavior of various species which are involved in electron transfer around Photosystem II and the role of manganese in O_2 evolution. The EPR signal of $Z^{+\cdot}$, the oxidized form of the primary donor to the Photosystem II reaction center chlorophyll, P_{680}, is an excellent probe for studying the oxidizing side of Photosystem II.

We have investigated the EPR characteristics of Photosystem II reaction center preparations from spinach, pokeweed and *Chlamydomonas reinhardtii*. Spin quantitation, with potassium nitrosodisulfonate as a spin standard, demonstrates that the Signal II species, $Z^{+\cdot}$, is present in approximately 60% of the reaction centers. This observation suggests that the donor Z is an integral component of the PSII reaction center complex.

The conditions for steady state Signal II formation in response to single turnover flashes in tris-treated,

DCMU-inhibited chloroplasts have been investigated. DCMU inhibits Signal II generation as the photoinactive state, $ZP_{680}Q_A^-$, accumulates. Potassium ferricyanide relieves this inhibition, so that Signal II can be fully developed on each flash in a flash series. The model most consistent with these observations postulates that ferricyanide interacts directly with Q_A^-. An endogenous acceptor other than Q_A does not appear to be involved.

The effects of ADRY reagents, a class of compounds which destabilize intermediates in the photosynthetic water-oxidizing process, on the reduction kinetics of $Z^{+\cdot}$ have been monitored in tris-washed chloroplasts by following the decay of Signal II. Our observations are most easily rationalized in terms of a model which proposes direct reduction of $Z^{+\cdot}$ by the ADRY reagent followed by regeneration of the reduced ADRY reagent in a nonspecific reaction with membrane components such as carotenoids, chlorophyll or protein.

Upon addition of hydroxylamine to chloroplasts or Photosystem II preparations, the EPR signal of $Z^{+\cdot}$ disappears and a new signal, which is identified with P_{680}^+, is observed. These observations indicate that in addition to its well-known inhibitory action on the oxygen evolving complex, hydroxylamine is also able to disrupt physiological electron flow to P_{680} itself.

We have also studied the effect of various other treatments which inhibit O_2-evolution at the oxidizing side of

Photosystem II in PSII particles. By monitoring the EPR properties of $Z^{+\bullet}$ we have explored the role of manganese and of polypeptides with molecular weights of 17 and 23 KD in the O_2 evolving process. The above two polypeptides seem to have a structural rather than a catalytic role in O_2 evolution activity. Removal of these polypeptides results in a condition whereby exogenous donors, such as benzidine, have ready access to components involved in the water splitting process.

To My Parents

and Sofia

ACKNOWLEDGEMENTS

I would like to thank Dr. Gerald T. Babcock for the independence and the encouragement he offered me throughout this study.

I am grateful to Dr. Charles F. Yocum for his help in the biochemical aspects of this work.

Finally I would like to thank all my fellow lab members for their general assistance.

TABLE OF CONTENTS

LIST OF TABLES

LIST OF FIGURES

ABBREVIATIONS

Asc^-	sodium ascorbate
ADRY	Accelerator of the Deactivation Reactions of the water-splitting system, Y.
ANT 2a	2-(4-chloro)anilino-3,5-dinitrothiophene
ANT 2p	2-(3-chloro-4-trifluoromethyl)anilino-3-5,dinotrothiophene
ANT 2s	2-(3,4,5-trichloro)anilino-3,5-dinitrothiophene
BZ	benzidine
CAPS	3-cyclohexylamino-1-propanesulfonic acid
CCCP	carbonylcyanide-m-chlorophenylhydrazone
DCMU	3-(3,4-dichlorophenyl)-1,1-dimethylurea
DPC	diphenylcarbazide
EPR	electron paramagnetic resonance
Fe^{III}_{CN} (or FeCN)	potassium ferricyanide
Fe^{II}_{CN}	potassium ferrocyanide
FCCP	carbonylcyanide-p-trifluoromethoxyphenyl-hydrazone
HEPES	N-2-hydroxyethylpiperazine-N'-2-ethane-sulfonic acid
H_2Q (or HQ)	hydroquinone
MES	4-morpholinoethane sulfonic acid
OEC	oxygen evolving complex
PMS	phenazine methosulfate
PS I	Photosystem I
PS II	Photosystem II
TPB	tetraphenylboron
Tris	Tris(hydroxymethyl)aminomethane

CHAPTER I.

INTRODUCTION

In 1771 Joseph Priestley showed that a mouse could not live in a container in which a candle flame had been allowed to burn out, but that a spray of mint restored the air so that after a few days a candle could burn again, or a mouse could live for a time. Thus Priestley showed that a plant could produce oxygen, or, in the language of his time, could dephlogisticate the air. In 1782 Senebier pointed out that plants need carbon dioxide to "oxygenate" the air and fourteen years later Ingenhousz suggested that this carbon dioxide was the source of all the organic matter in plant. In the middle of the nineteenth century Mayer suggested that the light energy was stored, in part, as chemical energy in the organic matter and in the early twentieth century the role of chlorophyll in photosynthesis was known.

Today, two centuries after Priestley's experiment, it is well known that of all the ways in which life interacts with light the most fundamental is photosynthesis, the biological conversion of light energy into chemical energy.

The overall chemistry of photosynthesis can be expressed in a simple equation. Six molecules of carbon dioxide are

taken up from the environment together with six molecules of water. In the presence of light these molecules are converted into a single molecule of glucose and six molecules of O_2 are released:

$$6CO_2 + 6H_2O \xrightarrow{h\nu} C_6H_{12}O_6 + 6O_2 \qquad (1.1)$$

For purposes of analysis, photosynthesis is most conveniently divided into two steps: a light reaction and a dark reaction. The light reaction captures energy from the sun in two comparatively unstable molecules: ATP and NADPH. In the dark reaction ATP and NADPH supply the energy needed to form glucose from CO_2. Both of these reactions, the light and the dark, take place in regions of the plant cell known as chloroplasts.

In chloroplasts the photosynthetically efficient photochemistry occurs at a limited number of sites in the pigment-containing membranes. These sites, so-called reaction centers, have a well-defined organization and positioning in the membranes. A reaction center contains a specialized chlorophyll a molecule, which, following electronic excitation, acts as the primary electron donor. At this point it is well known that there are two types of reaction centers in O_2-evolving photosynthetic organisms: the Photosystem I (PS-I)reaction center and the Photosystem II (PS-II) reaction center. These are present in a nearly 1:1 ratio and function in series to drive electrons from the O_2-evolving complex to $NADP^+$ [1].

A schematic representation of the light driven reactions is presented in Figure 1. As shown in this scheme, the reaction center of PS-II extracts electrons from a very oxidizing species and operates at high potential. By contrast, the reaction center of PS-I produces strongly reducing products and thus operates at a low potential. The reaction centers represent only a small fraction of the total pigments and the function of light absorption is fulfilled by other pigments which constitute the antenna system. Antenna pigments transmit their electronic excitation energy, resulting from light absorption, to the reaction centers, via both exciton and Forster transfer [2]. In general there are about 400 chlorophyll molecules per PS-I or PS-II reaction center [3].

A study of the flash induced difference spectrum indicates that photoexcitation of Photosystem II involves the bleaching of a special chlorophyll-a, P_{680}, with characteristic negative peaks around 430 and 690 nm [4], and the formation of a plastosemiquinone anion radical with a positive peak in the absorption difference spectrum around 320 nm, Q_A^- [5]. When the time resolution for measuring changes of optical absorbances was improved, the role of a pheophytin molecule as an intermediate acceptor between P_{680} and Q_A, emerged [6]. A second quinone, Q_B [7], a two electron acceptor, connects Q_A with the plastoquinone pool which in turn funnels electrons towards Photosystem I. The reduction of P_{680}^+ leads to the

FIGURE 1.

Flow of electrons from water to NADP (Z scheme).

Abbreviations: $\{S\}_n$, the oxygen evolving complex; Z, the primary donor to P_{680}; P_{680}, the PS-II reaction center; I, pheophytin, the primary acceptor of PS-II; Q_A, the primary stable acceptor of PS-II; Q_B, the secondary acceptor of PS-II; PQ_{pool}, plastoquinone pool; cyt f, cytochrome f; Pcy, plastocyanin; P_{700}, the PS-I reaction center; X, the primary acceptor of PS-I; Fd, ferredoxin, F_d-NADP, ferredoxin NADP reductase.

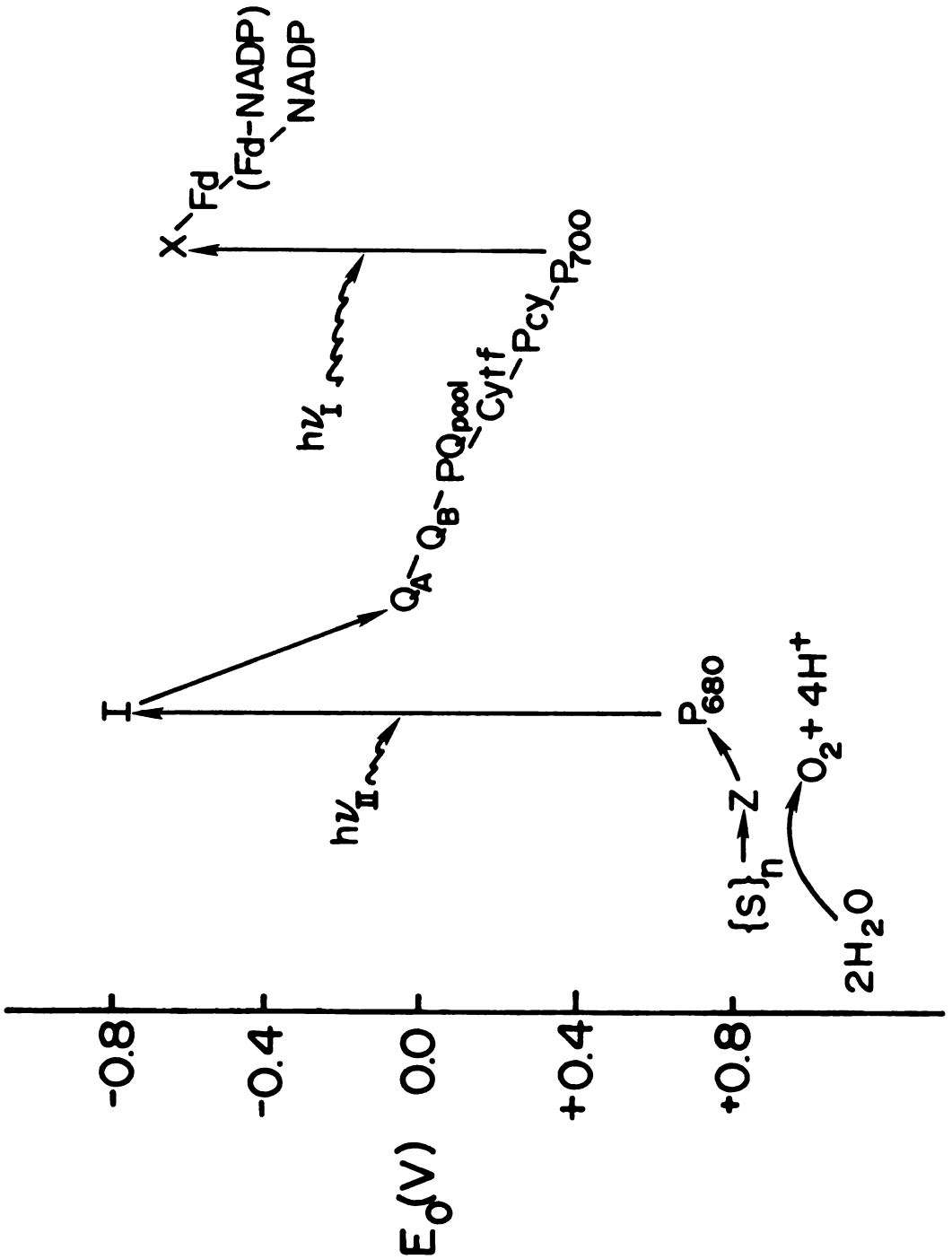
X
Fd
(Fd-NADP)
NADP
hν I
Q A
Q B
PQ pool
Cyt f
Pcy
P 700
I
hν II
P 680
Z
{S} n
O 2 + 4H +
2H 2O
-0.8
-0.4
0.0
+0.4
+0.8
E o (V)

formation of a strong oxidant, Z^+ ($E_m' \sim +1.1$ V, [8]), possibly a plastoquinone cation radical [9], which through the oxygen evolving complex (S-states), oxidizes water to molecular oxygen.

In an analogous manner, when light is absorbed by Photosystem I charge separation between the primary donor P_{700} and the primary acceptor X occurs. In the dark, following the photoexcitation of the reaction center, P_{700}^+ is rereduced by electrons transferred from Photosystem II whereas the reduced form of the primary acceptor is reoxidized by an iron sulfur center which in turn reduces NADP.

As the result of flash spectroscopic and polarographic studies of the microscopic phenomena, the photosynthetic electron transport from water to NADP has been inferred to be arranged in a zig-zag scheme [10], as shown in Fig. 2. Measurement, via the electrochromic effect, of the rise kinetics of the laser-flash-induced formation of an electric potential gradient across the thylakoid membrane [11] has led to the conclusion that the reaction center complexes span the membrane anisotropically with both primary donors, P_{680} and P_{700}, located near the inner side and the corresponding acceptors towards the outer side. From Fig. 2 it is apparent that electron flow from H_2O to NADP results in a development of both charge ($\Delta\psi$) and proton (ΔpH) gradients across the membrane. These two components make up what Mitchell

FIGURE 2.

Patterns of electron and proton transport in relation to the thylakoid membrane.

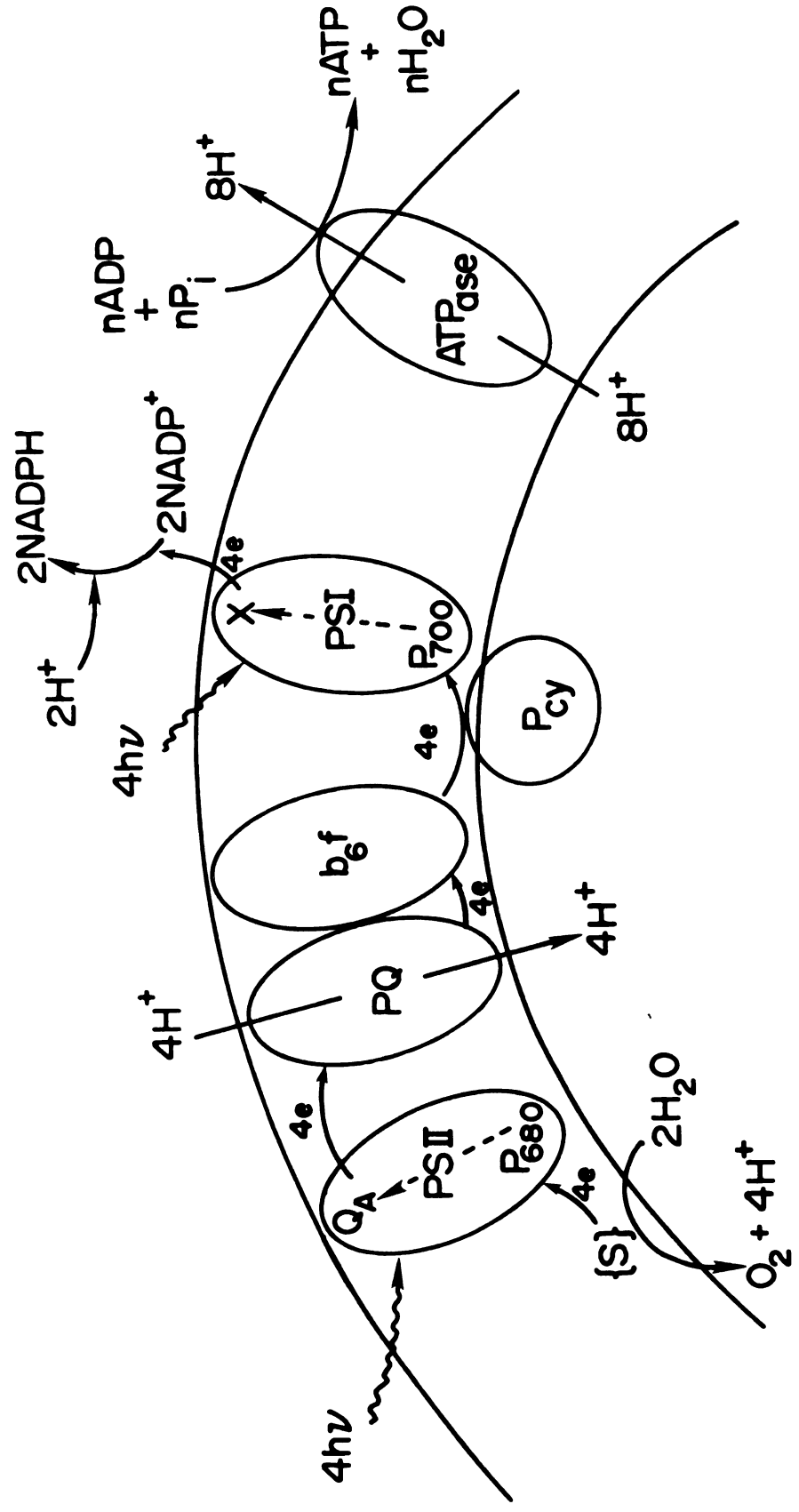
nATP
+
nH2O
8H+
nADP
+
nPi
ATPase
8H+
2NADPH
2NADP+
4e
X
PSI
P700
2H+
4hν
4e
Pcy
b6f
4e
4H+
4H+
PQ
4e
QA
PSII
P680
4e
{S}
2H2O
O2 + 4H+
4hν

called the protonmotive force, pmf:

$$pmf(volts) = 0.06(\Delta pH) + \Delta\psi$$

which provides the energy necessary for ATP synthesis [12].

The formation of a molecule of oxygen from water requires the removal of four electrons; at pH 7.0 the average oxidation-reduction potential of these four equivalents is +0.81 V

$$2H_2O \longrightarrow O_2 + 4H^+ + 4e \qquad (1.2)$$

Even though a considerable amount of knowledge has accumulated concerning the process of O_2 evolution, the photosynthetic photooxidation of water remains to be elucidated. A good deal of insight has been obtained by considering possible mechanisms for cleavage of water at the oxidizing side of Photosystem II.

Upon excitation of PS-II reaction center, the reaction center chlorophyll molecule P_{680} is oxidized and simultaneously, Q_A, the primary electron acceptor of PS-II, is reduced. In the dark following the excitation, P_{680} is reduced by the secondary donor, Z. The subsequent steps in the scheme shown below involve reduction of Z^+ by S_n, the charge-accumulator which carries out the actual oxidation of water, and reoxidation of the primary acceptor Q_A by the plastoquinone pool.

$$ZPQ(A) \xrightarrow{h\nu} ZP^{+}Q^{-}(A) \longrightarrow Z^{+}PQ^{-}(A) \longrightarrow ZPQ^{-}(A) \longrightarrow ZPQ(A^{-}) \qquad (1.3)$$

$$S_n \qquad S_{n+1}$$

In 1967 Joliot and co-workers [13] observed that the O_2 flash yield in a series of successive flashes varied with a period of four. In other words, the photosynthetic apparatus stores the oxidizing equivalents produced by four flashes and then breaks down two molecules of H_2O and produces one molecule of O_2. The results of such an experiment are shown in Fig. 3. The model proposed by Kok et al. [14], in order to explain the above periodicity is shown in Fig. 4. According to this model each O_2 center undergoes the cyclic series of reactions shown in the scheme. The states of the centers, S_n, differ by the number of oxidizing equivalents, indicated by n.

To fit this model to the experimental data, two assumptions were made:

(i) During each flash, a fraction (α) of the O_2 centers does not undergo a phototransition ('misses') and another fraction (β) undergoes a double transition ($S_n \longrightarrow S_{n+2}$ 'double hits').

(ii) The S_1 state and S_0 state are both stable in the dark. Since the S_2 and S_3 states have rather short lifetimes, the distribution of S states after about 15 minutes dark is $S_0:S_1:S_2:S_3 = 0.25:0.75:0:0$.

FIGURE 3.

O_2 flash yield sequence observed with isolated chloroplasts after a long dark period. (Ghanotakis, D.F. and Buttner, W.J., unpublished data).

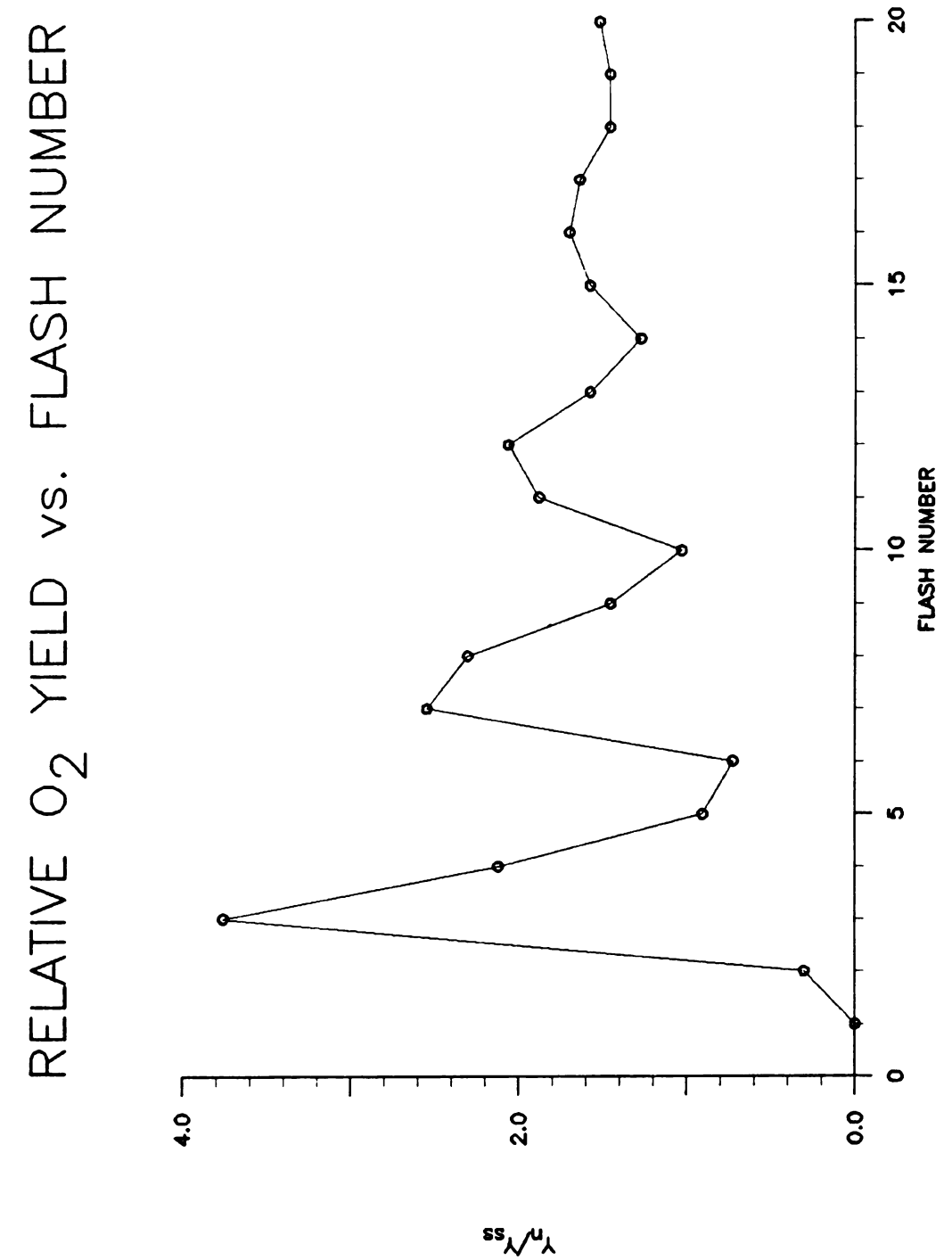
RELATIVE O_2 YIELD vs. FLASH NUMBER
Y_n/Y_{ss}
4.0
2.0
0.0
0
5
10
15
20
FLASH NUMBER

FIGURE 4.

Schematic diagram of the model of O_2 evolution proposed by Kok et al. [14]. The subscripts (n = 0-4) denote the oxidation state of the O_2 system. The steps $S_\eta \longrightarrow S_\eta^*$ represent phototransitions and the steps $S_\eta^* \longrightarrow S_{\eta+1}$ represent the subsequent dark relaxations.

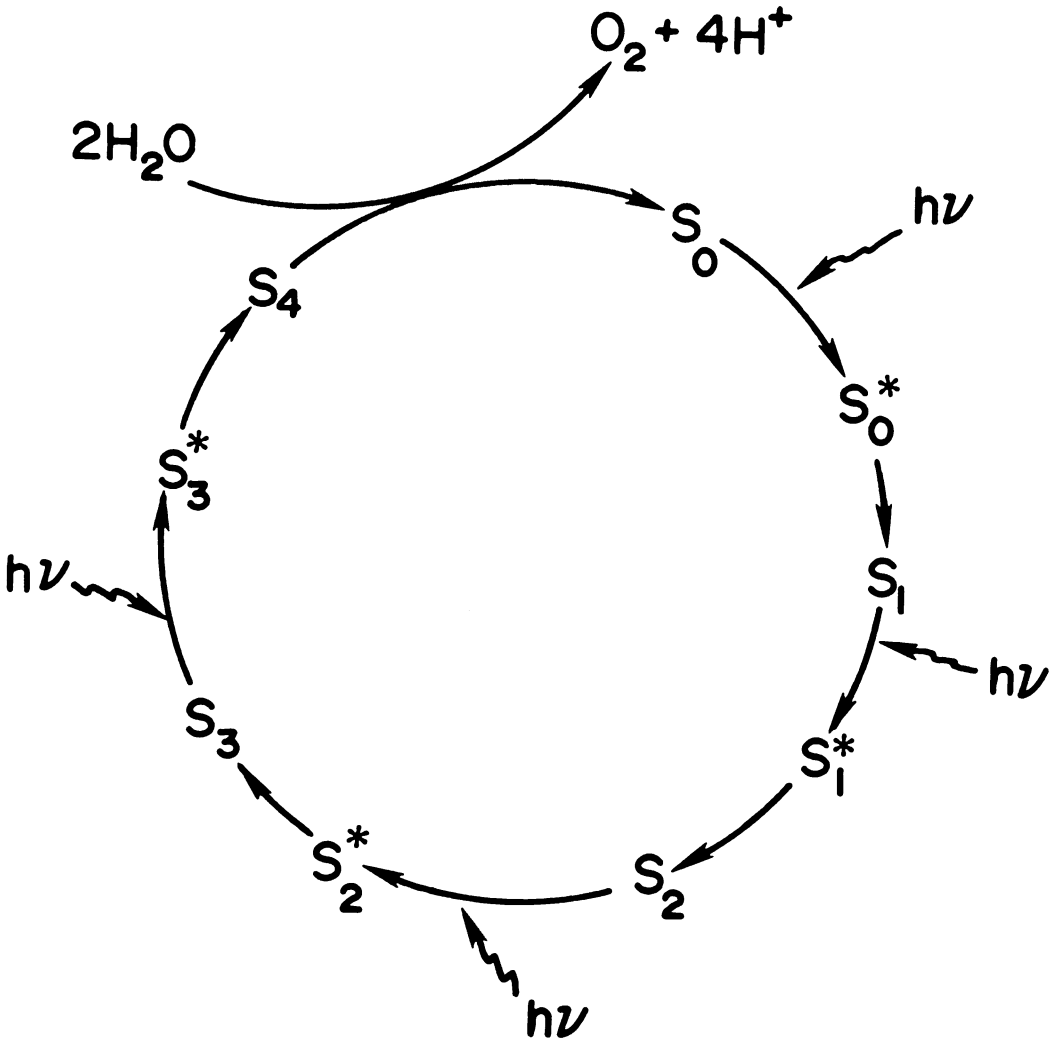
$O_2 + 4H^+$
$2H_2O$
S_0
$h\nu$
S_0^*
S_1
$h\nu$
S_1^*
S_2
S_2^*
$h\nu$
S_3
$h\nu$
S_3^*
S_4

Although the chemical identity of the charge collector (Oxygen Evolving Complex, OEC) has not been established, indirect evidence suggests that some form of thylakoid-bound manganese is involved. Depletion of manganese in plants or algae by withholding it from the growth medium leads to the loss of O_2 evolution capacity [15]. Activity can be restored upon readdition of Mn^{2+} to the growth medium. Various experiments point to a site on the donor side of Photosystem II as the location for the manganese requirement [16,17].

Manganese occurs in several pools in higher plant or algal cells. A portion of manganese occurs as aqueous Mn^{2+} and gives rise to an EPR signal characteristic of hexaaquomanganese (+2). It can be removed completely by cell rapture and washing of the pigment membranes with chelating agents such as EDTA [18]. Yocum et al. [19], using EPR spectroscopy, found that chloroplast thylakoid membranes isolated in the presence of EDTA retain high rates of O_2 evolution but contain no Mn^{2+} that is detectable by EPR at room temperature. The total Mn^{2+} content of these preparations is 4.6 per 400 chlorophylls; 0.6 Mn^{2+} can be released by addition of Ca^{2+}, a treatment that does not affect O_2 evolution. The remaining Mn^{2+} appears to be functionally associated with O_2 evolution activity. Inhibition by Tris, NH_2OH, or heat will release a small fraction of Mn^{2+} from these membranes ($\approx$25% with

Tris, for example). Addition of Ca^{2+} further enhances Mn^{2+} release so that for Tris and for NH_2OH, 2 and 3, respectively, Mn^{2+} per 400 chlorophylls are extracted from the O_2-evolving complex. Dismukes and Siderer [20] reported the observation of a multiline ESR signal in spinach chloroplasts given a series of laser flashes at room temperature and rapidly cooled to -140°C. The spectrum was attributed to a pair of antiferromagnetically coupled Mn ions, or possibly a tetramer of Mn ions, in which Mn(III) and Mn(IV) oxidation states are present. This manganese complex was identified with the S_2 state of the OEC.

In the process of H_2O oxidation four protons are released for every molecule of O_2 liberated. One might expect that these protons would be released concurrently with the O_2, as suggested in the early scheme of Kok et al. [14]. The experimental measurements show that this does not happen. Although the detection of proton release associated with water oxidation is complicated by other proton translocations across the thylakoid membranes that interfere and therefore must be subtracted out [21,22], each of the three groups that has carried out such studies agrees that the concerted process cannot be correct [22-24]. For the present the data do not justify going beyond the simplest whole-number values for the proton release pattern. Even so, there remains a disagreement between Fowler [22] and Saphon and Crofts [23],

on the one hand, who believe that the pattern is 1,0,1,2 for the number of protons released, respectively in the steps $S_0 \rightarrow S_1$, $S_1 \rightarrow S_2$, $S_2 \rightarrow S_3$ and $S_3 \rightarrow \{S_4\} \rightarrow S_0$, and Junge et al. [24] who believe that the pattern is 0,1,1,2. The experimental results of these groups clearly differ, especially with respect to the release of protons following the first flash and the amplitude of the oscillations of period 4. Although it is generally assumed that protons are released directly from H_2O, it is possible that protons are released from a protein in the OEC. It has been observed for hemoglobin that there is linkage between the binding of oxygen and the binding of protons by the protein. The oxygen-linked ionizable groups change pK upon addition or removal of oxygen, thereby exchanging protons with the solvent (the so-called Bohr effect) [25,26]. Further investigations of these measurements and the correlation of their kinetics with electron transfer kinetics are needed in order to establish the number and the origin of protons released in a series of flashes.

The close coupling between the reaction center and the oxygen evolving complex (OEC) can be disrupted by various physical and chemical treatments resulting in rather selective inactivation, or 'decoupling' of the OEC [4,27,28]. Exposure of isolated thylakoid membranes to Tris [29-31] or to NH_2OH [32-35] represent mild procedures for inactivation of the oxygen evolving reaction system. After the above treatments the decoupled

PS-II reaction center, though incapable of H_2O photooxidation, will still photooxidize a wide variety of chemically unrelated artificial electron donors, for example, ascorbate [27,36]. Apparently, the system after the treatments remains photochemically active, since the photooxidation of artificial electron donors via PS-II and PS-I proceeds with high quantum efficiency [33,37].

Among the compounds that have been known to inhibit oxygen evolution acting at the oxidizing side of PS-II are various amines, for example ammonia [38,39] and methylamine [39]. The inhibition by ammonia and methylamine appears to be rather direct and does not result in the release of bound Mn that occurs with higher concentrations of NH_2OH and high concentrations of Tris. Velthuys [40] and Frasch and Cheniae [31] proposed that water binds to manganese in the OEC by a Lewis acid-Lewis base mechanism and that amines, being better Lewis bases, are able to compete with H_2O for binding sites. Other treatments which result in inhibition of O_2 evolution at the oxidizing side of PSII are Cl^- depletion from chloroplasts [29,41] and extraction of certain polypeptides by using various techniques [41,42]. Izawa et al. [39] provided firm evidence for a specific function of Cl^- in reactions closely associated with O_2 evolution itself. Using mild techniques to deplete Cl^- from normal Cl^--containing chloroplasts, they obtained preparations which, upon addition of Cl^- (~5 mM), showed a 4- to 10-fold

increase in rates of O_2 evolution. The role of two polypeptides, the 17 and the 23 kd, has also been studied extensively in a series of extraction-reconstitution experiments [41,42].

A. Experimental Approaches

The experimental techniques which have been used to unravel the details of photosynthesis include such spectroscopic techniques as visible and UV absorption changes upon photoexcitation, prompt and delayed fluorescence (Luminescence), nuclear magnetic resonance (NMR) and electron spin resonance (ESR). Various biochemical approaches, for example, extraction of certain polypeptides followed by selective reconstitution, have also been used.

A summary of the various spectroscopic techniques is given below:

1. Optical and UV Changes

A primary use of optical spectroscopy is to characterize different molecular species or transient states and to follow *in vivo* their modifications during the photosynthetic process. Fast spectroscopic studies have provided a great amount of data on the primary reactions.

Döring et al. [4] obtained the absorption difference spectrum of P_{680} which showed major bleaching at 682 and 435 nm. The authors attributed the spectrum to a "sensitizer" which they designated chlorophyll a_{II}, but Butler [43] proposed, in a model which is now generally

accepted, that it is due to the oxidation of P_{680}. Absorption transients attributed to P_{680} include a small band at 820 nm [44], similar to that of a chlorophyll a cation-radical. This absorption band is very useful for kinetic studies, permitting relatively straightforward observation of P^{+}_{680} with excellent time resolution [45,46]. By monitoring the 820 nm absorption Van Best and Mathis [45] found that following a single flash on dark adapted chloroplasts P^{+}_{680} is rereduced in 30 ns, probably by the secondary electron donor, Z. In chloroplasts pre-treated with Tris, the primary donor of Photosystem II (P_{680}) is rereduced in a few microseconds in a pH sensitive reaction.

Pulles et al. [47] found that absorbance changes around 300 nm in O_2-evolving chloroplasts oscillate with flash number. One component of the oscillation has periodicity of two. It is obtained in a pure state in tris-washed chloroplasts supplied with artificial donors and it reflects the alternate one-electron reduction and oxidation of the secondary PS-II acceptor Q_B [47,48]. In untreated chloroplasts, however, the overall periodicity is four, which implies a contribution by donor side reactions [47,48]. Recently, Renger and Weiss [49], using trypsinized chloroplasts, eliminated the binary oscillation due to the reducing side of PS-II and observed a 320 nm absorption change which oscillated with a periodicity of four in phase with the oxygen yield as a function of the

number of the flash in the train. The transient 320 nm absorption change was attributed to a redox reaction within the water-splitting enzyme system (OEC). The secondary donor Z, probably a plastoquinone, is also a candidate for the 320 nm absorption change. Further investigation is necessary in order to unravel the chemical nature of the precursor.

2. Prompt Fluorescence

Fluorescence is emitted by photosynthetic systems upon absorption of light. The fluorescence intensity is at any moment proportional to the concentration of excited molecules of chlorophyll. The proportionality constant, however, is time dependent.

Duysens and Sweers [50] showed that the fluorescence yield of the antenna chlorophyll depended on the oxidation state of the primary acceptor Q_A. Oxidized Q_A is associated with low chlorophyll fluorescence whereas reduced Q_A results in an increase of fluorescence. In other words Q_A acts as if it is a "quencher" of fluorescence. To explain the low fluorescence yield observed for the $P_{680}Q_A$, $P^+_{680}Q^-_A$ and $P^+_{680}Q_A$, Butler et al., [51], on the basis of experiments at 77 K, proposed that P^+_{680} is also a quencher. Immediately after a flash, when the system is in the $P^+_{680}Q^-_A$ state, the fluorescence yield is low. It will subsequently rise upon rereduction of P^+_{680} by Z giving $Z^+P_{680}Q^-_A$, a state with no quenchers. The kinetics of the rise in fluorescence are, therefore,

generally interpreted as reflecting the rate of reduction of P_{680}^{+}. Fluorescence transients exhibit several phases that were extensively studied [52,53]. Sonneveld et al. [54] have used chlorophyll a fluorescence as a monitor of nanosecond reduction of P_{680}^{+}. For the first flash in dark adapted chloroplasts, they find a 35 ns reduction time. For the succeeding four flashes, the decay time of P_{680}^{+} is longer than 35 ns but correlated to the S states. Under steady state conditions, after damping of the period four oscillations, they find a 400 ns reduction time.

3. Luminescence

Luminescence is primarily a PS-II phenomenon. In addition to absorption of light, excitons are generated by a process which may occur in the dark. The resulting afterglow or delayed luminescence (d.l.) has been studied from submicroseconds to several minutes following illumination. The spectral emission of d.l. is nearly identical to that observed for fluorescence with the maximum intensity centered around 685 nm [55,56]. This suggests that d.l. and prompt fluorescence originate, in part, from the same pigment pool. D.l. is generally believed to result from a reversal of normal photoinduced electron transport [56]. Thus, based upon the recombination hypothesis, the immediate precursor of d.l. should be the state $[P_{680}^{+}Q_{A}^{-}]$. Zankel [57] found that the yield of luminescence, measured at 90 and 500 μs in a sequence of

flashes, oscillated in phase with O_2 yields. Luminescence emissions at longer times also reflect the state of the O_2-evolving system, although in this case the yields are not in phase with O_2 evolution [58,59].

An interesting modification to the delayed light experiment is a technique called electrophotoluminescence (EPL) pioneered by Arnold and Azzi [60,61]. In this technique a laboratory generated electric field is imposed after illumination and a dramatic enhancement in the yield of delayed light is observed, presumably because the field has forced recombination of the photoinduced hole and electron. This technique has been used to show that delayed light and EPL are both PS-II phenomena, by demonstrating a flash number dependence on the yield of period four [62].

4. NMR

Wydryzynski et al. [63] have used NMR to measure the spin lattice relaxation rates ($R_1 = 1/T_1$) of water protons under a variety of experimental conditions and have interpreted the results as arising from photoinduced oxidation state changes of membrane bound manganese. However, Robinson et al. [64] have challenged this interpretation by showing that the kinetics of the increase in R_1, produced by addition of NH_2OH to thylakoid suspensions from which non-functional contaminating Mn(II) has been removed [65], correlate closely with the inactivation of water oxidation as monitored by assays

of oxygen evolution. The species producing enhanced relaxivity has a dispersion profile characteristic of Mn(II) bound to sites of reorientationally restricted mobility [65]. These results indicate that water protons do not exchange quickly (ms time scale) with protons associated with functional manganese.

5. EPR

A series of articles from Sauer's laboratory demonstrated that one of the key intermediates at the donor side of PS-II can be monitored by EPR as a rapid kinetic component of the so-called "Signal II" [18,66]. Signal II_f, attributed to the oxidized form of the secondary donor Z, was first detected in tris-washed chloroplasts and its kinetic behavior was established by Babcock and Sauer [66]. Z^+ was also detected in untreated, oxygen-evolving chloroplasts and it proved to be transiently oxidized during the S_2 to S_3 and the S_3 to S_0 transitions [67]. The authors in reference 67 assumed a single secondary donor model and proposed the following scheme for the reduction of $Z^{+\cdot}$ by the various S states:

$$Z^{+\cdot} + S_0 \longrightarrow Z + S_1 \qquad t_{1/2} \lesssim 100\ \mu s \qquad (1.4)$$

$$Z^{+\cdot} + S_1 \longrightarrow Z + S_2 \qquad t_{1/2} \lesssim 100\ \mu s \qquad (1.5)$$

$$Z^{+\cdot} + S_2 \longrightarrow Z + S_3 \qquad t_{1/2} \simeq 400\ \mu s \qquad (1.6)$$

$$Z^{+\cdot} + S_3 \longrightarrow Z + S_4 \qquad t_{1/2} \simeq 1\ ms \qquad (1.7)$$

$$S_4 + 2H_2O \longrightarrow S_0 + 4H^+ + 4e^- + O_2 \qquad t_{\frac{1}{2}} < 1 \text{ ms} \tag{1.8}$$

Another model which would explain the results of ref. 67 is the two parallel secondary donors model [8] shown below:

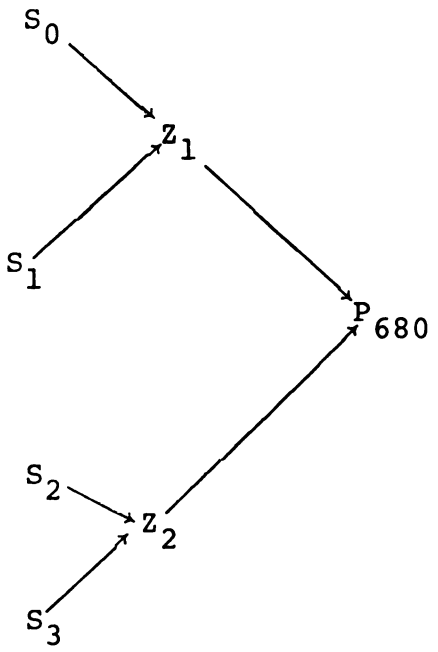

(1.9)

According to this model the S_0 and S_1 states interact with P_{680} through the donor Z_1 whereas S_2 and S_3 states interact with P_{680} through the donor Z_2, the species which gives rise to Signal II.

The EPR spectrum of P_{680}^+ has been also observed at low temperature, following flash excitation [68,69]. P_{680}^+ shows up as a free radical signal with g-value of 2.002 and a linewidth of 7-8 G. The narrow linewidth of the P_{680}^+ signal was taken as evidence that P_{680} is a dimer of chlorophyll *a*, as for P_{700}. The EPR spectrum of P_{680}^+ has also been observed at room temperature [70,71].

Davis et al. [72], on the basis of studies of models, proposed that the narrow EPR linewidth of P_{680}^+ results from a highly specific environment rather than from delocalization of the electron over two chlorophyll molecules. Recently, O'Malley and Babcock [73], based on the EPR and ENDOR spectra of model chlorophylls and P_{700}, proposed a monomer structure for both P_{700} and P_{680}.

The P_{680}^+ decay in dark adapted tris-treated chloroplasts was reported to be biphasic with a dominant pH dependent phase, ranging from a half-life of 44 μs at pH 4.0 to a half-life of 3.5 μs at pH 8.0 and a minor pH independent phase with a half-time of 100 to 200 μs [46]. The pH dependence of P_{680}^+ reduction was substantiated by parallel measurements on the decay of the EPR signal attributed to P_{680}^+ and the rise of Signal II_f [74]. In PS-II fragments with oxygen evolution activity inhibited by tris-washing, the kinetics of P_{680}^+ decay and Signal II_f rise were in good agreement with the optical data, thus directly verifying the role of Z as an electron donor to P_{680}.

At cryogenic temperatures, Dismukes and Siderer [20] have reported an EPR signal that they assign to a pair of antiferromagnetically coupled manganese ions in which Mn^{3+} and Mn^{4+} are present (possibly Mn^{III} 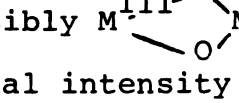 Mn^{IV}). They also report changes in the signal intensity with flash number, again of period four, suggesting a cyclic change

in manganese valence state. This multiline signal was attributed to the S_2 state.

Rutherford et al. [75] using EPR spectroscopy at liquid helium temperature have detected a light-induced spin polarized triplet state in a purified PS-II preparation. By analogy to bacterial photosynthesis the electron spin polarization pattern is interpreted to indicate that the triplet originates from radical pair recombination between the oxidized primary donor chlorophyll, P_{680}^{+}, and the reduced intermediate pheophytin, I^{-}. The dependence of the triplet signal on the redox state of I and of the primary acceptor, Q_A, are consistent with the origin of the triplet signal from the triplet state of P_{680}. The zero field splitting parameters of the triplet indicate that P_{680} is a monomeric chlorophyll.

Another species which has been observed by EPR at low temperatures is cytochrome b_{559}. There are two molecules of cytochrome b_{559} per four hundred chlorophyll molecules, one of which has an unusually high mid-point potential ($E_m' \sim +0.38$ V) and is associated with PS-II. PS-II mediated oxidation of the high potential form of cytochrome b_{559} has been observed at 77 K [76] and a rapid photooxidation and photoreduction have been reported in samples containing tetraphenylborate [77]. Low spin cyt b_{559} gives rise to an ESR signal with g value around 3.

CHAPTER II.

KINETIC STUDY OF SIGNAL II_f IN TRIS-TREATED CHLOROPLASTS AND PSII PREPARATIONS

A. Introduction

At room temperature oxygen-evolving photosynthetic materials generate two radical species which are detectable using EPR spectroscopy [78,79]. The first, Signal I, has rapid rise and decay kinetics and has been established as arising from P_{700}^{+}, the oxidized reaction center of PSI [80,81].

The second, Signal II, has been less well characterized. It has been reported to have a g-value of 2.0046 and a linewidth of about 20 G with partially resolved hyperfine structure. Kohl and coworkers [82-84] using extraction and readdition procedures, as well as studies on model compounds, have presented evidence suggesting that the molecular origin of Signal II may be plastoquinone or a related molecule. The microwave power saturation of Signal II is unusual in that the center of the spectrum saturates at a faster rate than the wings [85,86]. This led to the conclusion that more than one radical species was involved. However, the orientation studies of Hales and Gupta [85] and studies in our laboratory in which PSII

particle preparations were used [87,88] indicate that this effect is caused by varying saturation rates for different orientations of the single radical species involved. EPR as well as ENDOR studies of model compounds in conjunction with *in vivo* experiments on chloroplasts support the idea that Signal II is a plastoquinone cation radical [9]. Signal II has a fairly slow, light induced rise time ($t_{\frac{1}{2}} \sim 1$ s) and subsequent dark decay time ($t_{\frac{1}{2}} \sim 4$ h). These slow kinetics have led to its designation as Signal II_s [89].

A much faster component of Signal II has been observed in oxygen evolving chloroplasts by Babcock et al. [67]. It appears to have the same line shape as Signal II_s but very fast kinetics, which has led to designation as Signal II_{vf}. Signal II_{vf} was attributed to the oxidized form of Z, the donor to the reaction center chlorophyll P_{680}. After photooxidation Z^+ is rereduced by the oxygen evolving complex (S-states) in less than 1 ms (see Chapter 1). In addition to the different kinetic behavior Signal II_{vf} has also different power saturation properties compared to Signal II_s. Signal II_{vf} saturates at a slower rate, probably the result of a close interaction between Z and manganese in untreated chloroplasts [90].

Upon inhibition of the OEC by incubation in alkaline Tris-buffer, electron flow to Z^+ is interrupted and the lifetime of the free radical is extended well into the ms time range. Under these conditions, the Z^+ free radical

is referred to as Signal II_f and its reduction occurs at the expense of endogenous donors (e.g. ascorbate) in the chloroplast suspension [91]. Figure 5a shows spectra of Tris-washed chloroplasts before (1), during (2), and after (3) illumination. In Fig. 5 the behavior of pokeweed TSF-IIa particles (5b) and normal and DEAE *Chlamydomonas* particles (5c,5d) is also shown. The absence of PSI in the particles (5b-5d) is evident in that the strong P_{700}^+ free radical signal which dominates the central region of the spectrum in the tris-washed chloroplast sample is not observed in the particle preparations (all spectra from ref. 92).

In unfractionated thylakoid membranes, Babcock and Sauer [93] used P_{700}^+ as a spin standard and showed that Signal II was roughly (±50%) stoichiometric. A better approach, the use of Fremy's salt ($K_2(SO_3)_2NO$), was followed in ref. 92 and gave the results which are summarized in Table I (from ref. 92). Two trends are clear from these data: (a) the reaction center particles are enriched in Signal II concentration compared to either the unfractionated membranes or to the O_2-evolving PSII preparations [88] and (b) the Signal II spin concentration is roughly stoichiometric with P_{680} concentration in the particles, thus providing additional support for the association of Z with the reaction center complex.

FIGURE 5.

Dark and light-induced, room temperature EPR spectra in several membrane preparations: a) tris-washed spinach chloroplasts (2.76 mg Chl/ml), instrument gain = 1×10^6; b) pokeweed TSF-IIa particles (0.69 mg Chl/ml), instrument gain = 0.8×10^6; c) *Chlamydomonas* PSII particles (0.53 mg Chl/ml), instrument gain = 1.25×10^6; d) *Chlamydomonas* PSII DEAE particles (0.44 mg Chl/ml), instrument gain = 1×10^6. A modulation amplitude of 4 G and a time constant of 0.2 s were used in recording all spectra. (From ref. 92).

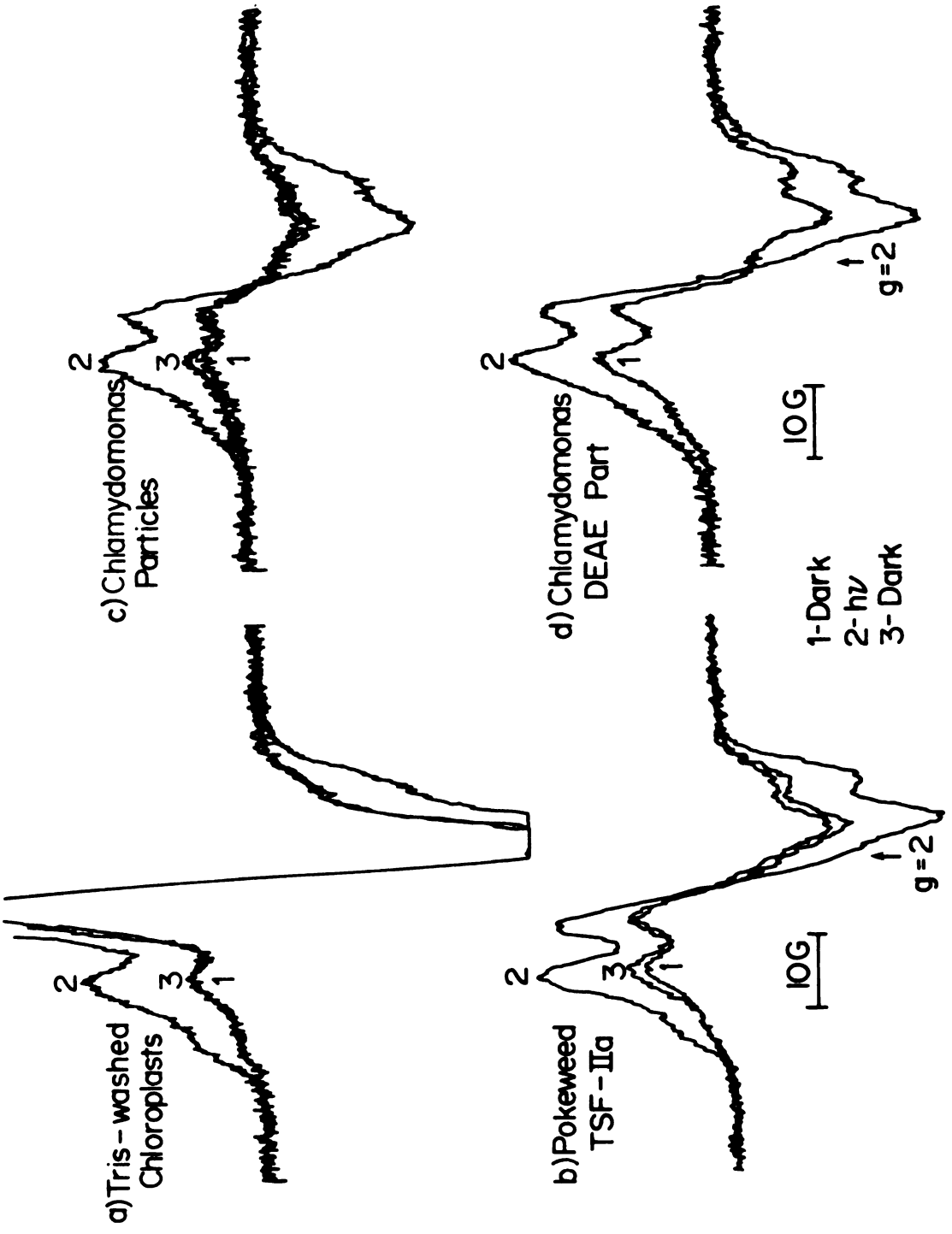
a) Tris-washed Chloroplasts
b) Pokeweed TSF-IIa
c) Chlamydomonas Particles
d) Chlamydomonas DEAE Part
1
2
3
g=2
10G
1-Dark
2-hν
3-Dark

TABLE I——Signal II (SII) Spin Quantitation (from Ref. 92).

Preparation	$\left(\frac{\text{Chl}^{a}}{\text{SII (dark)}}\right)$	$\left(\frac{\text{Chl}^{b}}{\text{SII (light)}}\right)$	$\left(\frac{\text{SII (dark)}^{c}}{\text{P680}}\right)$	$\left(\frac{\text{SII (light)}}{\text{P680}}\right)$	$\left(\frac{\text{SII (total)}}{\text{P680}}\right)$
O_2 evolving chloroplasts	388 ± 28	*d*	1.03	*d*	1.03
tris-washed chloroplasts	404	390	0.99	1.02	2.01
O_2 evolving spinach PSII particles	270	*d*	0.93	*d*	0.93
pokeweed TSF IIa	90	72	0.5	0.63	1.13
Chlamydomonas particles-preparation 1	115	94	0.39	0.48	0.87
Chlamydomonas particles-preparation 2	150	73	0.3	0.62	0.92
Chlamydomonas DEAE particles	52	66	0.86	0.68	1.54

[a] Chlorophylls per Signal II spin following 3' dark period.
[b] Chlorophylls per Signal II spin induced by continuous illumination.
[c] Estimates of dark, light and total Signal II spins per P680 in the various preparations were made by assuming 400 chlorophylls per P680 in unfractionated chloroplasts, 250 chlorophylls per P680 in the O_2 evolving PSII particles and 45 chlorophylls per P680 in the PSII reaction center preparations.
[d] No continuous light induced increase in Signal II spin concentration.

In the experiments reported here, we have studied the kinetic behavior of Z^+ in the various preparations. The decay of Signal II_f, which follows pseudo-first order kinetics in the presence of several commonly used electron donors, was studied in the presence of various cations. Addition of cations accelerated the reduction of Z^+ by negatively charged donors (e.g. ascorbate, ferricyanide) apparently due to a membrane surface charge effect. All cations used, except magnesium, had no effect on the decay time of Z^+ in the presence of neutral donors. Magnesium increased the decay time of Z^+ in the presence of neutral donors. At this point the effect of magnesium is not well understood.

B. Materials and Methods

Market spinach was used for preparing chloroplasts. Leaves were kept dark at 4°C prior to use, then washed in distilled water and deveined under low light conditions. They were broken in a Waring blender for 12 s in a standard reaction solution containing 0.4 M sucrose, 10 mM NaCl and 50 mM HEPES buffer (SHN), pH adjusted to 7.6. The homogenate was then strained through 8 layers of cheesecloth and centrifuged for 90 s (5000 r.p.m., SS-34 Sorvall rotor) at about 4°C. For tris-inactivation the pellets were resuspended in 0.8 M Tris buffer (pH = 8.0) and 0.5 mM EDTA and incubated under room light, at 4°C, for 20 min. The Tris washed samples were recentrifuged and resuspended in a

minimal volume of SHN. Chlorophyll concentrations ranged between 4 and 6 mg chlorophyll per ml as determined by the Sun and Sauer method [94]. 20 mg/ml spinach ferredoxin and 5×10^{-4} M NADP, obtained from Sigma, were added to the final chloroplast suspension as an electron acceptor system.

Photosystem II particles were isolated from mutant F54-14 of *Chlamydomonas reinhardtii* by using the digitonin and Triton X-100 solubilization procedure outlined in [95]; these are referred to in the text as "*Chlamydomonas* particles". Further fractionation of these particles to yield "*Chlamydomonas* DEAE particles" is also described in [95]. Triton-fractionated subchloroplast fragments (TSF-IIa particles) enriched in the reaction center components of PSII were isolated either from spinach or from pokeweed [96,97]. The above PSII preparations were kindly provided by Dr. Diner (*Chlamydomonas* particles) and Dr. Ke (TSF-IIa particles).

EPR spectroscopy was carried out on a Bruker ER200D spectrometer operated at X-band. A Varian TM_{110} mode cavity (model E238) was fitted to the microwave bridge by using appropriately modified waveguide and impedence matching circuitry. The sample cell was a Scanlon EPR flat cell. The microwave power was 20 mW and an effective modulation amplitude of 4 G, as determined by the method of Poole [98], was used in all experiments. Because

of the relatively low concentration of the paramagnetic species in the chloroplast suspension (~10 μM) the time course for the transient rise and decay of Signal II_f was enhanced through signal averaging in a Nicolet 1180 computer which is interfaced to the spectrometer. The instrument modifications necessary to permit efficient kinetic operation and the xenon flash lamp circuitry are described in detail in [99].

The chloroplast suspensions were kept in the dark on ice. Prior to each experiment, an aliquot of the sample was mixed with a known concentration of exogenous donors or salt. After stirring the sample with a Vortex the flat cell was filled under low light conditions. The EPR sample cell was then centered in the cavity and the detector diode allowed to stabilize. The number of scans averaged, time constant and other experimental conditions are noted in the figure captions.

C. Results

By using a potassium ferricyanide/ferrocyanide redox buffer system and magnesium chloride to shield surface charges, it is possible to carry out competitive flash signal averaging experiments on the transient kinetics of Signal II in the various particle preparations. Figure 6 shows kinetic traces at the indicated field values relative to the Signal II spectrum in *Chlamydomonas* DEAE particles. The amplitude and sense of the signal change and the

Figure 6.

Signal II kinetic transients as a function of magnetic field in *Chlamydomonas* DEAE PSII particles. The spectrum of Signal II recorded in the dark is shown in (a); field positions at which the kinetic traces shown in (b) were recorded are indicated as points A, B and C on the spectrum. Field point D is the zero crossing of Signal II. For the spectrum, the following instrument parameters were used: 0.2 s time constant, 200 s sweep, 4 G modulation amplitude, 20 mW microwave power. For the kinetic traces, 200 flashes, given at a rate of 0.25 Hz, were averaged, the instrument time constant was 500 μs. DEAE particles containing 0.44 mg Chl/ml were used.

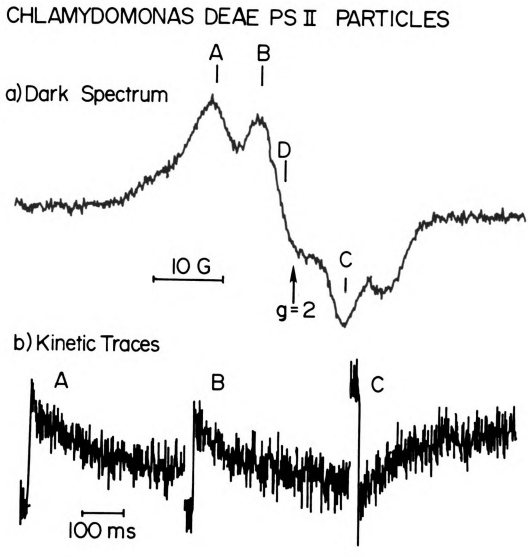
CHLAMYDOMONAS DEAE PS II PARTICLES
A
B
a) Dark Spectrum
D
10 G
C
g=2
b) Kinetic Traces
A
B
C
100 ms

decay kinetics all indicate that the light-induced changes observed arise from Signal II. Signal shape analysis of the light induced change in spinach TSF-IIa particles yielded results similar to those of Fig. 6 for the *Chlamydomonas* DEAE particles. A number of other experiments were carried out in order to determine the characteristics of Signal II transient kinetics in the reaction center preparations. The results (not shown) can be summarized as follow: (1) The risetime of the signal is instrument limited at 98 μs, consistent with the recent determination of the Signal II_f risetime in tris-washed chloroplasts [74] and with the properties of D_1 in *Chlamydomonas* particles [100]. (2) The light-induced signal increase shows microwave power saturation in the 20 mW range. This behavior is characteristic of Signal II when the enhanced relaxation induced by a nearby paramagnet, presumably manganese [19] has been removed. (3) The flash-induced increase in Signal II saturates at incident light intensities which are comparable to those required to saturate Signal II_f in tris-washed chloroplasts at comparable P_{680} concentrations. This indicates that Signal II responds with high quantum efficiency in the particle preparations. (4) The transient response of Signal II is fairly stable in the particle preparations. We noticed, for example, decreases of 25% and 50% of the initial flash amplitude after 600 flashes on *Chlamydomonas* DEAE particles and TSF-IIa particles, respectively.

In tris-washed chloroplasts, benzidine ($Em_7 = 0.55$ V), is an effective donor to Signal II_f [36]. The data of Fig. 7 demonstrate that in PSII reaction center preparations this species is also an efficient Signal II reductant. In Fig. 7a, the decay of Signal II in *Chlamydomonas* DEAE particles is at least biphasic and shows an overall half time of ~160 ms when only the potassium ferricyanide/ferrocyanide buffer is used. The kinetic trace in Fig. 7b shows that upon addition of 40 μM benzidine the decay of Signal II is markedly accelerated; the halftime is 23 ms. In Fig. 7c the benzidine concentration dependence of the acceleration in Signal II decay is summarized. From the slope, a second order rate constant of 7×10^5 M^{-1} s^{-1} can be obtained. The behavior of benzidine as a reductant to Signal II is observed in the other PSII reaction center preparations. Kinetic traces showing the effect of benzidine at various concentration levels in *Chlamydomonas* particles and in spinach and pokeweed TSF-IIa particles are shown in Fig. 8; the decay halftimes are given in the figure caption. The second order rate constants which we determined from the data of Figs. 7 and 8 are collected in Table II. In general, the benzidine rate constant is similar for the various particles and close to that observed for benzidine in tris-washed spinach chloroplasts [36]. The increased efficiency of benzidine in the *Chlamydomonas* particles was reproducible and thus appears to be a real effect. The origin of this

FIGURE 7.

Effect of donor addition on Signal II decay in *Chlamydomonas* DEAE PSII particles. The decay of Signal II in DEAE particles (0.44 mg Chl/ml) without (a) and with (b) the addition of 40 μM BZ is shown. Each trace is the average of 200 flashes, given at a frequency of 0.25 Hz. Instrument conditions: 0.5 ms time constant, 4 G modulation amplitude, 20 mW microwave power, field set at field point A (see Fig. 6). In (c), the BZ concentration dependence of the observed decay rate constant is summarized.

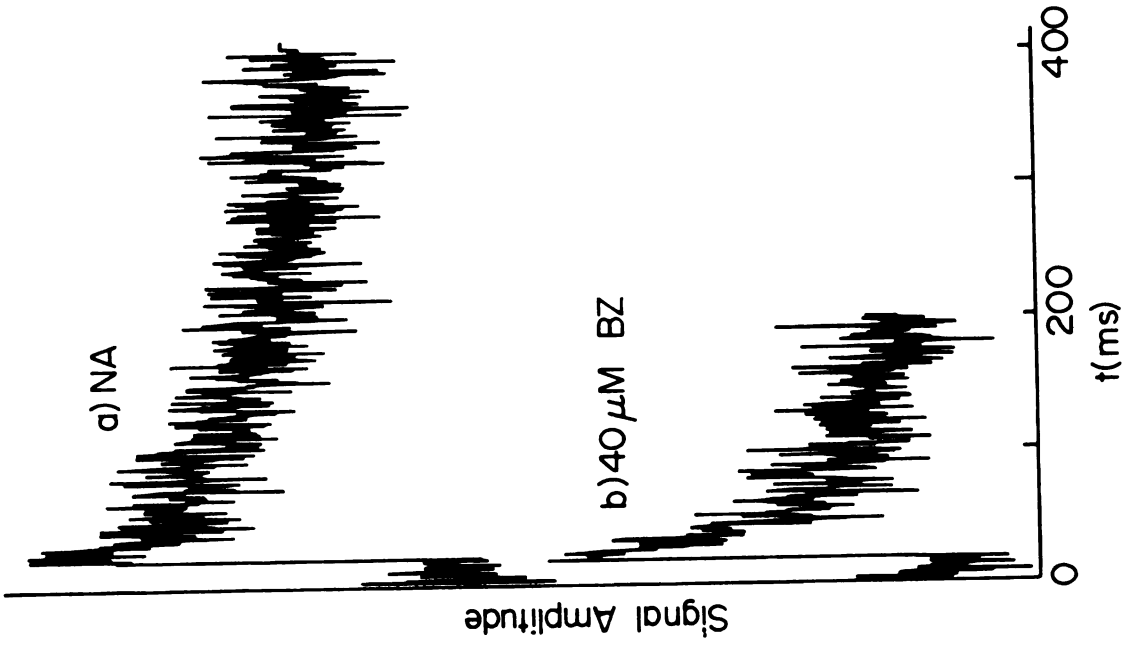
a) NA
b) 40 μM BZ
Signal Amplitude
0
200
400
t(ms)

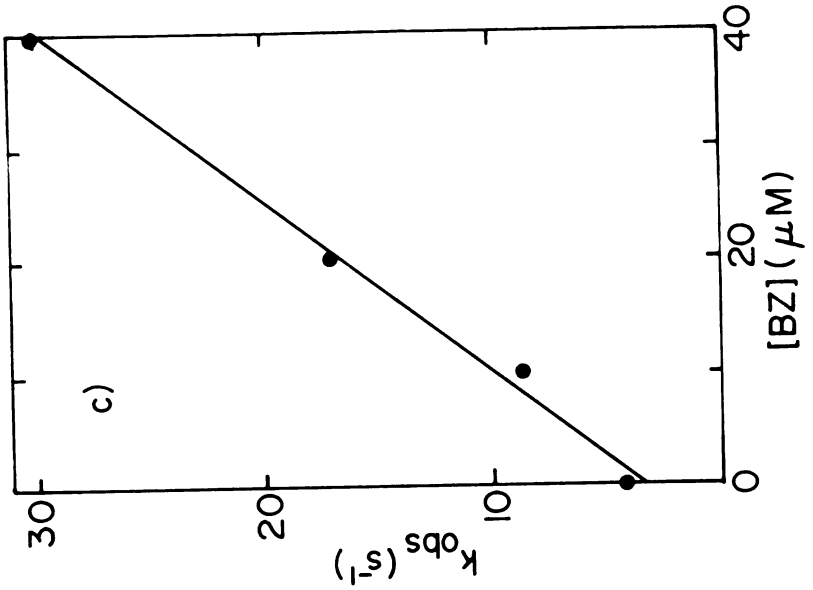
c)
k_{obs} (s^{-1})
30
20
10
0
0
20
40
[BZ] (μM)

FIGURE 8

Signal II kinetic transients in different PSII reaction center preparations. In (a) and (b), *Chlamydomonas* particles (0.39 mg Chl/ml) were used. No further additions were made in (a), overall decay halftime = 36 ms (see text); in (b) 40 μM BZ was added as an electron donor, decay halftime = 5 ms. Each trace is the average of 200 flashes, the instrument time constant was 200 μs. In (c) spinach TSF-IIa particles (0.78 mg Chl/ml) were used and 40 μM BZ was added as an electron donor. The decay halftime was 30 ms, the instrument time constant was 500 μs and 150 flashes were averaged. In (d), (e) and (f), pokeweed TSF-IIa particles (0.39 mg Chl/ml) were used. In (d) no further additions were made, decay halftime = 170 ms; in (e) 20 μM BZ was added, decay halftime = 45 ms; in (f) 40 μM BZ was added, decay halftime = 22 ms. For these traces, an instrument time constant of 200 μs was used and 255 flashes were averaged. In traces (a)-(f), a modulation amplitude of 4 G and microwave power of 20 mW were used. All kinetic traces were recorded at field setting A in Fig. 6.

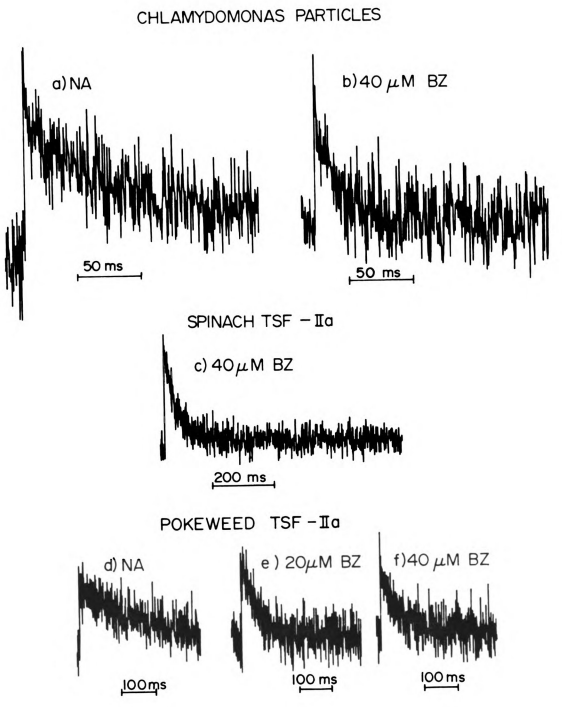
CHLAMYDOMONAS PARTICLES
a) NA
50 ms
b) 40 μM BZ
50 ms
SPINACH TSF - IIa
c) 40 μM BZ
200 ms
POKEWEED TSF - IIa
d) NA
100ms
e) 20μM BZ
100 ms
f) 40 μM BZ
100 ms

TABLE II——PSII Kinetic Parameters — Chloroplasts and Particles.

Preparation	Reagent	k (M^{-1} s^{-1}
spinach chloroplasts-tris washed [a]	BZ	1.3×10^5
spinach TSF-IIa	BZ	6×10^5
pokeweed TSF-IIA	BZ	8×10^5
Chlamydomonas particles	BZ	3×10^6
Chlamydomonas DEAE particles	BZ	7×10^6
spinach chloroplasts-tris-washed [b]	ANT2p	2.7×10^6
Chlamydomonas particles	ANT2p	6×10^6
Chlamydomonas particles	TPB	9×10^5
Chlamydomonas DEAE particles	ANT2p	1.3×10^6

[a] From reference 36.

[b] From reference 101.

phenomenon is unclear although it may represent an increased concentration of the lipophilic benzidine species in the vicinity of Z in this preparation relative to the others rather than some more subtle kinetic effect.

An interesting aspect of the data of Figs. 7 and 8 is that the decay halftimes of the transient Signal II increase in the presence of only the ferricyanide/ferrocyanide redox buffer system. In the DEAE particles (Fig. 7a) this halftime is ~160 ms whereas in the parent normal *Chlamydomonas* particle (Fig. 8a) the decay is more markedly biphasic and shows an initial fast decrease which accounts for roughly one-third of the total decay (separate, higher resolution experiments show that this initial rapid decrease occurs with a halftime of ~1.5 ms) followed by a slower phase with a halftime of 65 ms. Diner and Bowes [100] deduced the same type of behavior for the reduction of D_1 in these two types of *Chlamydomonas* particles from their double flash optical experiments on P^+_{680} decay kinetics, that is, that the rereduction of D_1 in the normal particles is significantly more rapid than is its rereduction in the DEAE-treated material. This observation and the results in ref. 74 support the identification of D^+_1 with the Signal II species, Z^+.

We also studied the effect of ADRY reagents on the decay of Signal II in *Chlamydomonas* particles. In tris-treated chloroplasts ADRY reagents act as reductants to Z^+ in that they accelerate the decay of Z^+ in a manner

which is first order in the ADRY reagent [101]. Figure 9 shows the effect of 20 μM tetraphenylboron (9a) or 5 μM ANT2p (9b) on Signal II amplitude and decay kinetics in normal *Chlamydomonas* particles and of 5 μM ANT2p on Signal II in the DEAE-treated material (9c). The signal amplitude in all three cases is 85-95% of that observed in the absence of the ADRY reagent. In the normal particles, the biphasic Signal II observed in the absence of the ADRY (e.g. Fig. 8a) is converted to what appears to be a monophasic decrease in signal amplitude. For tetraphenylboron we did not carry out a concentration dependence but from Fig. 9a we estimate a second order rate constant of 8×10^5 $\underline{M}^{-1}$ s^{-1} for the decay of Signal II in its presence. This and the second order rate constants for ANT2p in the *Chlamydomonas* particles are summarized in Table II.

The kinetic behavior of Signal II_f in tris-treated chloroplasts has been studied extensively in the past [36]. The decay of Z^+ has been reported to follow pseudo-first order kinetics in the presence of several commonly used electron donors (Ascorbate, hydroquine etc.). We have investigated the effect of various cations on the decay of Z^+ in the presence of negatively charged as well as neutral donors. As shown in Fig. 10, in the presence of negatively charged donors (2 mM ascorbate) addition of salt causes a faster decay of Signal II_f, apparently the result of the screening of the negative charge of the membrane by

FIGURE 9.

The effect of lipophilic anions on the decay of Signal II in *Chlamydomonas* particles PSII and DEAE PSII particles. In (a) and (b) *Chlamydomonas* particles (0.44 mg Chl/ml) were used. In (a) 20 µM TPB was added (decay halftime = 37 ms) and in (b) 5 µM ANT2p was added (decay halftime = 23 ms). Instrument conditions: 200 µs time constant, 200 scans averaged. In (c) DEAE particles (0.40 mg Chl/ml) to which 5 µM ANT2p was added were used. The decay halftime is 95 ms. Instrument conditions: 500 µs time constant, 200 scans averaged. Other settings as in Fig. 8.

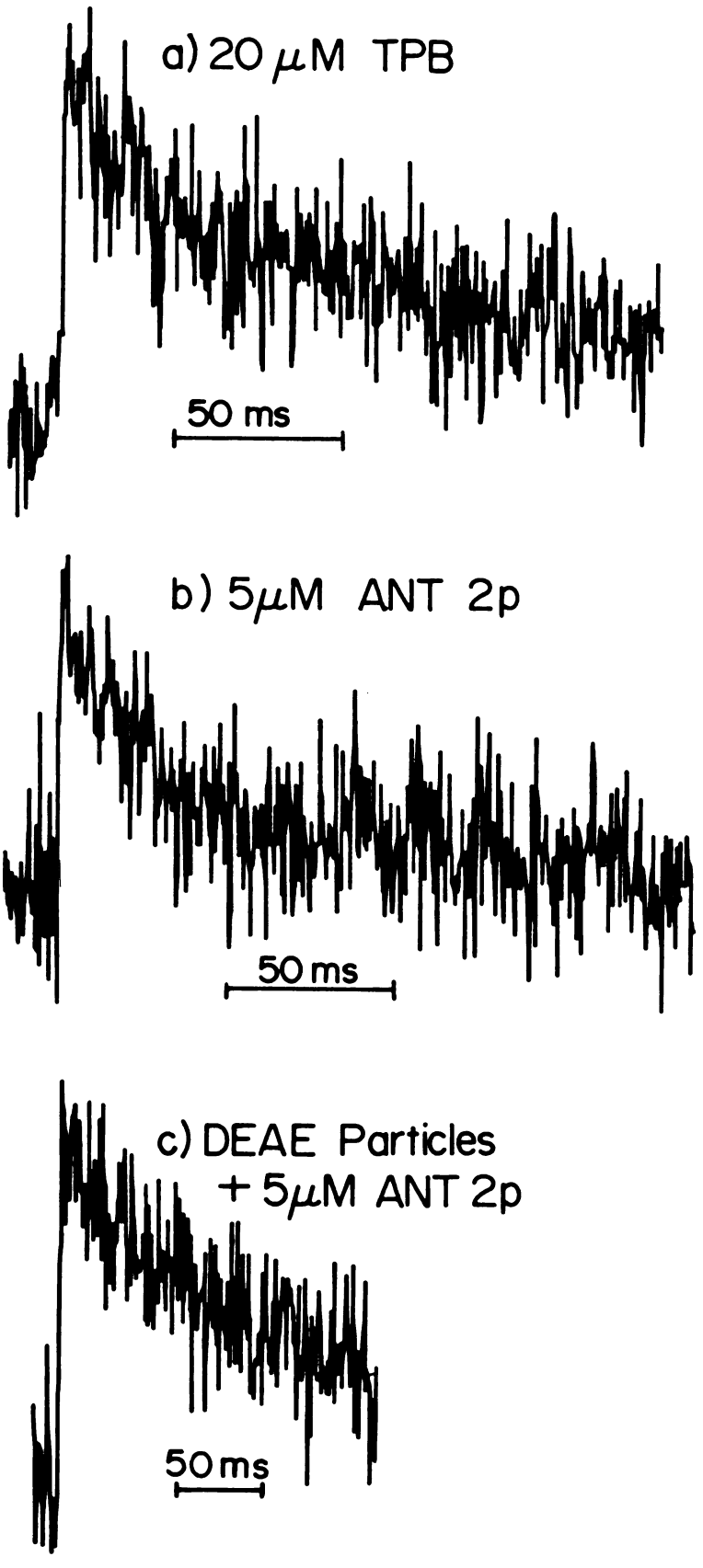
a) 20 μM TPB
50 ms
b) 5μM ANT 2p
50 ms
c) DEAE Particles
+ 5μM ANT 2p
50 ms

FIGURE 10.

The effect of cations on the decay kinetics of Signal II in tris-washed chloroplasts. Ascorbate (2 mM) was used as an exogenous donor. a) No further addition; b) 200 mM KCl; c) 50 mM $MgCl_2$; d) 50 mM $CaCl_2$; and e) 50 mM $SrCl_2$. A time constant of 1 ms was used in all the experimental traces which are each the average of 120 flashes given at a repetition rate of 0.25 Hz. The decay halftimes ($t_{\frac{1}{2}}$) measured from the experimental traces are: a) 350 ms; b) 290 ms; c) 285 ms; d) 94 ms; and e) 85 ms.

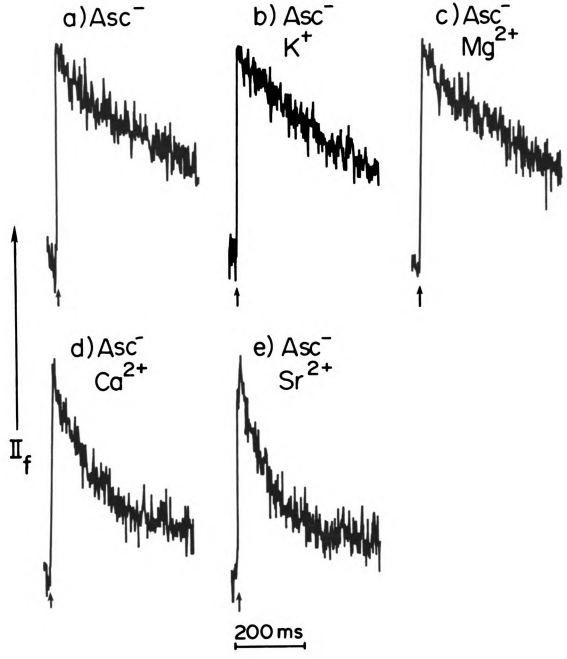
a) Asc⁻
b) Asc⁻ K⁺
c) Asc⁻ Mg²⁺
d) Asc⁻ Ca²⁺
e) Asc⁻ Sr²⁺
If
200 ms

the various cations [102]. In the absence of any salt the decay in the presence of 2 mM ascorbate is relatively slow (Fig. 10a, $t_{\frac{1}{2}} \sim 340$ ms), it becomes a little faster upon addition of 200 mM KCl (10b, $t_{\frac{1}{2}} \sim 280$ ms) and much faster upon addition of a divalent cation for example Ca^{2+} (10d, $t_{\frac{1}{2}} \sim 94$ ms) or Sr^{2+} (10e, $t_{\frac{1}{2}} \sim 86$ ms). The exception in this experiment was Mg^{2+} (10c) which did not show the screening effect of the other divalent cations. We also studied the effect of cations in the presence of neutral donors and the results of such an experiment are shown in Fig. 11. When DPC is used as a reductant addition of Ca^{2+} (11b) or Sr^{2+} (11c) has no effect on the decay time of Signal II_f whereas addition of Mg^{2+} slows it down. The same behavior is observed when benzidine is used as an exogenous donor (11e-g).

D. Discussion

The observation of Signal II in the particle preparations, particularly in the biochemically well-characterized *Chlamydomonas* preparations, suggests that the donor Z is an integral component of the PSII reaction center complex and also confirms the identification of D_1, the donor to P_{680}, with Z.

The kinetic studies we have performed have been concerned with the reduction kinetics of Z. Our results can be compared with previous P_{680}^+ optical work from which some of the characteristics of D_1^+ reduction have

FIGURE 11.

The effect of cations on the decay kinetics of Signal II_f in tris-washed chloroplasts in the presence of neutral donors. a) 0.4 mM DPC; b) 0.4 mM DPC and 50 mM $CaCl_2$; c) 0.4 mM DPC and 50 mM $SrCl_2$; d) 0.4 mM DPC and 50 mM $MgCl_2$; e) 30 μM benzidine and 2 mM ascorbate; f) 30 μM benzidine, 2 mM ascorbate and 50 mM $CaCl_2$; and g) 30 μM benzidine, 2 mM ascorbate and 50 mM $MgCl_2$. A time constant of 1 ms was used in a-d and 0.5 ms in e-g. The experimental traces in a-d are the average of 120 flashes given at a repetition rate of 0.25 Hz, whereas traces in e-g are the average of 150 flashes given at the same rate (0.25 Hz). The decay halftimes ($t_{\frac{1}{2}}$) measured from the kinetic traces are: a) 64 ms; b) 60 ms; c) 60 ms; d) 104 ms; e) 16 ms; f) 16 ms; and g) 29 ms.

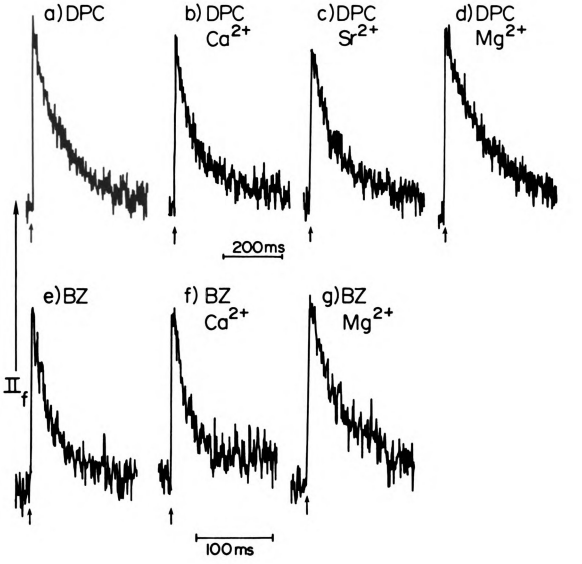
a) DPC
b) DPC
Ca2+
c) DPC
Sr2+
d) DPC
Mg2+
200ms
e) BZ
f) BZ
Ca2+
g) BZ
Mg2+
If
100ms

been inferred. For example, Diner and Bowes have concluded that D_1^+ is rereduced more rapidly in their normal *Chlamydomonas* particles than it is in DEAE particles [100]. The reduction kinetics of Z^+ which we measure in these two types of particles are in agreement with their results (Figs. 7a, 8a, see above). A corollary conclusion which can be drawn from a comparison of the optical work on the particles [100] and our results is that the kinetic characteristics of Signal II and of the reduced acceptor Q_A^- are quite dissimilar. From the second order rate constant for Q_A^- reoxidation by ferricyanide determined in ref. 100, we would predict that Q_A^- is reoxidized in the *Chlamydomonas* particles under the conditions we have typically used with a halftime of less than 1 ms. Signal II, on the other hand, decays with a halftime approximately two orders of magnitude longer, indicating that in the *Chlamydomonas* particles Q_A^- does not give rise to a Signal II-like spectrum. This point is important to establish in that if the iron associated with Q_A were removed during particle purification, we might expect a free radical type spectrum [97,103]. Our data indicate that this is not the case and are in agreement with recent PSII acceptor side EPR studies in the *Chlamydomonas* particles [104]. Renger and Reuter [105] have recently shown that D_1^+ reduction is accelerated both by reducing agents and ADRY reagents. The faster rereduction

of Z^+ in the presence of these species in PSII particles support the identification of Z and D_1.

A study of the effect of various cations on the decay of Signal II has revealed a specific effect of magnesium on the kinetic behavior of Z^+. As shown in Figs. 10 and 11, magnesium, in addition to its screening effect on the negative charge of the membrane, also causes a decrease of the decay time of Z^+ in the presence of neutral or negatively charged donors. At this point, the mechanism of this effect is not well understood. It is possible that magnesium causes a conformational change of the membrane at the region of Z, which alters its kinetic properties. Further kinetic, as well as biochemical, studies of the system are needed in order to understand this specific effect of magnesium.

CHAPTER III.

EXOGENOUS VERSUS ENDOGENOUS ACCEPTORS IN PHOTOSYSTEM II INHIBITED CHLOROPLASTS

A. Introduction

DCMU is known to block the oxidation of the reduced form of the primary acceptor Q_A by the secondary acceptor Q_B (or B) [50,106]. As a result, Q_A^- accumulates in the light and further electron flow through Photosystem II is inhibited.

In the presence of DCMU, Q_A^- can be oxidized by addition of ferricyanide. Two different mechanisms have been proposed to account for this observation. In the first, ferricyanide is postulated to oxidize Q_A^- directly [107,108]. Itoh [108] monitored the oxidation rate of the primary acceptor in the presence of exogenous electron acceptors by measuring the induction of chlorophyll fluorescence in the presence of DCMU. He found that the apparent rate constant for the oxidation of Q_A^- changed widely when either the medium pH or salt concentration was varied. By using acceptors having positive, negative, or no charge, he concluded that the membrane surface potential in the vicinity of the acceptor side of PSII had a dramatic effect on the value of the rate constant

observed for the reoxidation of Q_A^- by charged species. The interaction of the charged artificial acceptor with Q_A^- was explained in terms of the Gouy-Chapman theory [109,110]. In this treatment the apparent rate constant for the reoxidation reaction is dependent upon the local concentration of the acceptor at the membrane surface. The surface concentration of this species is a function of its charge and of the electrical potential difference at the surface of the membrane with respect ot the bulk aqueous phase. In the case of ferricyanide, for example, the relationship between its surface concentration and the surface potential, ψ_0, is given by the following equation:

$$[\text{Ferricyanide}]_s \cdot \gamma_s = [\text{Ferricyanide}]_b \cdot \gamma_b \exp(3F\psi_0/RT) \tag{3.1}$$

where s and b stand for surface and bulk phase, respectively, and γ denotes the activity coefficient. The rate of Q_A^- oxidation can be given as

$$-\frac{d[Q_A^-]}{dt} = k^\circ [Q_A^-] [Fe^{III}CN]_s \cdot \gamma_s \tag{3.2}$$

and

$$-\frac{d[Q_A^-]}{dt} = k [Q_A^-] [Fe^{III}CN]_b \tag{3.3}$$

where k° is the rate constant with respect to the surface activity of ferricyanide and k is the apparent rate constant (see ref. 108). From Eqs. (3.1) and (3.3), the relation between k and k° follows as

$$k = k^\circ \gamma_b \exp(3F\psi_0/RT) \tag{3.4}$$

In the second model, ferricyanide was envisioned as being the redox mediator in titrating an endogenous acceptor which is the species actually responsible for the reoxidation of Q_A^-. From the titration experiments, a midpoint potential of ~400 mV has been postulated for this endogenous species. An identification of this acceptor with cytochrome b_{559} has been ruled out [111]. In a recent review, Bouges-Bocquet summarized the properties of this species and proposed that it be referred to as A_H [8]. This A_H seems to be the same species observed in [68,100,111-116].

Babcock and Sauer [116] reported that the DCMU inhibition of Signal IIf, which arises from the oxidized form of the P680 donor, $Z^{+\cdot}$ [74,92], was relieved if sufficiently high reduction potentials ($E_h > 480$ mV) were maintained in tris-washed chloroplast suspensions. The explanation they offered for their results was that by keeping the potential high they maintained A_H (in Bouges-Bocquet's notation [8]) in its oxidized form so that, under their flashing light conditions, it could act as an additional acceptor for Q_A^- in their DCMU-inhibited chloroplasts.

In the work reported here we have used EPR spectroscopy to reinvestigate the conditions for Signal II_f formation in tris-treated, DCMU-inhibited chloroplasts. We are able to interpret our data without invoking an A_H species and thus we conclude that the reoxidation of Q_A^-

in DCMU-inhibited preparations depends on the effectiveness of ferricyanide in interacting directly with Q_A.

B. Materials and Methods

Chloroplasts were prepared from market spinach and tris-washing and chlorophyll determinations were carried out as described in Chapter II. The chlorophyll concentration in the EPR experiments was 3 mg/ml. The buffer system used consisted of 0.4 M sucrose, 0.05 M HEPES and 0.01 M NaCl which was adjusted to pH 7.6. Reagents were of the highest purity commercially available and were used without further treatment. Redox potentials of the chloroplast suspensions were measured with a platinum /Ag-AgCl electrode (Broadley-James Corp.) which was connected to an Orion 701 A pH/mV meter. The electrode was initially calibrated vs. saturated quinhydrone [117] and was periodically checked by using an equimolar mixture of ferri- and ferrocyanide in the above buffer (SHN). The potential for the couple was measured to be 430 mV in the absence of and 458 mV in the presence of 40 mM Mg^{++}. The redox potentials measured in specific experiments are noted in the figure captions. Electron paramagnetic resonance (EPR) spectroscopy was carried out by using a Bruker 200D instrument operating at X-band and interfaced to a Nicolet 1180 computer. Instrument modifications and the flash lamp are described in [99]. Light induced changes in Signal II_f amplitude were measured by setting the magnetic

field value at the low field maximum of the Signal II spectrum; a modulation amplitude of 4 G was used. The flash repetition rate, instrument time constant, and number of passes averaged in specific experiments are detailed in the figure captions.

C. Results

Upon inhibition of the oxygen-evolving complex, electron flow to $Z^{+\cdot}$ is interrupted, its lifetime is increased, and its EPR signal is referred to as Signal II_f. In a signal-averaged, flashing light experiment, the formation of $Z^{+\cdot}$ is inhibited by DCMU [100]. Previously [101] we showed that the DCMU inhibition of Signal II_f formation is relieved if relatively high concentrations of $Fe^{III}CN$ and divalent cations were added. Ferricyanide addition restores Signal II_f amplitude under these conditions by regenerating the photoactive state, Z P680 Q_A, from Z P680 Q_A^- in the dark time between flashes. The action of $Fe^{III}CN$ can be explained by either of the two models described above. To decide between the alternatives, we have explored the ferricyanide effect in more detail by examining its dependence on dark time between flashes, salt concentration, redox potential and acceptor ionic charge.

As shown in Fig. 12a, the amplitude of Signal II_f is a function of the dark time (t_d) between successive flashes in DCMU inhibited, tris-washed chloroplasts. At

FIGURE 12A.

Effect of the dark time (t_d) between flashes on the magnitude of Signal II_f [$A = (A_{II_f})/(A^{max}_{II_f})$, where A_{II_f} is the measured amplitude and $A^{max}_{II_f}$ is the amplitude in the absence of DCMU]. 3 m$\underline{M}$ $Fe(CN)^{3-}_6$, 20 m$\underline{M}$ Mg^{++} and 100 μM DCMU were added to a suspension of tris-washed chloroplasts at pH 7.6. The instrument time constant was 1 ms; 150 flashes were averaged. The dashed lines show the theoretical fit of these data according to Eq. (3.8).

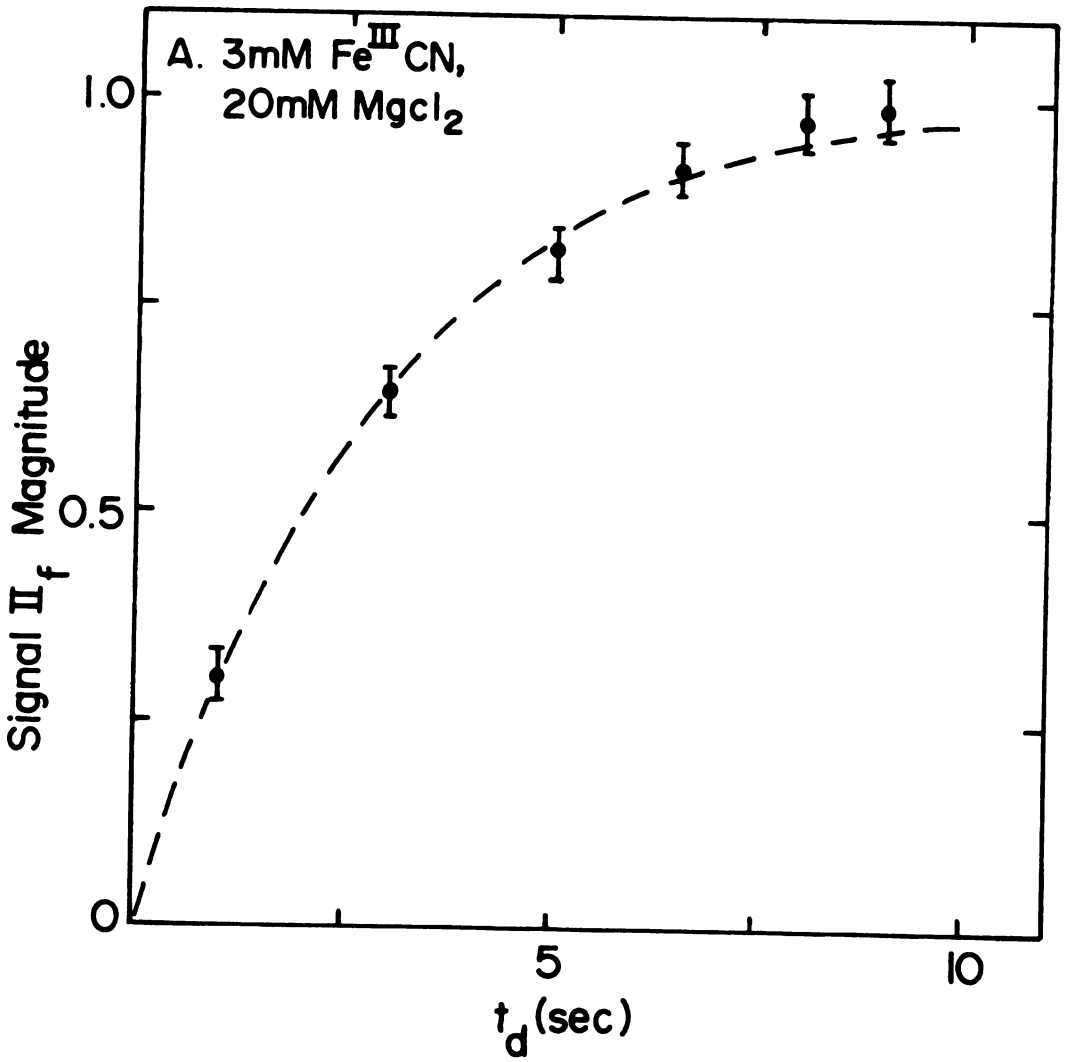
A. 3mM $Fe^{III}CN$,
20mM $Mgcl_2$
1.0
0.5
0
Signal II_f Magnitude
5
10
t_d(sec)

FIGURE 12B.

Graphical determination of the apparent rate constant of Q_A^- reoxidation by ferricyanide (see text for details).

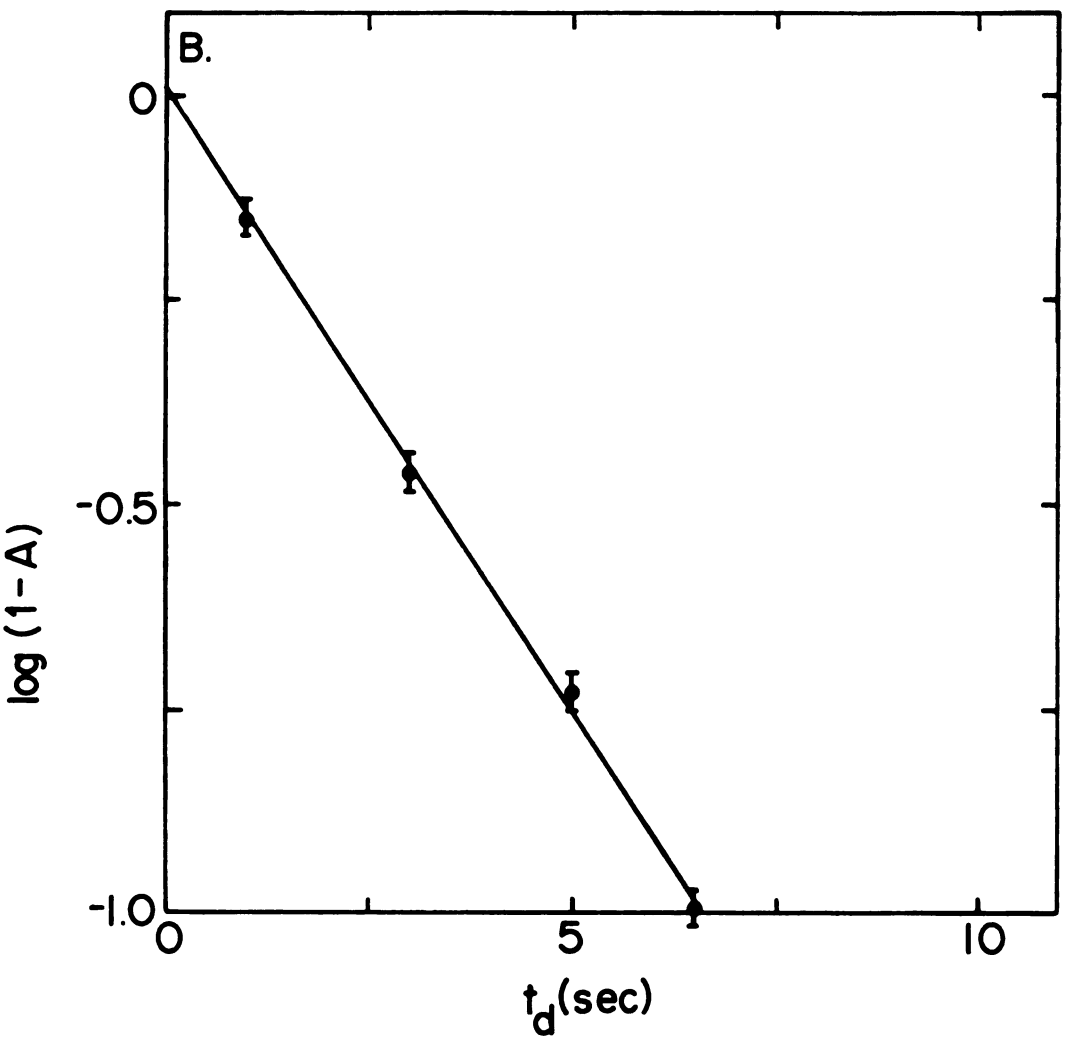
B.
0
-0.5
-1.0
log (1-A)
0
5
10
t_d(sec)

sufficiently long dark times the effect saturates and full Signal II_f amplitude, as determined by controls carried out in the absence of DCMU, is observed. The data in Fig. 12A were obtained with 3 m$\underline{M}$ $Fe^{III}CN$ and 20 m$\underline{M}$ $MgCl_2$ and show half maximal Signal II_f amplitude at $t_d \cong 2$ sec.

The interplay between Signal II_f amplitude and flash repetition rate in the presence of DCMU is influenced by both the salt and the ferricyanide concentration. As shown in Fig. 13, the oxidation of Q_A at constant $Fe^{III}CN$ concentration and dark time between flashes is facilitated by addition of Mg^{++}, apparently due to the effect of the divalent cation on the surface potential in the vicinity of System II as reported by Itoh [108]. The Mg^{++} effect of Fig. 13 is nonspecific since it is also given by other divalent (Ca^{++}, Sr^{++}) as well as monovalent (K^+, Na^+) cations, with divalents being more effective (not shown).

Figure 14 shows the effect of $Fe^{III}CN$ concentration on the amplitude of Signal II_f under conditions where Mg^{++} was present and the ratio of ferri- to ferrocyanide was kept constant. Increasing the ferricyanide concentration in the absence of ferrocyanide gave similar results, i.e., an increase in Signal II_f magnitude with increased acceptor concentration (data not shown). With ferricyanide alone, however, we found fluctuations in redox potential; by maintaining a constant ferricyanide to ferrocyanide ratio, the redox potential remained constant at ~460 mV during a given experiment and did not change significantly between

Figure 13.

Effect of Mg^{++} concentration ($MgCl_2$) on the magnitude of Signal II_f. 3 m$\underline{M}$ $Fe(CN)_6^{3-}$ and 100 μM DCMU were added to a suspension of tris-washed chloroplasts at pH 7.6. The instrument time constant was 1 ms; 150 flashes were averaged at a frequency of 0.33 Hz (t_d = 3 sec).

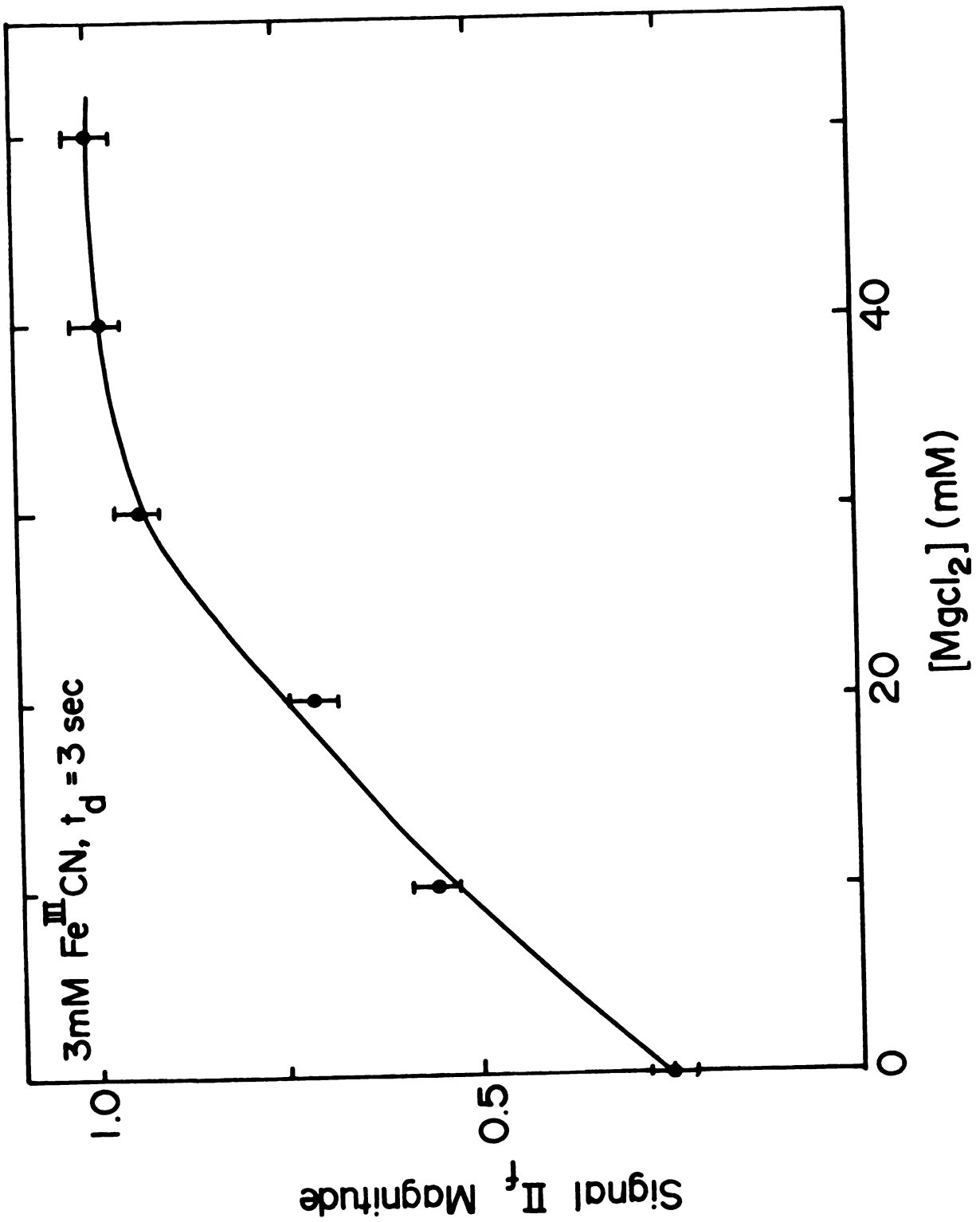
Signal Π_f Magnitude
1.0
0.5
0
20
40
[$MgCl_2$] (mM)
3mM $Fe^{III}CN$, t_d = 3 sec

FIGURE 14.

Effect of ferricyanide concentration on the magnitude of Signal II_f. The amounts of ferri- and ferrocyanide shown above were added to a suspension of tris-washed chloroplasts at pH 7.6, which contained 40 m$\underline{M}$ Mg^{++} and 100 μM DCMU. The redox potential in all samples was ~460 mV. 150 flashes were averaged at a frequency of 0.5 Hz and with an instrument time constant of 1 ms.

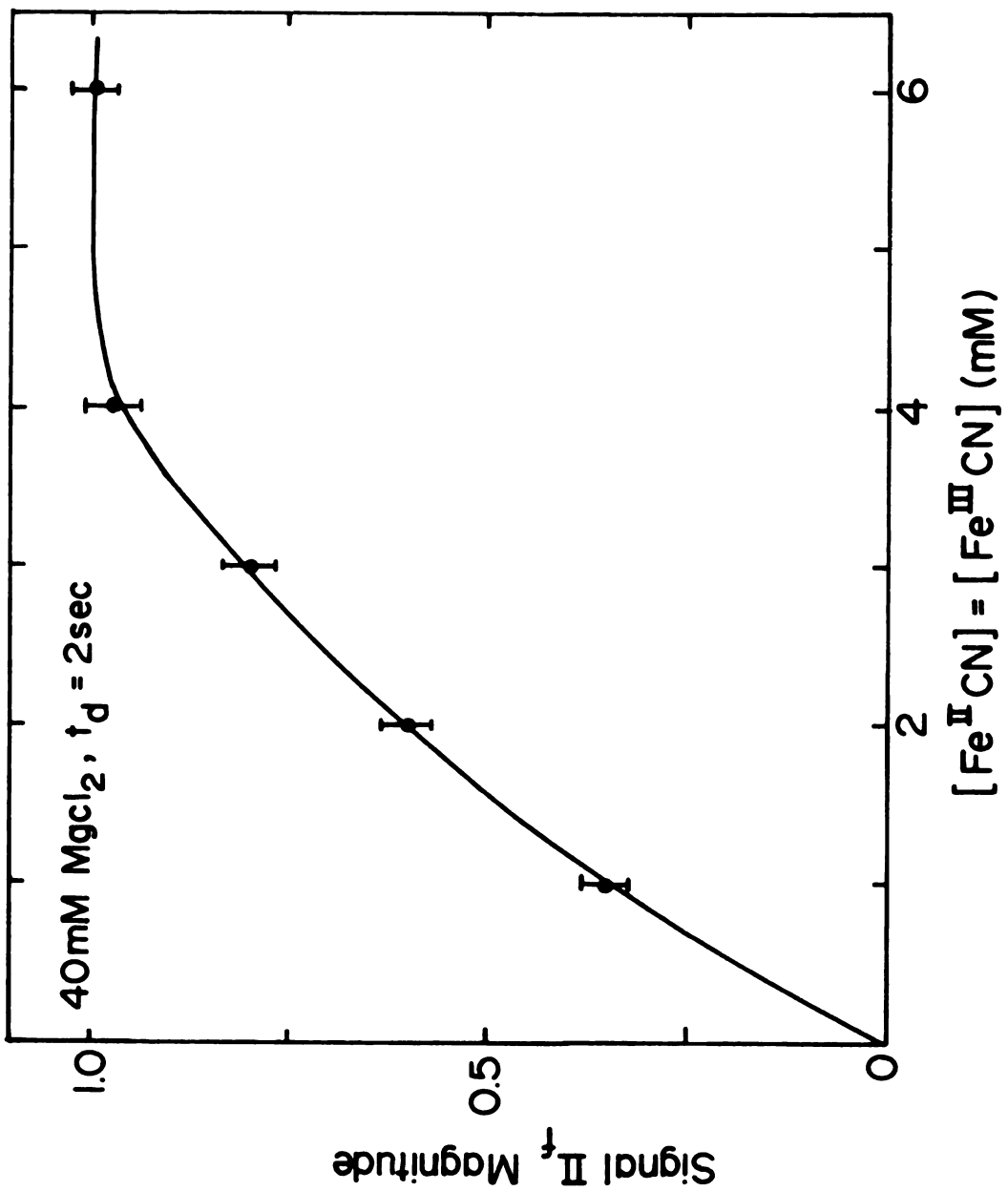
Signal Π_f Magnitude
1.0
0.5
0
40mM $MgCl_2$, t_d = 2sec
2
4
6
$[Fe^{II}CN] = [Fe^{III}CN]$ (mM)

samples. The increase in II_f magnitude with increasing ferricyanide concentration apparent in Fig. 14 can be interpreted according to the direct acceptor model for ferricyanide action: according to Eq. (3.1) the surface concentration of ferricyanide is increased when its bulk concentration is increased, which, because of Eq. (3.2), results in a faster reoxidation of Q_A^-.

The results above indicate that, at constant redox potential (i.e. constant ferricyanide to ferrocyanide concentration ratio), the amplitude of Signal II_f observed depends on the flash repetition rate, the absolute ferricyanide concentration and the concentration of the shielding cation. If we maintain these factors constant and decrease the redox potential of a chloroplast sample by adding additional ferrocyanide, we observe a progressive decrease in the Signal IIf amplitude when divalent cations are used to screen the membrane surface charge, but not when monovalent cations are used as the shielding species. Typical results from such a set of experiments are shown in Fig. 15. Using just $Fe^{III}CN$ (6 m$\underline{M}$) and Mg^{++} (40 m$\underline{M}$), full Signal II_f amplitude is generated (Fig. 15a). Upon addition of $Fe^{II}CN$ (60 m$\underline{M}$), the redox potential of the chloroplast suspension decreases to 405 mV and a partial inhibition in Signal II_f formation is observed (Fig. 15b) which is relieved when we increase the dark time between flashes (Fig. 15c). If the same experiments are carried

FIGURE 15.

Effect of negatively charged species on Signal II_f in tris-treated DCMU-inhibited chloroplasts, pH 7.6, in the presence of 40 m$\underline{M}$ Mg^{++} and 6 m$\underline{M}$ $Fe(CN)_6^{3-}$. a) No further addition, $t_d = 3.5$ sec; b) 60 m$\underline{M}$ $Fe(CN)_6^{4-}$, $t_d = 3.5$ sec; c) 60 m$\underline{M}$ $Fe(CN)_6^{4-}$, $t_d = 8$ sec; d) 200 m$\underline{M}$ $SO_4^{=}$ (Na_2SO_4), $t_d = 3.5$ sec and e) 200 m$\underline{M}$ $SO_4^{=}$, $t_d = 8$ sec. The redox potential in (a) was 582 mV, in (b) and (c) 405 mV and in (d) and (e) 566 mV. The instrument time constant was 1 ms and each trace is the average of 150 flashes.

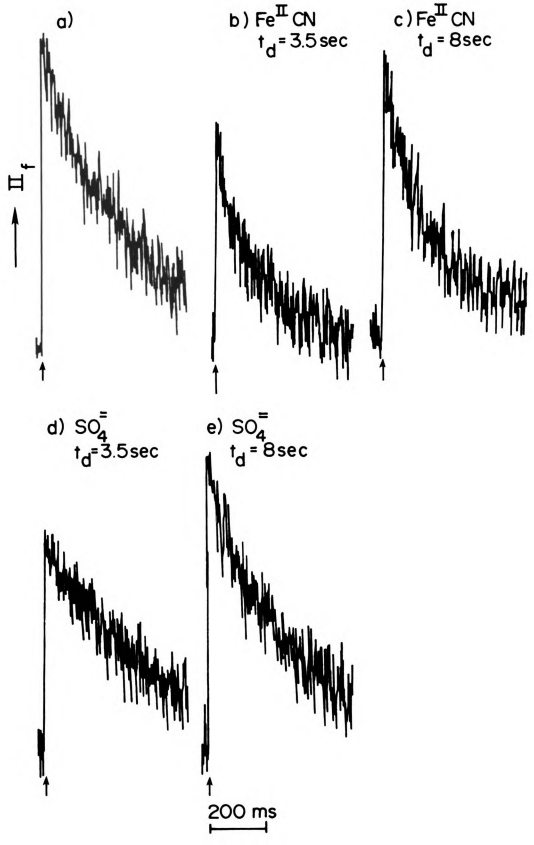
a)
b) $Fe^{II}CN$
t_d = 3.5 sec
c) $Fe^{II}CN$
t_d = 8 sec
Π_f
d) $SO_4^=$
t_d = 3.5 sec
e) $SO_4^=$
t_d = 8 sec
200 ms

out with 500 m$\underline{M}$ KCl (or NaCl) as the only screening species, we find maximal Signal II_f amplitude independent of the ferrocyanide concentration (not shown).

Two explanations for the observations in Fig. 15a and 15b are possible as follows. 1) In an A_H endogenous acceptor model, the added ferrocyanide lowers the solution redox potential sufficiently to reduce a significant fraction of A_H in the dark. As a result, only partial reoxidation of Q_A^- occurs on subsequent flashes and formation of $Z^{+\cdot}$ is suppressed. 2) In an exogenous acceptor model, by introducing high concentration of $Fe^{II}CN$ we decrease the apparent rate constant of the reaction between Q_A^- and $Fe^{III}CN$ and under these conditions an increase in the dark time (t_d) is necessary for complete reoxidation of Q_A^- to occur between flashes. That full Signal II_f amplitude can be generated even in the presence of high $Fe^{II}CN$ concentrations simply by increasing the dark time between flashes (Fig. 15c), or by using monovalent instead of divalent cations to screen the surface charge, appears to favor the second explanation. High concentration of $Fe^{II}CN$ could decrease the rate of the reoxidation reaction simply by decreasing the surface concentration of $Fe^{III}CN$. The decrease of the surface concentration of $Fe^{III}CN$ could be either the result of a simple displacement of $Fe^{III}CN$ by $Fe^{II}CN$ (according to Stern's theory there is a limited number of sites at the membrane [118]) or the result of a decrease in the surface potential (i.e., the

surface potential becomes more negative) caused by addition of the polyvalent anion, $Fe^{II}CN$ (see below).

To distinguish between the exogenous and endogenous acceptor models we used high concentrations of Na_2SO_4 instead of $Fe^{II}CN$ at constant $Fe^{III}CN$ concentration. The sulfate anion is simlar to $Fe^{II}CN$ in that it is polyvalent. It is, however, redox inactive and therefore its addition does not significantly decrease the solution redox potential (see caption to Fig. 15). The results of this experiment (Fig. 15d) show that a decrease in Signal II_f amplitude occurs with increases in $SO_4^=$ concentration. Moreover, the sulfate induced suppression of Signal II_f amplitude, like that observed in the presence of ferrocyanide, could be relieved by increasing the dark time between flashes (Fig. 15e). (Controls carried out in the absence of DCMU showed that 200 m$\underline{M}$ Na_2SO_4 had no effect on the extent or kinetics of Signal II_f formation and decay when $t_d = 3$ sec was used.) These experiments indicate that the decrease in Signal II_f amplitude observed upon increasing the $Fe^{II}CN$ concentration (Fig. 15b) is not the result of a decrease in the solution redox potential but rather arises from a perturbation to the surface potential induced by this polyvalent anion. As a result of the altered surface potential, the surface concentration of $Fe^{III}CN$ is decreased.

We noted above that one mechanism by which the polyvalent anion induced inhibition of Signal II_f amplitude

could occur was by simple displacement of ferricyanide in the double layer. However, the inhibition occurred only when polyvalent anions ($Fe^{II}CN$, $SO_4^{=}$) were added to solutions in which divalent cations (e.g. Mg^{2+}) were used to screen membrane surface charge. No inhibition in Signal II_f amplitude occurred with either monovalent anions (e.g., Cl^-) or with monovalent screening cations (K^+ or Na^+). These observations suggest that ion-pair association occurs between the added polyvalent anion and the divalent which results in a decrease in the effective concentration of the screening cation [119]. Such an ion pair association will be more pronounced when a divalent cation is used to shield the surface charge for two reasons. First, the higher charge of the divalent compared to the monovalent leads to more efficient ion-pair formation [119]. Second, the divalent cation is effective in screening surface charge at much lower concentrations compared to that of the monovalent and, because of its lower concentration, its screening capacity is more susceptible to the effects of ion-pair formation. A decrease in the effective concentration of the divalent cation results in an incomplete shielding of the membrane surface and, consequently, a decrease in the surface concentration of $Fe^{III}CN$. As predicted by this model, the $Fe^{II}CN$ inhibition observed in Fig. 15b was relieved by addition of higher concentrations of $MgCl_2$ (data not shown).

The results above indicate that, under our experimental conditions, Q_A^- is reoxidized directly by the exogenous acceptor rather than by an intermediate endogenous species and that the factor which controls the oxidation of Q_A^- is not a relatively high redox potential in the medium but rather the presence of an efficient acceptor. Since the midpoint potential of the ferricyanide-ferrocyanide couple was measured to be 458 mV (in the presence of 40 m$\underline{M}$ Mg^{++}), it was difficult to decrease the solution potential to values much below 390 mV and, at the same time, keep the concentration of ferricyanide at levels where it would be an effective acceptor. Thus, we looked for an acceptor with a lower midpoint potential. Itoh [108] has shown that the positively charged species, PMS, is a very efficient acceptor under conditions where the surface potential of the membrane was negative. Figure 16a shows that in the presence of PMS, and under conditions where A_H should be reduced ($E_h = 260$ mV, measured before and after the experiment), Q_A^- is reoxidized in the dark time between flashes. This result strongly suggests that PMS reacts directly with Q_A^-. The decay halftime of Signal II_f in the presence of PMS is fast owing to the reduction of $Z^{+\cdot}$ by the reduced form of PMS at that potential. When the potential was increased to 520 mV by addition of $Fe^{III}CN$, the decay rate of $Z^{+\cdot}$ was slowed down because the concentration of reduced PMS was minimized (Fig. 16b). We also tried to use various quinones to

FIGURE 16.

Phenazinemethosulfate (PMS) as an artificial acceptor in tris-treated DCMU-inhibited chloroplasts at pH 7.6. a) 1 m$\underline{M}$ PMS; redox potential 260 mV; b) 1 m$\underline{M}$ PMS and 1 m$\underline{M}$ $Fe(CN)_6^{3-}$; redox potential 520 mV. 150 flashes were averaged at a frequency of 0.25 Hz. The instrument time constant was 200 μs in (a) and 1 ms in (b).

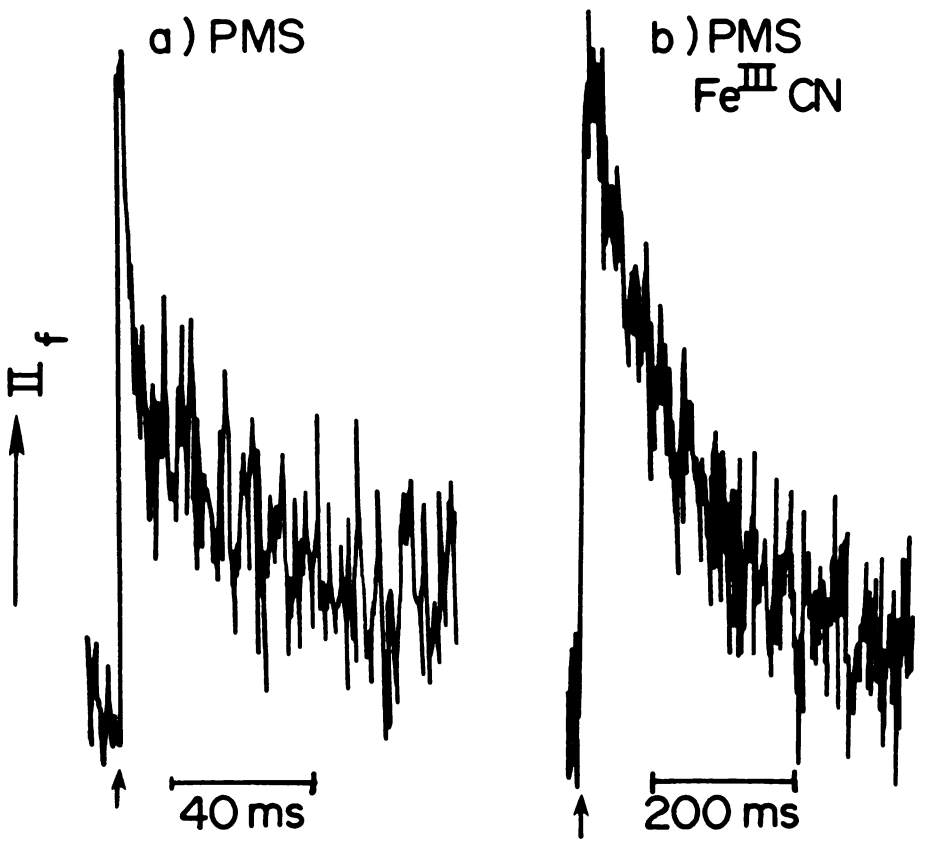
a) PMS
b) PMS
Fe^{III} CN
Π_f
40 ms
200 ms

adjust the redox potential, but our kinetic data were complicated by the presence of very strong, g = 2.0 EPR signals from the semiquinones. PMS also shows a weak EPR signal in this region (g ~ 2.0), but it does not effect the kinetic traces of Signal II_f, as shown by repeating the experiment at various magnetic field positions on the Signal II spectrum.

D. Discussion

In the presence of DCMU, oxidation of Q_A^- by the endogenous secondary electron acceptor is blocked. The EPR results presented above indicate that the release of this DCMU inhibition observed upon ferricyanide addition results from a direct oxidation of Q_A^- by the added acceptor. It thus becomes unnecessary to postulate an endogenous component, A_H, to explain this observation. To develop this in more detail, we begin with Itoh's observation that after continuous illumination the oxidation of Q_A^- in the presence of ferricyanide in DCMU inhibited chloroplasts occurs by a pseudo-first order reaction with respect to the bulk concentration of ferricyanide [120]. From Eq. (3.3) we can calculate the amount of Q_A which remains in the reduced form $[Q_A^-]_t$, after time, t, under a given set of experimental conditions as

$$[Q_A^-]_t = [Q_A^-]_0 \, e^{-k\,[Fe^{III}CN]_b \cdot t} \qquad (3.5)$$

where $[Q_A^-]_0$ is the concentration of Q_A^- produced by the

flash. From Eq. (3.5) we calculate the halftime of the reaction to be

$$t_{\frac{1}{2}} = \frac{\ln 2}{k\,[Fe^{III}CN]_b} \tag{3.6}$$

From Eqs. (3.5) and (3.6), and assuming that single-turnover, saturating flashes are used, we obtain

$$[Q_A]_t / [Q_A] = 1-2^{-t/t_{\frac{1}{2}}} \tag{3.7}$$

where $[Q_A]_t$ is the amount of Q_A in the oxidized form after time t and $[Q_A]$ is the total concentration of the acceptor irrespective of its valence state. Thus, in a series of flashes t_d time apart the amount of Q_A oxidized between two flashes will be given by Eq. (3.7) with $t = t_d$. Because the amount of Signal II_f generated by a flash under steady state conditions is proportional to the amount of Q_A oxidized between flashes we can write

$$A_{II_f}/A^{max}_{II_f} = 1-2^{-t_d/t_{\frac{1}{2}}} \tag{3.8}$$

or

$$1-A = 2^{-t_d/t_{\frac{1}{2}}} \tag{3.9}$$

where $A = A_{II_f}/A^{max}_{II_f}$. This can be rewritten as

$$\log (1-A) = -0.43\ k\,[Fe^{III}CN]_b t_d \tag{3.10}$$

Application of Eq. (3.10) to the data of Fig. 12a gives a plot shown in Fig. 12b. The slope of the straight line which results is -0.16 and therefore, $-k\,[Fe^{III}CN]$

TABLE III——Apparent Rate Constants for Q_A^- Oxidation by Ferricyanide in the Presence of Various Concentrations of $MgCl_2$.

$[Mg^{++}]$ (m$\underline{M}$)	$10^{-2} \times k$ ($\underline{M}^{-1}$ s^{-1})
0	0.3
10	0.9
20	1.2

(0.43) = -0.16. Since the concentration of $Fe^{III}CN$ used is 3 m$\underline{M}$ we calculated the apparent rate constant k to be 1.2×10^2 $\underline{M}$ s^{-1} under the experimental conditions of Fig. 12. Using the data of Fig. 13 and Eq. (3.10), we can calculate the value of the apparent rate constant for various concentrations of Mg^{++}. The results are summarized above in Table III.

From Itoh's work (ref. 108, Fig. 2) we obtain a k value of 0.4×10^2 $\underline{M}^{-1}$ s^{-1} for the reoxidation of Q_A^- by $Fe^{III}CN$ in the presence of 20 m$\underline{M}$ $MgCl_2$, which is in good agreement with our k value for similar conditions. Therefore, the results from two different kinds of experiments, Itoh's work on fluoresence detection of Q_A^- reoxidation [108] and our present data on Z^+ by EPR detection, converge and indicate that the ferricyanide relieves DCMU inhibition by oxidizing Q_A^- directly.

According to the model proposed here, the decrease in Signal II_f observed by Babcock and Sauer [116] when they decreased the solution potential by titrating the ferricyanide containing suspension with ascorbate, can be attributed to the decrease in the ferricyanide concentration rather than to the drop in the redox potential upon addition of ascorbate. Although these authors were aware of possible ferricyanide specific effects and repeated their titration with a different redox mediator, cyanotungstate, it is likely that the surface charge effects apparent for ferricyanide will also be in force for cyanotungstate.

From the results and arguments presented above, it is apparently unnecessary to invoke the high potential acceptor component, A_H, in order to rationalize steady state EPR results in tris-washed chloroplasts. The A_H species has also been postulated to account for results obtained in low temperature optical and EPR experiments and in room temperature fluorescence measurements (see [8]). These studies involved essentially single flash techniques applied to dark-adapted material. They are thus quite distinct in terms of experimental protocol from our measurements and it becomes uncertain as to whether an extrapolation of our results to these systems is appropriate. Nonetheless, it is possible to explain these results in terms of direct exogenous acceptor oxidation of Q_A^- rather than in terms of the endogenous

A_H species. Two additional observations regarding these earlier studies support this hypothesis: a) the $Fe^{III}CN/Fe^{II}CN$ redox couple has been used to poise the solution redox potential in all previous studies in which A_H has been proposed [68,100,111-116] and b) no known redox component occurs endogenously in PSII which has the A_H midpoint potential (since A_H is not cyt b_{559} [111]).

CHAPTER IV.

THE ROLE OF ADRY REAGENTS IN DESTABILIZING HIGH-POTENTIAL OXIDIZING EQUIVALENTS IN CHLOROPLAST PHOTOSYSTEM II

A. Introduction

At least three components have been implicated in the molecular events which lead to oxygen evolution in chloroplast Photosystem II (for reviews, see [8] and [121]). The first of these, the reaction center chlorophyll complex P_{680}, is involved in photon absorption and subsequent primary charge separation. Good progress in understanding these processes has been made recently owing to the strong analogy which has emerged between the photochemistry which occurs in the Photosystem II and that which occurs in the photosynthetic bacterial reaction center [97,122, 123], although the state of chlorophyll aggregation in the two different reaction centers may be distinct [72]. The second component, usually designated as D_1 or as Z, is an intermediate electron carrier which appears to be a quinone species [81,85,116,124]. When oxidized during P_{680}^+ rereduction, $Z^{+\cdot}$ gives rise to EPR Signal II_{vf} in oxygen evolving chloroplasts [125] and to EPR Signal II_f in inhibited chloroplasts [91]. The kinetics of the

electron transfer reactions of this intermediate have been studied extensively by EPR [36,67,90,102], by optical [45,126,127], by luminescence [128] and by fluorescence [54] techniques and a reasonably clear picture of its involvement in P_{680}^{+} rereduction has emerged. The possibility that a parallel donor alternates with Z as a P_{680}^{+} reductant has also been raised [8]. The third component on the oxidizing side of Photosystem II is the oxygen evolving complex (OEC) which carries out the actual water splitting reaction. Kok and coworkers have shown that the oxidizing equivalents required in this process are accumulated linearly with P_{680} turnover and have developed the S-state terminology to describe the formal oxidation state of the oxygen evolving complex [14]. Proton release data suggest that the higher oxidation states may actually correspond to partially oxidized water intermediates which remain bound to the OEC [22,23,29,130]. Manganese has been implicated as a cofactor in the water splitting reaction (for review, see [131]); recent work has provided additional support and insight into the role of manganese in this process [19,20,31].

In the reactions which occur on the oxidizing side of PSII, these components (P_{680}, Z and OEC) are often postulated to form a linear chain so that oxidizing equivalents generated by photon absorption in the reaction center are transferred via Z into the OEC. Within this formulation the redox potential of these components can be

roughly estimated. At pH 7, the midpoint potential of the water/oxygen couple is 815 mV; however, photosynthetic water oxidation appears to occur such that the protons released in this process appear in the acidic internal thylakoid volume [22] where the steady state pH value may be as low as 4.5. Thus the OEC operates under conditions where the midpoint potential of its reductant, water, is at least 965 mV. From work which has been done with both P_{680} [45,126] and with EPR Signal II_{vf} [67], it appears that the equilibrium constants for the reaction of P_{680}^{+} with Z and of $Z^{+\cdot}$ with the OEC must be at least 10. Thus the midpoint potential of $Z^{+\cdot}$ is more positive by at least 60 mV relative to that of the OEC and that of P_{680}^{+} is at least 60 mV more positive than that of the $Z/Z^{+\cdot}$ couple.

Despite these strongly oxidizing potentials, the water oxidizing system appears to be remarkably specific for H_2O. Commonly used reductants are completely ineffective in competing with water for the oxidants generated in PSII [132]. Only those species which are structurally similar to H_2O (e.g. H_2O_2, NH_2OH) appear to be oxidized by PSII at the expense of water. Part of this specificity, no doubt, arises from the extremely rapid redox reactions which occur during the transfer of photogenerated oxidizing equivalents from P_{680}^{+} through Z to the OEC. These reactions proceed with halftimes in the sub-ms time range and even the slowest step in this process, the actual generation of

O_2, occurs with a 1 ms halftime [67,133]. Thus exogenous reductants, which react with Z^{+} in tris-washed chloroplasts with second-order rate constants in the 10^2-10^7 $\underline{M}^{-1}$ s^{-1} range [36], are excluded at normal concentration levels ($\leq$100 μM) simply by the kinetics of the membrane bound transfers. The intermediate states of the OEC, however, are reasonably stable, even though they are held at high redox potentials, and only decay (i.e. are reduced to lower formal oxidation states) when the interval between successive absorbed photons extends well into the seconds range [13,14]. The chemical basis for the remarkable stability of the higher S states is at present unknown.

Over the past decade, a class of compounds has been found which increases the rate by which the intermediate formal oxidation states of the OEC decay [134-137]. Much of this work has been carried out by Renger and coworkers who refer to these species as ADRY reagents. Little is known regarding the mechanism by which they destabilize higher S-states. However, some members of the ADRY class are remarkably efficient at S-state deactivation even at very low concentrations (~1 per PSII reaction center), and, as a consequence, models in which ADRY reagents activate a cyclic pathway for the reduction of the OEC, rather than participate directly in the redox chemistry, appear to be favored. That one of the requirements for the ADRY effect appears to be an acidic proton on a lipophilic anion has also attracted comment [138]. Recently, Renger and

Eckert [139] and Renger and Reuter [105], using optical techniques to monitor P_{680}^{+} decay, have shown that in tris-washed chloroplasts, ADRY reagents promote the rereduction of $Z^{+\cdot}$ following flash excitation. Thus ADRY reagents appear to be general in increasing the rate at which the highly oxidizing equivalents generated by PSII are reduced. In the work described here, we have used EPR spectroscopy to monitor the effect of ADRY reagents on the behavior of $Z^{+\cdot}$ in tris-washed chloroplasts in signal-averaged, flashing light experiments. Our results can be interpreted to indicate that ADRY reagents act by reducing $Z^{+\cdot}$ directly in a bimolecular reaction with second-order rate constants on the order of 10^5-10^7 $\underline{M}^{-1}$ s^{-1}.

B. Materials and Methods

Chloroplasts were prepared from market spinach and tris-washing and chlorophyll determinations were carried out as described in Chapter II. Chlorophyll concentrations in EPR experiments ranged from 3 to 6 mg/ml. The buffer system used in most experiments consisted of 0.4 $\underline{M}$ sucrose, 0.05 $\underline{M}$ HEPES, 0.01 $\underline{M}$ NaCl which was adjusted to pH 7.6. Addition of other reagents is indicated in the figure captions as is the buffer system used when experiments were carried out at pH values other than 7.6. Ferredoxin and NADP were added as an acceptor system [36] to maintain electron flow under signal-averaging conditions. Standard chemicals were obtained commercially and were of

the highest purity available. DCMU was from Dupont and was recrystallized prior to use. ANT 2p was a gift from Dr. G. Renger; ANT 2a was a gift from Dr. R. Blankenship. Care was taken to maintain the organic solvent volume at less than 1% the volume of the chloroplast suspension when they were used in order to solubilize the various reagents. At this concentration the solvents used had no discernible effect on the reactions being monitored.

Electron paramagnetic resonance (EPR) spectroscopy was carried out with a Bruker ER 200D instrument operating at X-band and interfaced to a Nicolet 1180 computer. The instrument has been modified slightly primarily in that we increased the effective Q of the phase sensitive signal detector by imposing either a passive 50 KHz high pass filter or a PAR 189 selective amplifier between it and the detector diode preamplifier. The rationale for and effects of these modifications have been discussed by Yerkes [99]. A Varian TM mode cavity (E238), modified for operation with the Bruker spectrometer [19], and Scanlon TM mode flat cell (S-814) were used in the experiments described. In flashing light experiments, a critically damped xenon flashlamp (ILC, Sunnyvale, CA), which provides saturating pulses 14 μs in duration (full width, 1/3 maximum intensity), was used in conjunction with laboratory constructed capacitor discharge and timing circuitry [99]. Light induced changes in Signal II_f

amplitude were measured by setting the magnetic field value at the low field maximum of the Signal II spectrum; a modulation amplitude of 4 G was used. The flash repetition rate, instrument time constant and number of passes averaged in specific experiments are detailed in the figure captions.

C. Results

In oxygen-evolving chloroplasts, $Z^{+\cdot}$ is rereduced by the OEC in the submillisecond range following excitation [67,125]; the free radical state of Z observed under these conditions is referred to as Signal II_{vf}. Upon inhibition of the OEC electron flow to $Z^{+\cdot}$ is interrupted and the lifetime of the free radical is extended well into the ms time range. Under these conditions, the $Z^{+\cdot}$ free radical is referred to as Signal II_f and its reduction occurs at the expense of endogenous donors (e.g. ascorbate) in the chloroplast suspension [91]. Upon addition of exogenous donors, the lifetime of $Z^{+\cdot}$ is decreased owing to a direct bimolecular reaction of the donor with $Z^{+\cdot}$. This pathway is the principal route by which exogenous donors restore PSII electron flow in inhibited chloroplasts [66]. The efficiency of various donors in restoring this flow can be judged by the second-order rate constant for their reaction with $Z^{+\cdot}$ which have been tabulated recently [36]. Figure 17 shows typical Signal II_f data we obtain with the hydroquinone/ascorbate couple. In the absence of

FIGURE 17.

The effect of donor addition on the decay of Signal II_f in tris-washed chloroplasts. In (a) 2 mM sodium ascorbate was added as a donor, the observed rate constant for Signal II_f decay is 4.2 s^{-1}; in (b) 100 μM hydroquinone and 2 mM sodium ascorbate comprised the donor system, $k_{obs} = 16.4\ s^{-1}$; in (c) 200 μM hydroquinone and 2 mM sodium ascorbate were used, $k_{obs} = 34\ s^{-1}$. The instrument time constant in (a) was 1 ms which was decreased to 500 μs in (b) and (c). Each trace is the average of 180 flashes given at a frequency of 0.25 Hz.

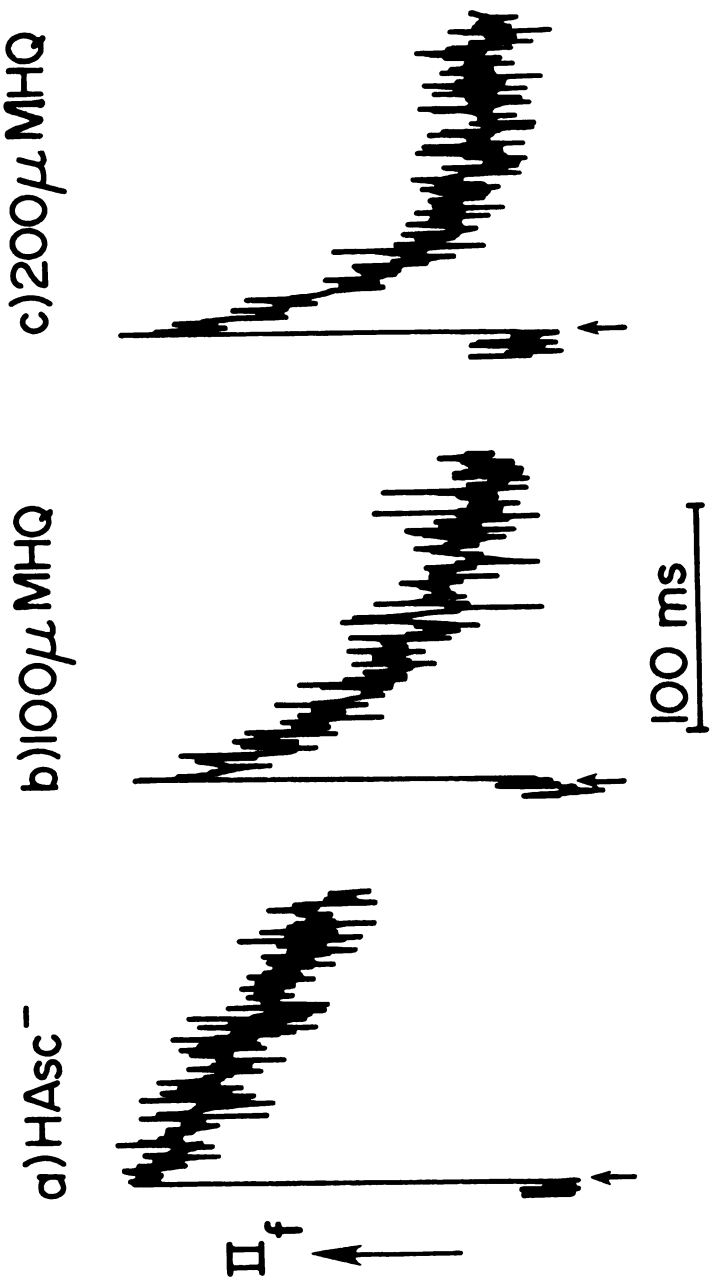
a) HAsc⁻
b) 100μ MHQ
c) 200μ MHQ
100 ms
Πf

exogenous donors the decay halftime is slow, typically in the 500 ms—1 s time range [91]. Addition of ascorbate at substrate levels increases the decay rate (Fig. 17a) and increasing concentrations of the more efficient donor, hydroquinone, accelerates the $Z^{+\cdot}$ rereduction further (Figs. 17b,c). From these data, k_2, the second-order rate constant for the reaction between H_2Q and $Z^{+\cdot}$ (Eqn. 4.1)

$$H_2Q + Z^{+\cdot} \xrightarrow{k_2} Z + H_2Q^{+\cdot} \qquad (4.1)$$

can be extracted by plotting the observed (pseudo-first order) rate constant (k_{obs}) versus the H_2Q concentration corresponding to the particular value of k_{obs}. The value we obtain in the series of experiments of Fig. 17, 1.7×10^5 $\underline{M}^{-1}$ s^{-1}, is in good agreement with the value reported earlier [36].

If we now carry out a similar experiment but replace the exogenous donor couple with an ADRY reagent we can probe the mechanism by which this class of compounds accelerates the reduction of $Z^{+\cdot}$. Figure 18 shows typical data we have obtained with the ADRY reagent, ANT 2p. In the absence of the ADRY reagent, Signal II_f exhibits a slow decay similar to that described in conjunction with Fig. 17. Increasing ANT 2p concentration from 2.5 μM (Fig. 18a) through 5 μM (18b) to 15 μM (18c) leads to progressively more rapid Signal II_f decay. Figure 18d shows a first-order plot for the decay of Signal II_f in

FIGURE 18.

The effect of ANT 2p on the decay kinetics of Signal II_f in tris-washed chloroplasts. ANT 2p at the indicated concentrations was used in (a), (b) and (c). A time constant of 500 μs was used in all three experimental traces which are each the average of 180 flashes given at a repetition rate of 0.25 Hz. In (d), a semilog plot of the decay of Signal II_f in (b) is presented. A hand-drawn curve was fitted to the data and the amplitude of Signal II_f at various times was extracted from this curve.

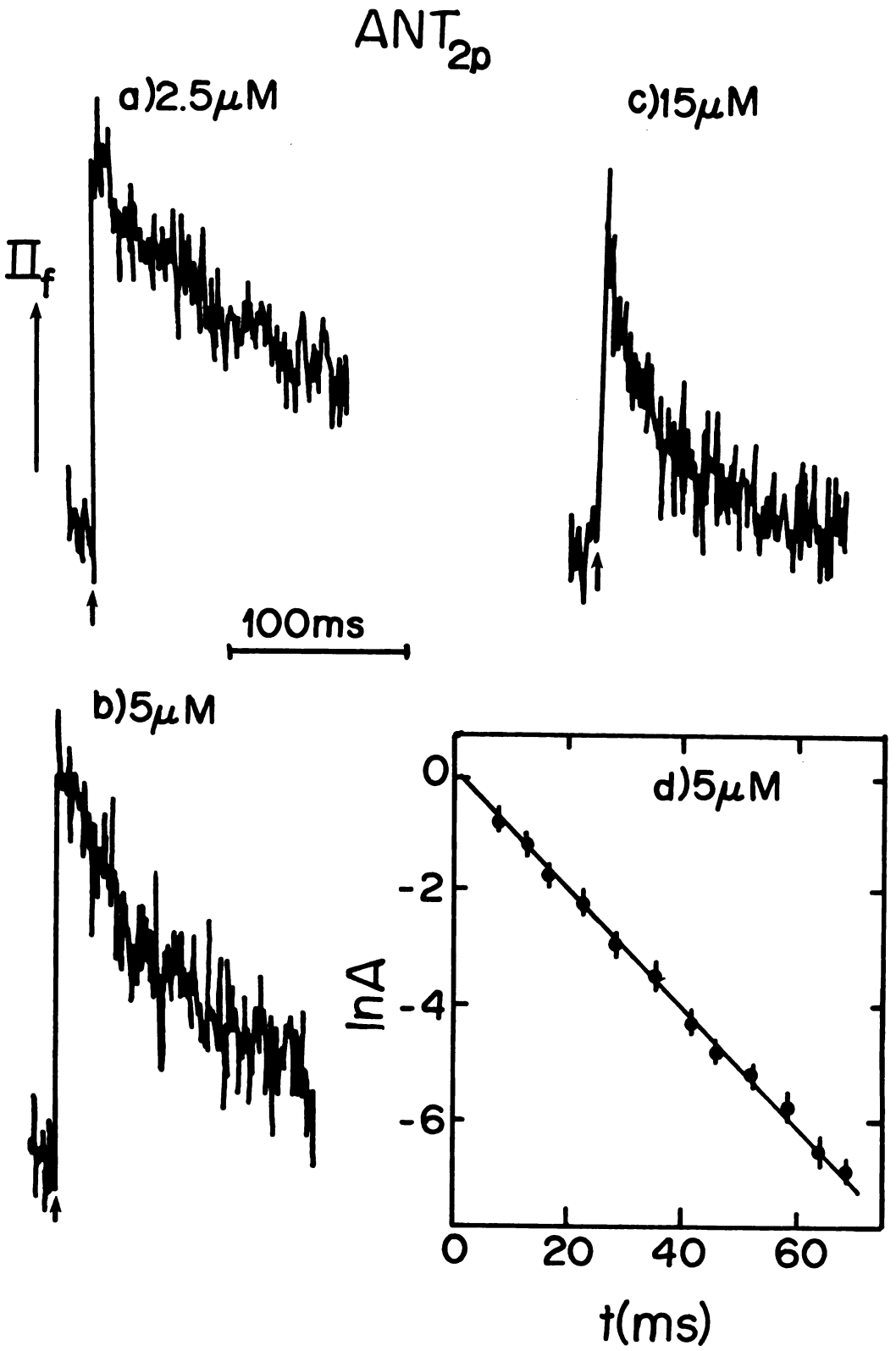
ANT2p
a)2.5μM
c)15μM
If
100ms
b)5μM
d)5μM
0
-2
-4
-6
lnA
0
20
40
60
t(ms)

the presence of 5 μM ANT 2p. Its linearity indicates that the time course of $Z^{+\cdot}$ reduction is exponential and hence that the reaction is proceeding under pseudo-first order conditions. By plotting k_{obs} for the experimental traces in Fig. 18 versus the corresponding ANT 2p concentration we can extract the second-order rate constant which describes the decay of $Z^{+\cdot}$ in the presence of this ADRY reagent (see Figure 20 and Table IV).

We have investigated a number of other ADRY reagents including picrate [140], CCCP and ANT 2a, in their effects on the decay kinetics of $Z^{+\cdot}$. The data for picrate are shown in Fig. 19 where we show Signal II_f kinetic transients for picrate concentrations between 15 μM and 180 μM (Figs. 19a-e). The increase in Signal II_f decay rate is apparent as the halftime of exponential

TABLE IV——Calculated Second Order Rate Constants for the Rereduction of $Z^{+\cdot}$ in the Presence of Various ADRY Reagents.

ADRY Reagent	$k(M^{-1}\ s^{-1})$
ANT 2p	2.7×10^6
CCCP	1.9×10^6
ANT 2a	0.5×10^6
picrate	0.2×10^6

FIGURE 19.

The effect of picrate addition on the decay kinetics of Signal II_f in tris-washed chloroplasts. In (a)-(e) 9 mM $K_3Fe(CN)_6$ and 40 mM $CaCl_2$ were added to a suspension of tris-washed chloroplasts at pH 7.6 and picrate at the indicated concentrations was added. Note that the time axis is compressed by a factor of 2 in (a) compared to the other traces in the figure. In trace (f), the $K_3Fe(CN)_6$ and $CaCl_2$ were omitted from the reaction mixture which was 180 μM in picrate; in (g) 9 mM $K_3Fe(CN)_6$ and 180 μM picrate were present but the $CaCl_2$ was omitted. The instrument time constant was 500 μs; 150 flashes were averaged at a frequency of 0.25 Hz.

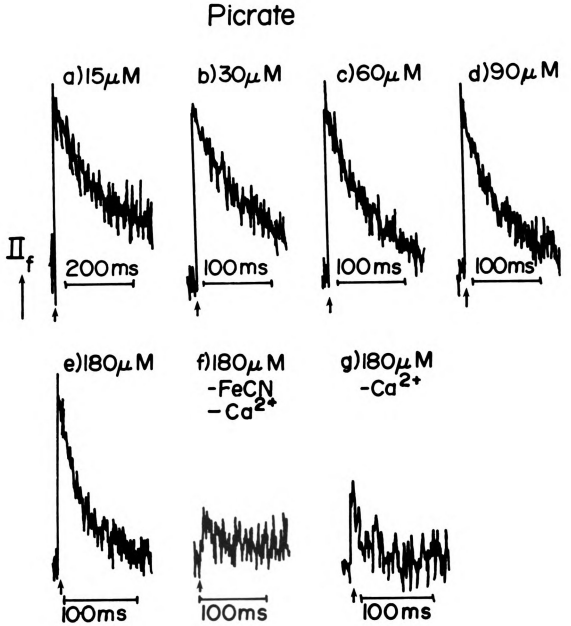
Picrate
a)15μM
b)30μM
c)60μM
d)90μM
Π_f
200ms
100ms
100ms
100ms
e)180μM
f)180μM
-FeCN
$-Ca^{2+}$
g)180μM
$-Ca^{2+}$
100ms
100ms
100ms

FIGURE 20.

Graphical determination of the second-order rate constants for the decay of Signal II_f in the presence of various ADRY reagents. The observed rate constant for the decay of Signal II_f in the presence of the indicated ADRY reagent is plotted against the corresponding ADRY concentration. The slope of the straight lines which results is the second-order rate constant. These are tabulated in Table IV.

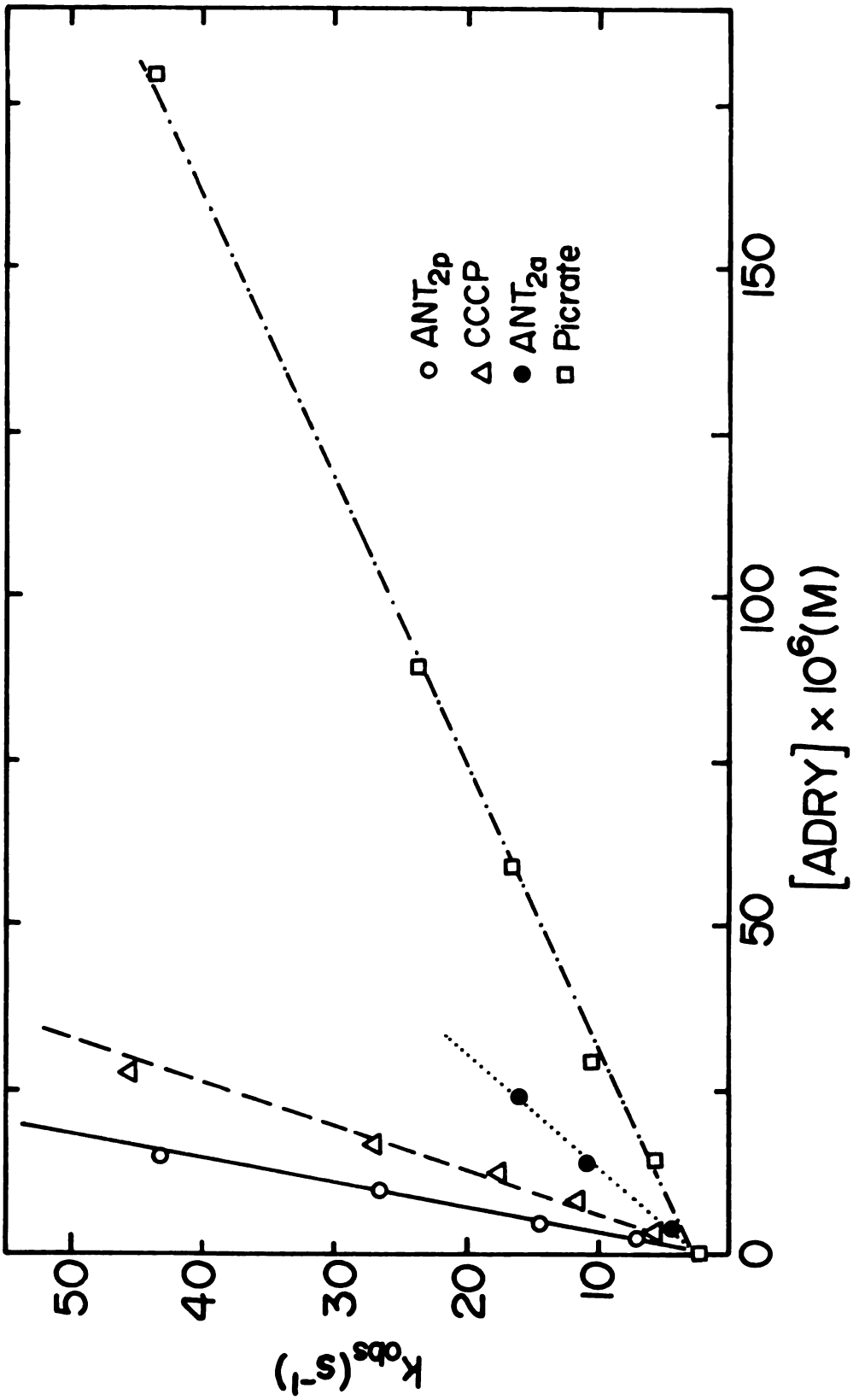
$k_{obs}(s^{-1})$
50
40
30
20
10
0
50
100
150
[ADRY] x 10^6(M)
○ ANT_{2p}
△ CCCP
● ANT_{2a}
□ Picrate

decay of Signal II_f decreases progressively from 126 ms in Fig. 19a to 16 ms in Fig. 19e. The picrate experiments were carried out in the presence of 9 mM ferricyanide and 40 mM Ca^{2+} owing to an apparent inhibiting effect on the reducing side of PSII by this ADRY reagent, similar to that described for other ADRY reagents [141], which leads to an inhibition of Signal II_f formation at high picrate concentrations (Fig. 19f). Addition of ferricyanide alone relieves this inhibition to some extent, (Fig. 19g), but full development of II_f requires both salt addition and ferricyanide. The salt requirement is non-specific and most likely involves a surface charge shielding effect as originally described by Itoh [142].

The kinetic data we have obtained for four ADRY reagents are collected in Fig. 20 where we have plotted the observed first-order rate constants (k_{obs}) for Signal II_f decay versus the corresponding ADRY concentration. That these plots are linear for all four reagents indicates that the relationship, $k_{obs} = k[ADRY]$, holds. From the slopes of the lines we can extract values for the second-order rate constant, k, for each of the ADRY reagents. These values are summarized in Table IV and indicate that the effectiveness of ADRY reagents in stimulating $Z^{+\cdot}$ reduction in tris-washed chloroplasts increases in the order picrate < ANT 2a < CCCP < ANT 2p. A similar ordering of these reagents has been observed

for their effectiveness in deactivating high S states in oxygen-evolving chloroplasts (see below).

The data of Figs. 18-20 indicate that there is a first-order dependence of the decay rate of Signal II_f upon the ADRY concentration. Two different mechanisms can be proposed to account for this dependence. In the first of these, which we will call a direct reduction model, ADRY reagents act in a manner analogous to the H_2Q/ascorbate couple of Fig. 17 and reduce $Z^{+\cdot}$ in a direct bimolecular reaction as follows:

$$Z^{+\cdot} + \text{ADRY(red)} \xrightarrow{k} Z + \text{ADRY(ox)} \qquad (4.2)$$

Here ADRY(red) represents the reduced form of the reagent and ADRY(ox) its oxidation product. In this model, the second-order rate constants for the various ADRY reagents in Table IV correspond to the rate constant, k, in Eq. (4.2) above. To account for the exponential decay of $Z^{+\cdot}$ even at low ADRY concentration we must also postulate a fast regeneration of ADRY(red) from its oxidation product so that during the course of $Z^{+\cdot}$ reduction the concentration of this species remains constant, i.e.,

$$\text{ADRY(ox)} + D_r \xrightarrow{\text{fast}} \text{ADRY(red)} + D_o \qquad (4.3)$$

where D_r and D_o represent the reduced and oxidized form of an electron donor in the chloroplast suspension. Taken together, the mechanism proposed in Eqs. (4.2) and (4.3)

leads to an exponential rate law for $Z^{+\cdot}$ reduction of the following form:

$$- \frac{d[Z^{+\cdot}]}{dt} = k_{obs}\, Z^{+\cdot} \qquad (4.4)$$

where

$$k_{obs} = k[\,ADRY] \qquad (4.5)$$

In the second mechanism, which we will call a catalytic model, ADRY reagents are not redox active in their interaction with $Z^{+\cdot}$ but rather catalyze a faster rereduction by other electron donors in the suspension. The following set of reactions can be proposed for this model:

$$Z^{+\cdot} + ADRY \underset{k_{-1}}{\overset{k_1}{\rightleftharpoons}} Z^{+\cdot}ADRY \qquad \frac{k_1}{k_{-1}} = K \qquad (4.6)$$

$$Z^{+\cdot} + D_r \xrightarrow{k_2} Z + D_o \qquad (4.7)$$

$$Z^{+\cdot}ADRY + D_r \xrightarrow{k_3} Z + ADRY + D_o \qquad (4.8)$$

The equilibrium in (4.6) represents the catalytic interaction between $Z^{+\cdot}$ and ADRY which results in a more reactive conformation, $Z^{+\cdot}ADRY$. This form of $Z^{+\cdot}$ is reduced by the donor D_r more rapidly than is the free form, $Z^{+\cdot}$, i.e., $k_3 > k_2$. For the decay of Signal II_f, which reflects the reduction time course of $Z^{+\cdot}$, we have

$$- \frac{d[Z^{+}\cdot]}{dt} = k_2[Z^{+}\cdot][D_r] + k_3[Z^{+}\cdot ADRY][D_r] \qquad (4.9)$$

To obtain the observed first-order dependence on the ADRY reagent concentration (figs. 18-20) we must postulate that the equilibrium in reaction (4.6) is established quickly, i.e. that k_1, $k_{-1} >> k_2$ or k_3. Then we solve the equilibrium expression in (4.6) and express $[Z^{+}\cdot ADRY]$ in terms of $[Z^{+}\cdot]$ and [ADRY] as

$$[Z^{+}\cdot ADRY] = \frac{k_1}{k_{-1}}[ADRY][Z^{+}\cdot] = K[ADRY][Z^{+}\cdot] \qquad (4.10)$$

and substituting into (4.9) we obtain

$$- \frac{d[Z^{+}\cdot]}{dt} = k_{obs}[Z^{+}\cdot] \qquad (4.11)$$

where

$$k_{obs} = (k_2[D_r] + k_3K[D_r][ADRY]) \qquad (4.12)$$

In the absence of an ADRY only the first term in Eq. (4.12) survives, whereas in the presence of an ADRY reagent the second term dominates. In this formulation the second-order constants for the various ADRY reagents in Table IV correspond to the product $k_3K[D_r]$. The donor D_r may be a soluble component, either endogenous (e.g. ascorbate [93]) or exogenous, or it may be a membrane bound component. In the experiments described below we have attempted to test these two models in order to decide which is more appropriate.

If D_r is a soluble component, then the two models above make different predictions as to the decay of Signal II_f under conditions where both an ADRY reagent and an added donor are present. In the direct reduction model, $Z^{+\cdot}$ may be reduced either by the ADRY or by the added donor and thus we expect the observed rate constant to be simply the sum of the rate constants observed when each of the components is present separately. The catalytic model, on the other hand, predicts that an ADRY reagent should sharply increase the rate of $Z^{+\cdot}$ reduction when present with added donor owing to the increased concentration of the faster reacting $Z^{+\cdot}$ADRY conformation. Thus the catalytic model predicts that there should be a synergistic effect when exogenous donor and an ADRY reagent are added to the same chloroplast suspension. Figure 21 presents the results of two sets of experiments which were carried out to test the contrasting predictions. In Fig. 21a-c CCCP was used in conjunction with the H_2Q/ascorbate donor system. In the presence of 5 μM CCCP alone, the decay halftime was 75 ms (Fig. 21a); with 150 μM H_2Q alone, the decay halftime was 20 ms (Fig. 21b). When the ADRY and the exogenous system were used together, the decay halftime was 21 ms (Fig. 21c). These results indicate that there is essentially no synergism between the two compounds in the rate at which $Z^{+\cdot}$ is reduced. In the second series of experiments (Figs. 21d-h), ANT 2p was used in conjunction with the H_2Q/ascorbate

FIGURE 21.

The effect of an ADRY reagent in conjunction with an electron donor system on the decay kinetics of Signal II_f. In (a)-(c) the ADRY, CCCP, and the donor system, hydroquinone/ascorbate, were used. The CCCP concentration in (a) and in (c) was 5 μM; no CCCP was present in (b). Hydroquinone (150 μM) and sodium ascorbate (2 mM) were added in (b) and (c), but were absent in (a). A time constant of 1 ms was used for traces (a)-(c), each of which is the average of 150 flashes given at a repetition rate of 0.25 Hz. In traces (d)-(h) the ADRY, ANT 2p, and the hydroquinone/ascorbate donor system were used. In (d) and in (f), the hydroquinone concentration was 20 μM and ascorbate was present at 2 mM; the donor system was omitted in the other traces. The ANT 2p concentration in traces (e)-(h) was 10 μM; it was omitted from the chloroplast suspension used in obtaining trace (d). In (g), 12 mM $K_3Fe(CN)_6$ and 40 mM $CaCl_2$ were present and in (h) 40 mM $CaCl_2$ was added. An instrument time constant of 500 μs was used in obtaining the experimental data in (d)-(h). 180 flashes, given at a rate of 0.25 Hz, were averaged to obtain the final decay curves.

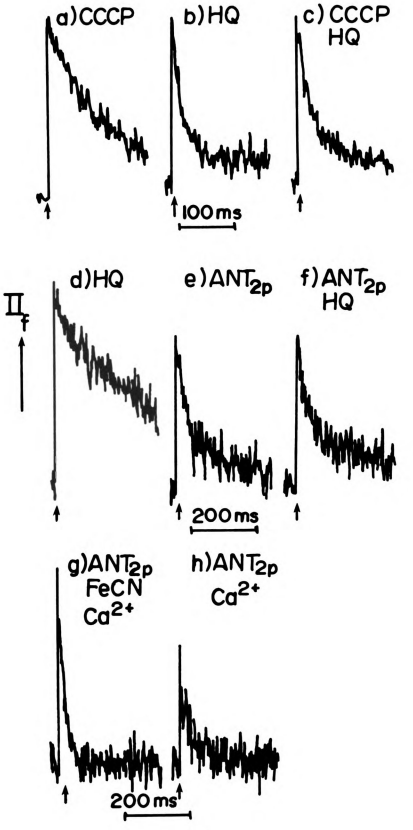
a) CCCP
b) HQ
c) CCCP HQ
100 ms
d) HQ
e) ANT2p
f) ANT2p HQ
Πf
200 ms
g) ANT2p FeCN Ca2+
h) ANT2p Ca2+
200 ms

couple. The conditions were chosen so that Signal II_f decay in the presence of only H_2Q (20 μM, $t_{½}$ = 190 ms, Fig. 21d) was slower than that in the presence of ANT 2p alone (10 μM, $t_{½}$ = 38 ms, Fig. 21e). When the two were used together (Fig. 21f), the observed halftime, 38 ms, again indicates that there is no synergism between an ADRY reagent and a soluble electron donor. Figure 21g is a control carried out to demonstrate that the decrease in Signal II_f amplitude in Figs. 21e and f relative to that in 21d is the result of a slight PSII reducing side inhibition induced by ANT 2p, analogous to that observed above for picrate, which can be relieved by addition of ferricyanide and a divalent cation. Figure 21h shows that the acceleration in $Z^{+\cdot}$ decay rate observed in Fig. 21g comes about because of the presence of the divalent cation, most likely because at the pH used in the experiment ANT 2p is largely in its anion form [135] and subject to surface charge effects as has been shown previously for the ascorbate monoanion [36,102].

The results of Fig. 21 indicate that if the catalytic role envisioned for ADRY reagents in the second model described above is correct, the source of electrons for the reduction of $Z^{+\cdot}$ cannot be a soluble reductant. A second potential reductant pool which may be activated by ADRY addition involves reduced components in the electron transport chain on the acceptor side of PSII [105]. The results of experiments designed to test this

hypothesis are shown in Fig. 22. When DCMU is added to tris-washed chloroplasts, Signal II_f formation and decay are no longer observed under signal-averaged, flashing light conditions [116]. This inhibition can be relieved by addition of ferricyanide and a divalent cation to insure approach of the oxidant to the thylakoid membrane [102,142] (Fig. 22a, decay halftime = 85 ms). Upon addition of the ADRY, ANT 2p, a stimulation in the rate of $Z^{+\cdot}$ reduction is observed (Fig. 22b, $t_{\frac{1}{2}}$ = 15 ms). This result apparently eliminates B, the PQ pool and cytochrome b_{559} as reductants susceptible to ADRY action owing to the facts that DCMU inhibits transfer of electrons to B and PQ and that in the presence of ferricyanide we expect these species as well as b_{559} to remain oxidized in the dark. The oxidizing conditions were apparent in that high concentrations of the P_{700}^{+} free radical were present in these samples. Figure 22c is a control which shows that the rate of $Z^{+\cdot}$ reduction is independent of the presence or absence of DCMU. Figure 22d shows that if the divalent cation and ferricyanide are omitted, no Signal II_f formation in the presence of DCMU is observed. This experiment indicates that ADRY reagents are unable to catalyze a direct $Z^{+\cdot}Q^{-}$ back recombination which agrees with a similar conclusion obtained earlier by Renger et al. [136]. We conclude from the experiments of Fig. 22 that ADRY reagents can exert their accelerating

FIGURE 22.

The effect which conditions on the acceptor side of Photosystem II exert on the decay kinetics of Signal II_f in the presence of an ADRY reagent. The decay of Signal II_f was recorded in tris-washed chloroplasts in which the final concentration of added reactants was as follows: (a) 100 μM DCMU, 12 mM $K_3Fe(CN)_6$, 40 mM $CaCl_2$; (b) 100 μM DCMU, 12 mM $K_3Fe(CN)_6$, 40 mM $CaCl_2$, 10 μM ANT 2p; (c) 12 mM $K_3Fe(CN)_6$, 40 mM $CaCl_2$, 10 μM ANT 2p; (d) 100 μM DCMU, 10 μM ANT 2p. For each trace, 180 flashes were averaged at a flash repetition rate of 0.25 Hz. The instrument time constant was 1 ms.

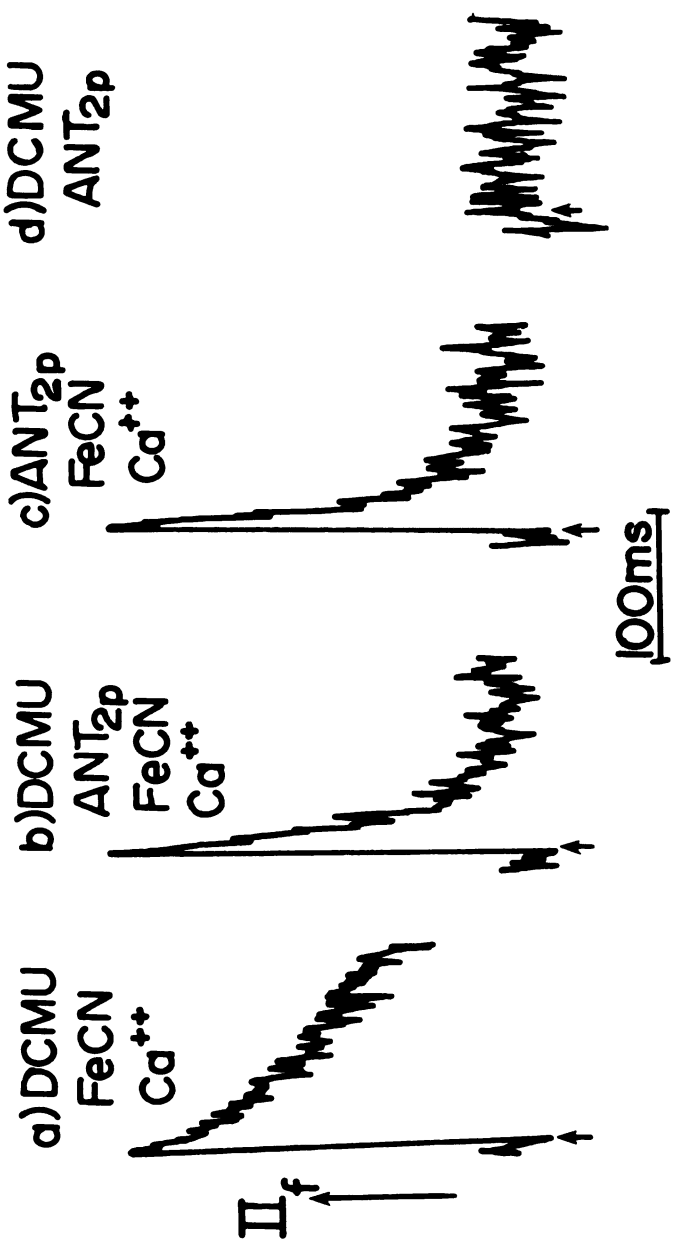
a) DCMU
FeCN
Ca++
b) DCMU
ANT2p
FeCN
Ca++
c) ANT2p
FeCN
Ca++
d) DCMU
ANT2p
100ms

effect on $Z^{+\cdot}$ decay independent of the redox state of the acceptor side components and thus the primary model of ADRY action does not appear to involve catalysis of cyclic flow to $Z^{+\cdot}$ from these compounds. Taken together, the results of Figs. 18-22 provide no evidence for the catalytic model of ADRY action, rather they indicate that these reagents are likely to reduce $Z^{+\cdot}$ in tris-washed chloroplasts in a bimolecular reaction as outlined in the direct reduction model.

Renger has pointed out that effective ADRY reagents possess an acidic proton which, upon dissociation, generates a lipophilic anion. Moreover, the anion form appears to be more effective in stimulating ADRY action than is the neutral form [143]. The results of Fig. 23 show that similar behavior is exhibited by ANT 2a ($pK_a = 7.0$, [134]) during its reaction with $Z^{+\cdot}$. At pH 5.8, where this species is over 90% in its protonated form, the decay halftime of $Z^{+\cdot}$ is 53 ms (Fig. 23a); at pH 8.2, where 90% is in the anion form, the decay halftime of Signal II_f decreases to 33 ms (Fig. 23b). Assuming pseudo-first order behavior and the pK_a value above, one calculates that the anion form of ANT 2a is 1.7 times more effective than the neutral species in $Z^{+\cdot}$ reduction.

D. Discussion

In addition to their uncoupling activity [144] and inhibitory action on the reducing side of PSII [141], ADRY

FIGURE 23.

The effect of pH on the decay of Signal II_f in tris-washed chloroplasts in the presence of ANT 2a. In (a) tris-washed chloroplasts were resuspended in a buffer which contained 0.4 M sucrose, 0.01 M NaCl and 0.05 M MES. The pH was 5.8 and 15 μM ANT 2a was present. In (b) a buffer consisting of 0.4 M sucrose, 0.01 M NaCl and 0.05 M HEPES at pH 8.2 was used. The ANT 2a concentration was 15 μM. Each trace is the average of 180 flashes, 0.25 Hz repetition rate and 1 ms time constant.

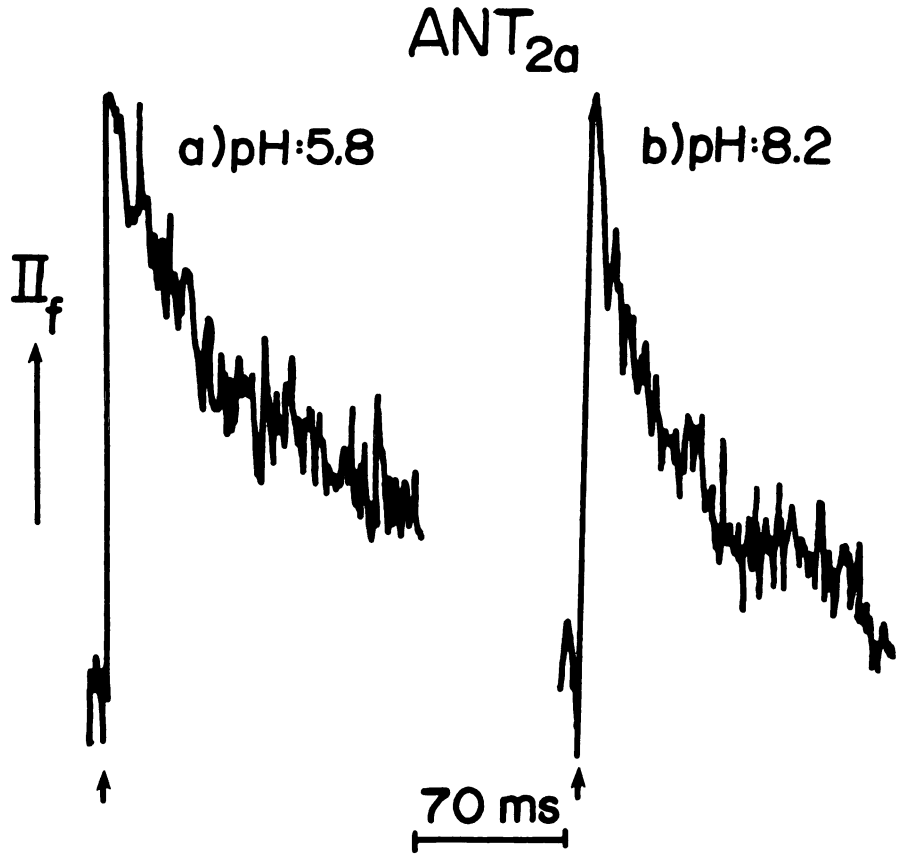
ANT2a
a)pH:5.8
b)pH:8.2
If
70 ms

reagents destabilize oxidizing equivalents generated by P_{680}. States and species which are susceptible to this destabilization effect include the OEC intermediates S_2 and S_3 [105,136], the free radical species Signal II_s [145-147] and the electron transport component $Z^{+\cdot}$ [139, this work]. Moreover, ADRY reagents alter significantly the behavior of two other species which appear to be linked to PSII function, cytochrome b_{559} and carotenoids [77,148-151].

In the work reported here, we have shown that the rate of $Z^{+\cdot}$ decay shows a first-order dependence on the concentration of ADRY reagent and have listed in Table IV the second-order rate constants for this reaction for four ADRY reagents: ANT 2p, CCCP, ANT 2a and picrate. These data show that the efficiency of these four species in exerting the destabilization effect varies by a factor of about 14 and decreases in the order ANT 2p > CCCP > ANT 2a > picrate. This ordering and the magnitude of the second order rate constants provide a basis from which the relationship between the effect we observed for ADRY reagents in their interaction with $Z^{+\cdot}$ and that observed for their destabilization of S_2 and S_3 can be explored. Renger, Vater and their coworkers have reported S_2 and S_3 decay curves for a variety of ADRY reagents at various concentrations [105,135-137,139,140,143]. In general the decay of the OEC intermediates in the presence of an ADRY follows an exponential time course (although there are

exceptions [140]) and the rate constant for this process increases as the ADRY concentration is increased. This behavior is qualitatively similar to that which we observe for $Z^{+\cdot}$ decay in the presence of an ADRY and implies that S_2 and S_3 exhibit pseudo-first-order decay behavior upon ADRY addition. To put this observation in more quantitative terms, we have tabulated data on the ADRY-induced destabilization of OEC intermediates which have been reported over the past decade (Table V). The halftimes ($t_{\frac{1}{2}}$) were taken from the data reported and converted to pseudo-first-order rate constants by using the relationship, $k_{obs} = \ln 2/t_{\frac{1}{2}}$. The apparent second-order constants, k, were calculated as $k_{obs}/[ADRY]$. The results show that there is remarkably consistent behavior observed for the various species and that the second-order formulation appears reasonable. For ANT 2p, for example, the second-order rate constant varies by no more than a factor of two even when the concentration is varied over an order of magnitude. Moreover, inspection of the ANT 2s and ANT 2a data indicates that this factor of two may be more a function of experimental error (e.g. two separate measurements at 1×10^{-6} M ANT 2a shows a twofold variation), than a real concentration dependence in the second-order rate constants. Focusing on the data in Table V for the four ADRY reagents we have studied in their interaction with $Z^{+\cdot}$, we see that the efficiency of these species declines in the order

TABLE V——Calculated Second Order Rate Constants for Various ADRY Reagents in the Deactivation of Higher Formal Oxidation States of the Oxygen-Evolving Complex.

Reagent	Concentration (M)	$t_{½}$ (s)	k_{obs} (s^{-1})	k (M^{-1} s^{-1})	Ref.
ANT 2p	1×10^{-7}	0.47	1.5	1.5×10^{7}	105
ANT 2p	3×10^{-7}	0.33	2.1	7×10^{6}	105
ANT 2p	3×10^{-7}	0.26	2.7	9×10^{6}	105
ANT 2p	4×10^{-7}	0.21	3.3	8.4×10^{6}	136
ANT 2p	5×10^{-7}	0.18	3.9	7.7×10^{6}	105
ANT 2p	1×10^{-6}	0.10	7.0	7×10^{6}	143
ANT 2p*	1×10^{-6}	1.9	0.4	0.36×10^{6}	136
				average = 9×10^{6}	
ANT 2s	2×10^{-7}	0.39	1.8	9×10^{6}	137
ANT 2s	4×10^{-7}	0.12	5.7	1.4×10^{7}	137
ANT 2s	4×10^{-7}	0.20	3.3	8.4×10^{6}	135
				average = 10×10^{6}	

Table V Continues.

Table V Continued.

Reagent	Concentration (M)	$t_{½}$ (s)	k_{obs} (s^{-1})	k (M^{-1} s^{-1})	Ref.
ANT 2a	4×10^{-7}	1.2	0.6	1.5×10^{6}	135
ANT 2a	10^{-6}	0.43	1.6	1.6×10^{6}	135
ANT 2a	10^{-6}	1.0	0.7	0.7×10^{6}	143
ANT 2a	2×10^{-6}	0.32	2.2	1.1×10^{6}	135
				average = 1.2×10^{6}	
FCCP	10^{-6}	0.11	6.3	6.3×10^{6}	137
CCCP	10^{-5}	0.09	7.7	7.7×10^{5}	137
picrate	10^{-6}	1.25	0.55	5.5×10^{5}	140
2,4 dinitrophenol	10^{-4}	2	0.35	3.5×10^{3}	140

*Carried out at a bare platinum electrode where its redox activity may have led to spurious results [105,136]; not included in determining the average value of the second order rate constant.

ANT 2p > ANT 2a > CCCP > picrate. The relative inefficiency of CCCP with respect to ANT 2a in Table V may be an example of experimental variation in that in ref. 135, Renger indicates the reverse, i.e., that CCCP is more efficient than ANT 2a. In addition, the ADRY efficiencies, as judged by the value of the second-order rate constants, vary by a factor of about 16 as one goes through the series of four. Finally, the magnitude of the rate constants for a given ADRY reagent in Tables IV and V are within a factor of four (e.g., Table IV: $k(\text{ANT 2p}) = 2.7 \times 10^6\ \underline{M}^{-1}\ s^{-1}$; Table V: $k(\text{ANT 2p}) = 9 \times 10^6\ \underline{M}^{-1}\ s^{-1}$).

These observations, in conjunction with the data in Fig. 23 indicating that the anion is the more effective form, suggest that the mechanism by which ADRY reagents destabilize S_2 and S_3 in oxygen-evolving chloroplasts is the same as that which we observe for the ADRY-induced rereduction of $Z^{+\cdot}$ in tris-washed chloroplasts. Note, however, that we do not intend to convey the idea that ADRY reagents destabilize S_2 and S_3 by intercepting oxidizing equivalents at $Z^{+\cdot}$ in water-splitting chloroplasts. The data of Table V indicate that S_2 and S_3 destabilization is observed in the hundreds of ms time range under the ADRY concentration conditions usually employed, whereas it has been shown [67,125] that $Z^{+\cdot}$ transfers its oxidizing equivalent into the OEC in the sub-ms range in O_2 evolving chloroplasts. Thus in

uninhibited chloroplasts the site of ADRY action is the OEC itself, whereas in tris-washed chloroplasts the much longer lifetime of $Z^{+\cdot}$ makes it susceptible to ADRY attack.

Within the context of the data of Tables IV and V, it is worthwhile to consider briefly the effect of ADRY reagents on the decay of Signal II_s. Lozier and Butler [145] originally demonstrated that a number of reagents, including CCCP, destabilized the free radical species which gives rise to this EPR signal so that its decay halftime decreased from hours in the absence of CCCP to seconds in the presence of this reagent. They also showed that subsequent illumination led to Signal II_s regeneration [145]. Subsequently, Babcock and Sauer confirmed these results and showed that the Signal II_s precursor, which they designated as F, was oxidized to its free radical form by a redox interaction with the OEC intermediate states S_2 and S_3 [93,146]. They also carried out a detailed study of the CCCP concentration dependence of the Signal II_s decay rate and presented data on the decay halftime of Signal II_s which showed that increasing CCCP levels led to increased destabilization of the radical (see Fig. 3 in ref. 146). From the decay halftime data they presented, we have calculated observed rate constants and have plotted k_{obs} versus the CCCP concentration in Fig. 24. The four points fall on a reasonably good straight line and from the slope we obtain an apparent second order rate constant for the

FIGURE 24.

Graphical determination of the second-order rate constant for the decay of Signal II_s in oxygen-evolving chloroplasts in the presence of CCCP. The data from Fig. 3 in ref. 146 were used to obtain the pseudo-first order rate constant, k_{obs}, for the decay of Signal II_s at various CCCP concentrations. This rate constant is plotted against the corresponding CCCP concentration in order to determine the second-order rate constant as the slope of the straight line which results.

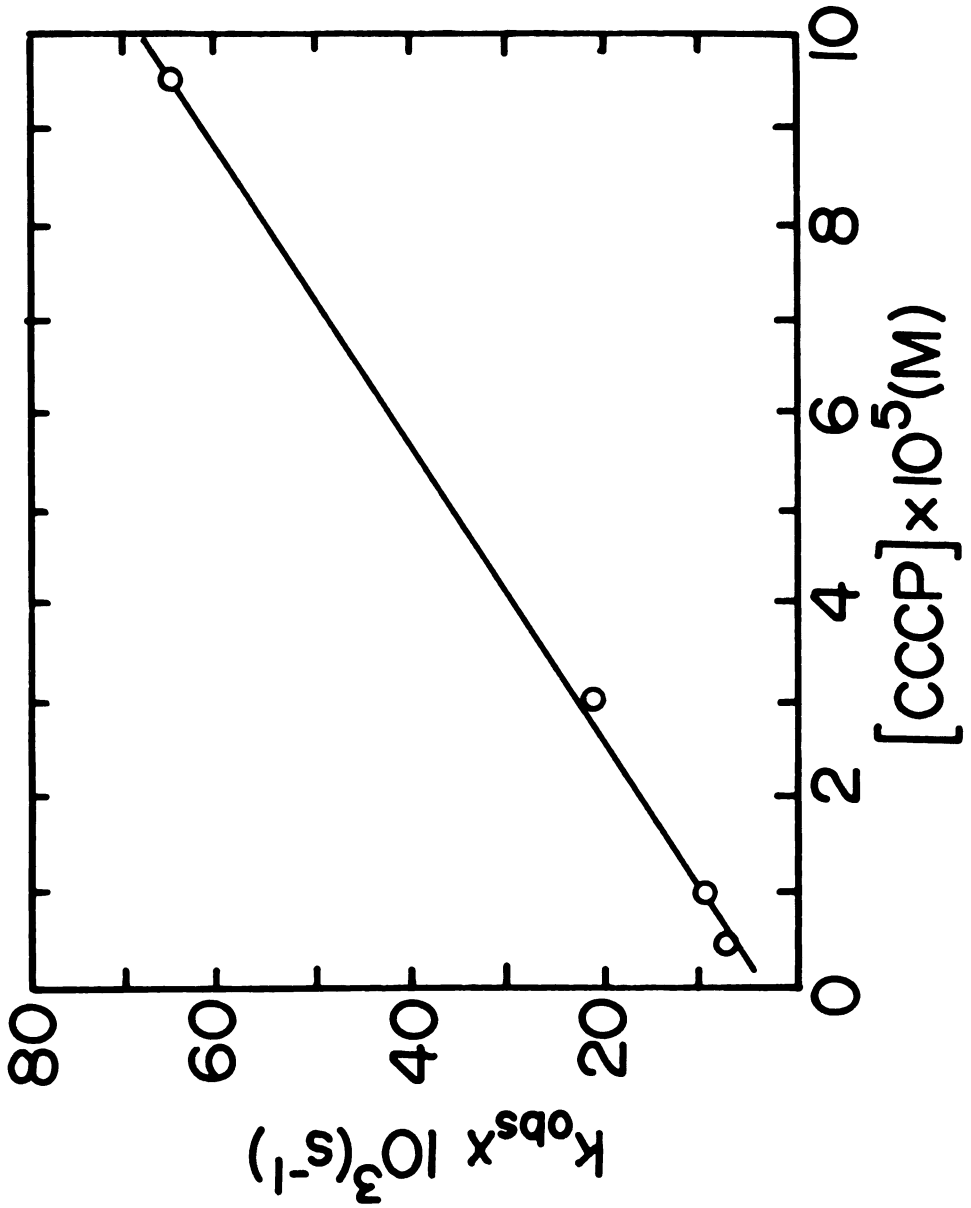
80
60
40
20
0
2
4
6
8
10
$k_{obs} \times 10^3 (s^{-1})$
$[CCCP] \times 10^5 (M)$

CCCP-induced destabilization of Signal II_s of 6.5×10^2 $\underline{M}^{-1}$ s^{-1}. This value is approximately three orders of magnitude smaller than the second order rate constant for the CCCP induced destabilization of $Z^{+\cdot}$ (Table IV) or for the destabilization of S_2 and S_3 (Table V). This observation indicates that, although II_s is mechanistically similar to $Z^{+\cdot}$ and to S_2 and S_3 in its susceptibility to the action of ADRY reagents, it is much more sluggish in terms of its response time. Nonetheless, these results show that the action of ADRY reagents appears to be general in that oxidized species generated by the light reaction of PSII are susceptible to destabilization by ADRY reagents and that the decay process which results shows a first order dependence on ADRY concentration.

The data we have presented above can be used to provide several insights into the mechanism by which ADRY reagents act on oxidizing equivalents generated by PSII. Previous considerations of this problem [105,135-140] had focused on essentially two alternative possibilities as follows: (1) ADRY reagents are redox active cofactors and act by reducing the stored oxidizing equivalents directly; (2) ADRY reagents act in a catalytic manner and, by inducing conformational or configurational changes in PSII, facilitate a cyclic reaction which accelerates the decay of the stored oxidizing equivalents. While several ADRY reagents are clearly redox active (e.g.

tetraphenylboron [77,152] and dichlorophenol-indophenol [140]), the catalytic mechanism has generally been preferred on the basis of stoichiometric arguments over the direct reduction mechanism [e.g. 137]. Consistent with the catalytic mechanism is the well-known observation that cytochrome b_{559} is photooxidized, apparently by PSII, in the presence of ADRY reagents [148,151] and recent discussion of the ADRY catalytic mechanism has focused on an involvement of b_{559} in the process [77,105,139].

In the experiments presented above we have attempted to explore these two possibilities. The first-order dependence on ADRY reagent concentration which is observed for $Z^{+\cdot}$ decay in tris-washed chloroplasts (Fig. 20) appears to be characteristic of the general mechanism by which these species destabilize PSII oxidizing equivalents (see Table V and Fig. 24) and leads one to the alternative kinetic models, direct reduction (Equations 4.2-4.5) <u>versus</u> catalytic (Equations 4.6-4.12) presented and discussed briefly in the Results section. In developing experimental tests aimed at identifying the source of electrons for the catalytic mechanism we have been able to eliminate an ADRY-catalyzed increase in the efficiency with which soluble endogenous or exogenous donors reduce $Z^{+\cdot}$ (Fig. 21). Likewise, the data of Fig. 22 argue against the possibility that the source of reducing equivalents mobilized by ADRY reagents is either on the reducing side of PSII or originates in

cytochrome b_{559}. In fact, the decay of $Z^{+\cdot}$ in the presence of an ADRY reagent is remarkably insensitive to any perturbation supplied to the acceptor side of the photoreaction. For example, if one compares the decay of $Z^{+\cdot}$ in the presence of 10 μM ANT 2p under conditions where electron transfer is blocked at Q (Fig. 22b) to the analogous experiment in which there is no acceptor side inhibition (Figs. 22c,21g), one finds that the flash-induced $Z^{+\cdot}$ amplitude and decay time (14 ms) remain constant. Similarly, if one carries out the experiment in the absence (Fig. 21b) or presence of (Fig. 22c,21g) ferricyanide, it is again apparent that the decay of Signal II_f in the presence of 10 μM ANT 2p remains constant at 14 ms. The amplitude difference in these experiments is the result of the slight acceptor side inhibition of PSII observed by us and others [14] at relatively high ADRY concentrations. Finally, if one takes into account the salt effect described below, the data of Figs. 21e,f and g indicate that the reduction of $Z^{+\cdot}$ by ANT 2p proceeds independent of the redox state of cytochrome b_{559}. These observations eliminate both this species and PSII acceptor side components as necessary sources of reducing equivalents in an ADRY-catalyzed $Z^{+\cdot}$ rereduction reaction.

The only significant means by which we have been able to influence the decay rate of $Z^{+\cdot}$ at a given ADRY

concentration is through salt addition. For example, in Fig. 2le, $Z^{+\cdot}$ decays with a 38 ms halftime in the absence of salt which decreases to the 14 ms lifetime of Fig. 2lh when 40 mM Ca^{2+} is added. This salt is independent of the identity of the divalent cation and is the sort of screening effect one expects for an anion, in this case the deprotonated form of ANT 2p, interacting with a reaction partner associated with a negatively charged membrane [142]. It has been shown recently that the inner membrane surface in the vicinity of PSII is negatively charged and that this surface charge does influence the reduction kinetics of $Z^{+\cdot}$ by anionic species [102].

The results discussed above argue against the catalytic model of ADRY action, but are clearly consistent with the predictions of the direct reduction mechanism. The latter model, however, requires a substrate level reductant (D_r in Equation 4.3) in order to regenerate the reduced form of the ADRY reagent from its oxidation product. That this requirement is significant is evident from the sustained ADRY effect observed even at low reagent concentration which was originally noted and commented on by Renger [137] and confirmed in the experiments reported here. An inspection of the literature indicates that this reductant pool is likely to consist of membrane components, such as carotenoids, chlorophyll and protein, which are susceptible to non-specific

oxidation by ADRY(ox). This possibility is indicated by the results of Yamashita et al. [149] and of Itoh et al. [150] which showed that addition of the ADRY, CCCP, to either oxygen-evolving or tris-washed chloroplasts led to the photobleaching of both carotenoids and chlorophylls. Similarly, Homan has noted photodestruction of PSII in the presence of the ADRY reagents, CCCP or tetraphenylboron, and has suggested that these species funnel oxidizing equivalents generated within the photosystem into destructive side reactions [152,153]. Finally, it is well established that if reduced cytochrome b_{559} is available, it is oxidized in the presence of an ADRY reagent and light by a Photosystem II-driven reaction [77,148,151]. Taken together, these results suggest that a fairly non-specific oxidation reaction occurs upon illumination of ADRY-treated chloroplasts and that the direct reduction model outlined above may be rewritten as the following two step sequence:

$$Z^{+}_{\bullet} + \text{ADRY} \xrightarrow{k} Z + \text{ADRY(ox)} \qquad (4.13)$$

$$\text{ADRY(ox)} + \begin{cases} \text{carotenoid} \\ \text{chlorophyll} \\ b_{559}^{2+} \\ \text{soluble reductants} \end{cases} \xrightarrow{\text{fast}} \text{ADRY(red)} + \begin{cases} \text{carotenoid}^{+} \\ \text{chlorophyll}^{+} \\ b_{559}^{3+} \\ \text{soluble oxidation products} \end{cases} \qquad (4.14)$$

Although we cannot provide definitive evidence to eliminate a catalytic mechanism which invokes an ADRY-

mediated direct oxidation of carotenoids and chlorophylls by $Z^{+\cdot}$, we favor the mechanism outlined in Equations 4.13 and 4.14 for several reasons. First, it accounts for the exponential decay of Signal II_f we observed in the presence of low concentrations of an ADRY reagent under an extended flash regime (typically 150-200 flashes) without postulating a specialized structural arrangement between $Z^{+\cdot}$ and carotenoid, chlorophyll or b_{559}. Second, this model accounts for the oxidation of b_{559} in the presence of an ADRY reagent if the cytochrome is in its reduced state prior to initiation of a flash train. However, it does not make the oxidation of this species mandatory for ADRY action, consistent with our data described above and with experimental results which indicate that in the presence of FCCP, b_{559} oxidation is non-stoichiometric [A.R. Crofts, personal communication]. Third, it explains the inhibition of carotenoid bleaching which is observed if an exogenous reductant is added to CCCP treated chloroplasts [149,150]. Fourth, it accommodates those ADRY reagents which are known to be redox active (e.g. tetraphenylboron, dichlorophenolindophenol). Finally, the model is supported by Renger and Reuter's observation of redox activity for ANT 2s at a platinum electrode [105] and by our own observation of redox activity for several ADRY reagents (picrate, ANT 2p, ANT 2a, CCCP) by cyclic voltammetry (Ghanotakis, D.F. and Babcock, G.T. unpublished). Picrate has also been studied elsewhere and its electrode

reactions appear to be complex [154]; we are in the process of exploring the electrochemical behavior of various ADRY reagents in more detail.

The scheme presented in Fig. 25 summarizes the model developed above for the behavior of ADRY reagents on the oxidizing side of PSII. The strongly oxidizing species generated by P_{680}^{+} are susceptible to reduction by an ADRY reagent in a manner which depends on the ADRY concentration, its second order rate constant and the lifetime of the specific intermediate. In O_2-evolving chloroplasts, ADRYs act primarily on the states S_2 and S_3 and, in a much slower reaction, on the species $F^{+\cdot}$ which gives rise to Signal II_s. In chloroplasts inhibited at the OEC, the lifetime of $Z^{+\cdot}$ is extended significantly and it becomes a site of ADRY action at fairly low ADRY concentrations. The interaction between the ADRY reagent and the PSII oxidant generates the oxidized form of the ADRY reagent, itself a good oxidant which is able to oxidize the indicated chloroplast components in a fairly non-specific reaction. The net result of these reactions is the regeneration of the ADRY reagent, the oxidation of a variety of endogenous components and the accelerated decay of stored oxidizing equivalents in Photosystem II.

FIGURE 25.

A model for the role of ADRY reagents in destabilizing oxidizing equivalents generated in PSII. The solid arrows denote proposed reactions in oxygen-evolving chloroplasts, dashed arrows indicate proposed reactions in tris-washed chloroplasts and the dotted lines indicate inhibitor action. See text for other details.

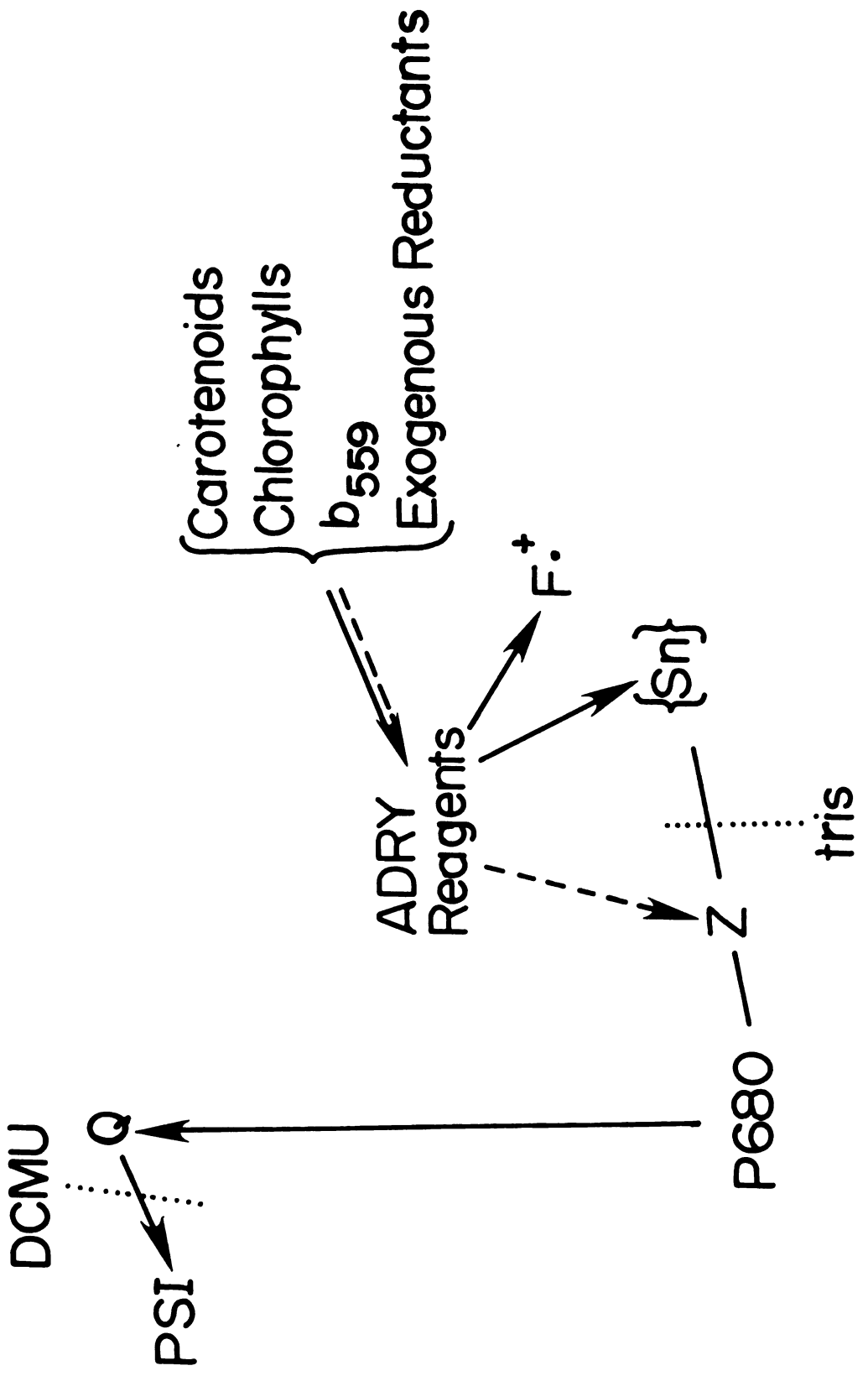
Carotenoids
Chlorophylls
b_{559}
Exogenous Reductants
$F^+\cdot$
ADRY
Reagents
{Sn}
tris
Z
P680
Q
DCMU
PSI

CHAPTER V.

HYDROXYLAMINE AS AN INHIBITOR BETWEEN Z AND P_{680} IN PHOTOSYSTEM II.

A. Introduction

Exposure of isolated thylakoid membranes to NH_2OH is known to be a mild treatment for inactivation of the oxygen evolving reaction system [32-35]. Cheniae and Martin [33] reported that the mechanism of NH_2OH inactivation of the oxygen evolving complex (OEC) is different from that of tris-inactivation: inhibition by tris is accelerated by low light intensities [30,31], whereas NH_2OH produces a rapid inactivation at low concentrations in the dark. In the same work [33], the authors report that NH_2OH-inhibition occurs by two different mechanisms. One is the extraction of Mn from the photosynthetic membrane while the other mechanism, which has an immediate but reversible effect, was not localized. Sharp and Yocum [155], using NMR relaxation techniques, proposed that higher S-states are immune to attack by NH_2OH and that NH_2OH-induced Mn extraction occurs only from the lower S-states. Den Haan et al. [156] studied the fluorescence kinetics in *Chlorella Pyrenoidosa* in the

presence of NH_2OH and suggested that an inhibition site could be localized between Z, the physiological donor, and the oxidized reaction center pigment, P_{680}. This inhibition was reversed during illumination of a washed sample. These authors also reported that for a series of high frequency flashes in the presence of NH_2OH, P_{680}^+ was rereduced by a back reaction with the reduced form of the primary acceptor, Q_A^-.

In this work we have used EPR spectroscopy to monitor the formation of Signal II_f and P_{680}^+ directly in order to localize the immediate NH_2OH inhibition observed in the past [33,156]. Since the EPR signal which arises from P_{680}^+ is reported to have the same shape and g-value as that which arises from P_{700}^+, we used PSII preparations free of Photosystem I in addition to unfractionated thylakoids in these experiments. In agreement with [156], we find that NH_2OH exerts an immediate and reversible inhibition which results in a blocking of electron flow from Z to P_{680}.

B. Materials and Methods

Intact thylakoid membranes were prepared as described in Chapter II. Subchloroplast membranes, free of Photosystem I and capable of oxygen evolution, were prepared as in [88] except that the initial Triton extraction and subsequent washings were carried out at pH 6.0. We have found that by using lower pH values during the isolation,

PSII particles with higher O_2 rates result. The buffer system used contained 0.4 M sucrose, 0.01 M NaCl and either 0.05 M HEPES for pH 7.6 or 0.05 MES for pH 6.0. Chlorophyll concentrations were determined as described in [94]. EPR spectroscopy was carried out on a Bruker ER-200D spectrometer operated at X-band and interfaced to a Nicolet 1180 computer. Instrument modifications as well as the xenon flash lamp circuitry and the protocol followed in signal-averaged, flashing light kinetic experiments are described in [99].

C. Results

When O_2 evolution is inhibited at the oxygen evolving complex, the lifetime of the intermediate electron carrier, Z^+, is extended into the hundreds of ms time range and becomes detectable as EPR Signal II_f. Yocum et al. [19] reported that incubation of chloroplasts in the dark with NH_2OH followed by washing of the system with buffer resulted in complete inhibition of O_2 evolution and conversion of Signal II_{vf} to Signal II_f. When we incubated chloroplasts with NH_2OH in the dark and then, without removing the inhibitor, transferred them to the EPR spectrometer we found that neither Signal II_{vf} nor Signal II_f was present. After washing the system twice with buffer Signal II_f could be observed. We repeated the above experiment with tris-treated chloroplasts and noted the same behavior, i.e., the presence of NH_2OH

in the system inhibited Signal II_f formation, whereas its removal allowed full development of Signal II_f. PSII subchloroplast preparations showed analogous behavior in the presence of hydroxylamine except that lower concentrations of NH_2OH were required. Indeed when we measured the O_2 rates of PSII preparations immediately following addition of NH_2OH (Fig. 26), we noticed that low concentrations of NH_2OH were very effective in inhibiting O_2 evolution. Intact chloroplasts required higher concentrations of NH_2OH in order to obtain the same extent of inhibition. For example, under the conditions of Fig. 26, 50% inhibition of O_2 evolution in PSII preparations occurs at ~1 m$\underline{M}$ NH_2OH; in chloroplasts under these conditions ~5 m$\underline{M}$ NH_2OH was required for 50% inhibition.

Reflecting the behavior of O_2 evolution in response to NH_2OH addition, Signal II_{vf} of untreated PSII preparations and Signal II_f of tris-treated preparations disappears and a new signal, which rises within the 50 μs response of our instrument and had a decay halftime of less than 200 μs, is present (Fig. 27). Removal of NH_2OH from tris-treated PSII preparations restores the system to its initial state (full Signal II_f, no new signal, data not shown).

The shape of the new signal, as determined by signal-averaged experiments at different field values, is shown in Fig. 28. Its peak-to-peak width is 7-8 Gauss and its g-value is 2.002; these values are in agreement

FIGURE 26.

Effect of NH_2OH concentration on the O_2 rate of PSII preparations at pH 6.0. PSII preparations (10 µg Chl/ml) were suspended in the polarograph vessel with the exogenous acceptors, $Fe(CN)_6^{3-}$ (3.5 m<u>M</u>) and 2,5-dichloro-p-benzoquinone (250 µM). Addition of NH_2OH was followed by immediate illumination to determine the rate of O_2 evolution.

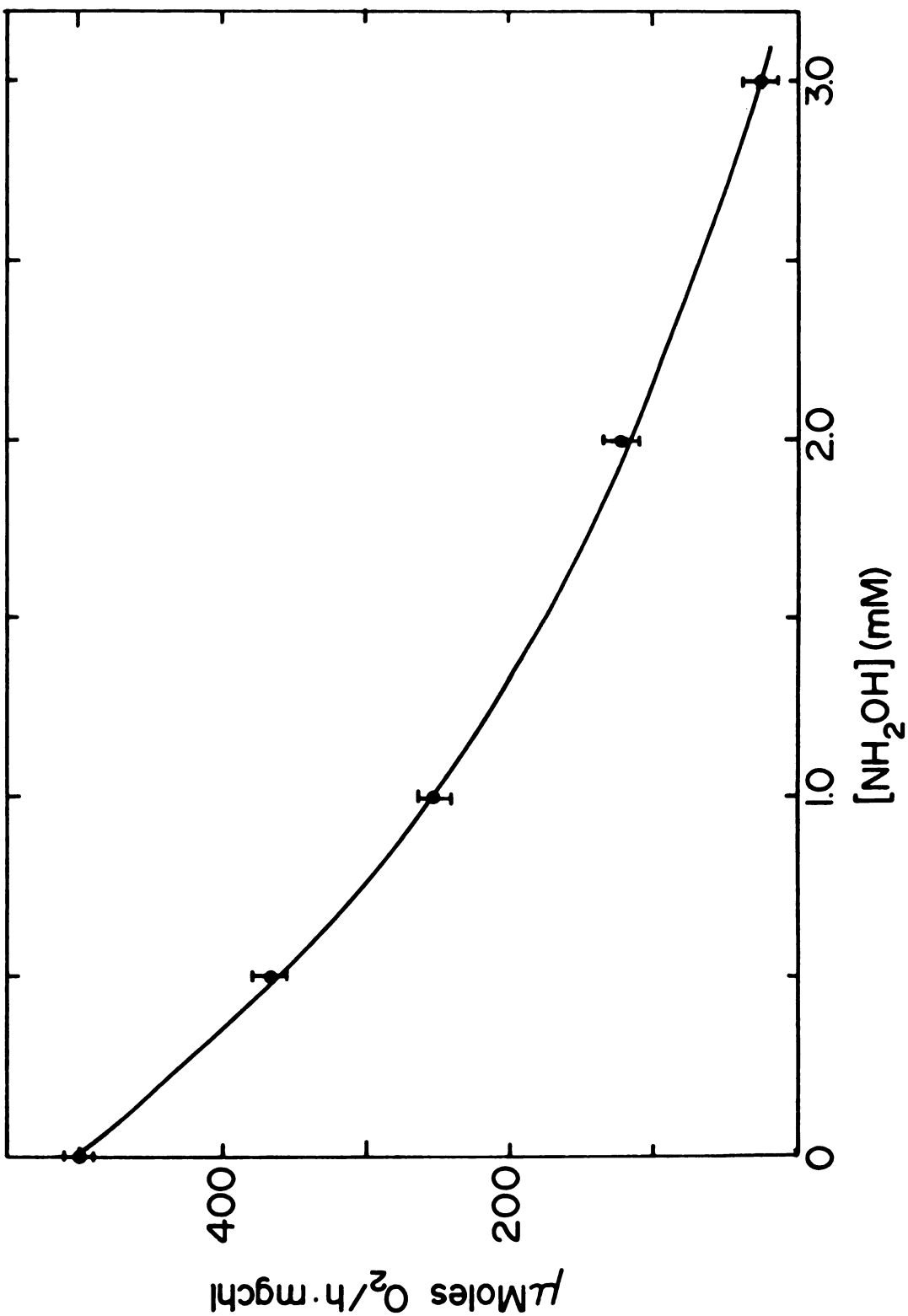
μMoles O2/h.mgchl
400
200
0
1.0
2.0
3.0
[NH2OH] (mM)

FIGURE 27.

Kinetic transient of the P_{680}^{+} EPR signal. 1 m$\underline{M}$ $Fe(CN)_6^{3-}$, 1 m$\underline{M}$ $Fe(CN)_6^{4-}$ and 2 m$\underline{M}$ NH_2OH were added to a suspension of PSII particles at pH 6.0. The instrument time constant was 50 μs; 150 flashes were averaged at a frequency of 0.1 Hz.

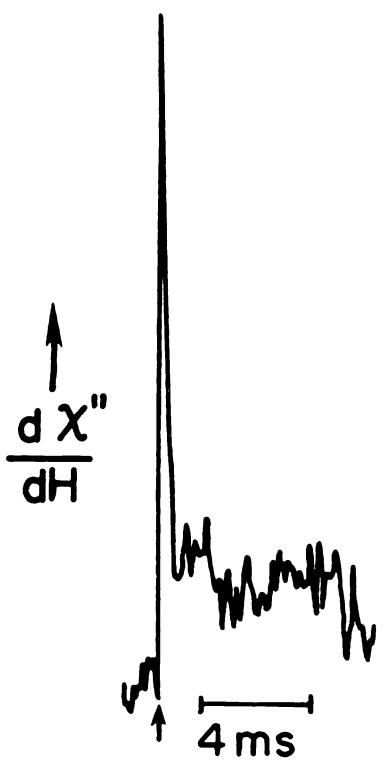
d χ"
dH
4 ms

FIGURE 28.

Shape of Signal P_{680}^{+} (solid line) in PSII preparations obtained by kinetic experiments at the indicated field values. The shape of Signal II_s is also shown (dotted line). Insert: Saturation properties of Signal P_{680}^{+} in PSII preparations at pH 6.0. Each point represents the amplitude of the P_{680}^{+} EPR signal at the indicated microwave power. The conditions were the same as those in Fig. 27.

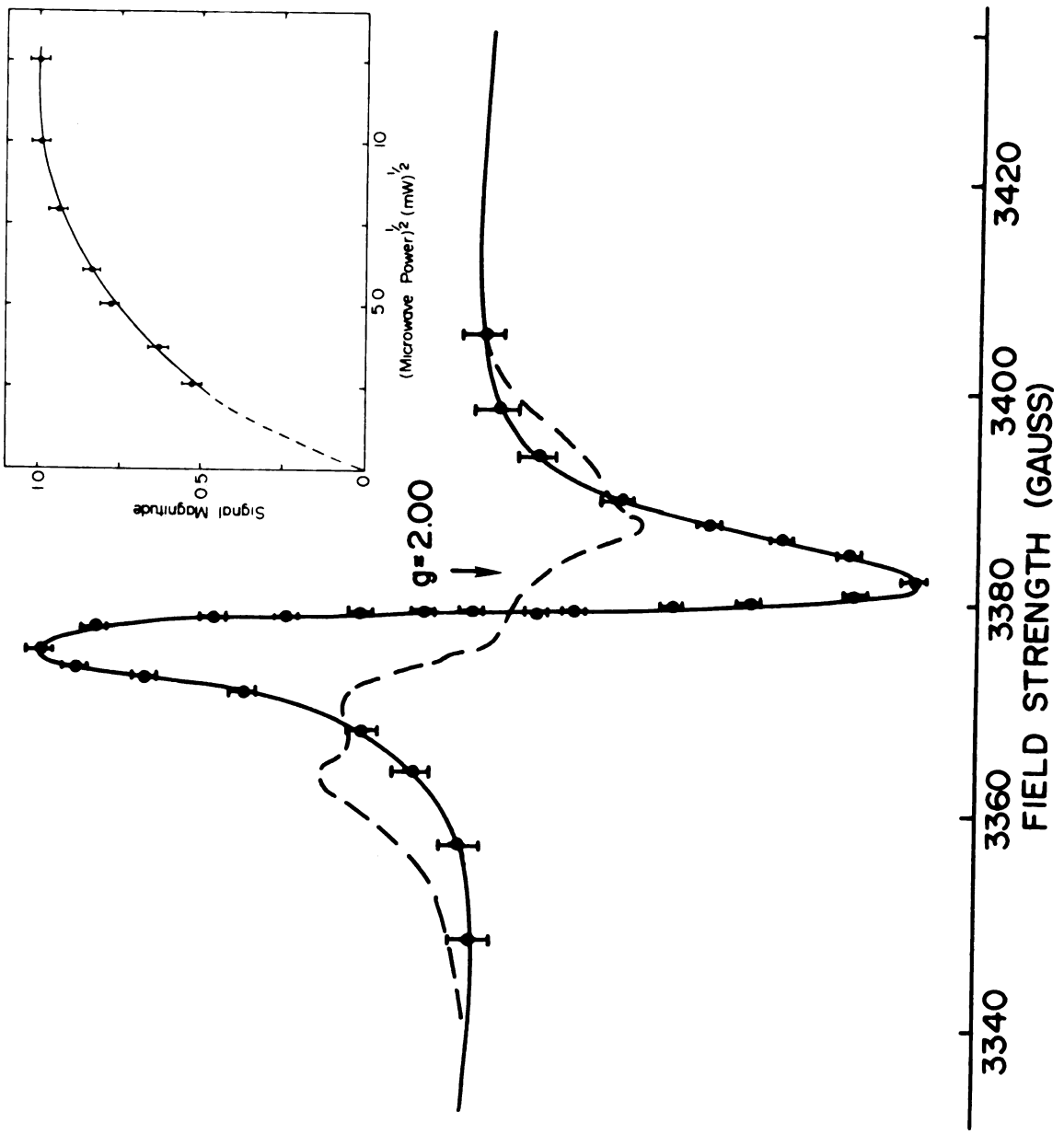
Signal Magnitude
0
5
10
(Microwave Power)$^{\frac{1}{2}}$ (mW)$^{\frac{1}{2}}$
0
5
10
g=2.00
3340
3360
3380
3400
3420
FIELD STRENGTH (GAUSS)

with those reported for P_{680}^+ [68,70]. Quantitation of the new signal, by double integration and correction for the instrument time constant, showed that it is stoichiometric (±20%) with Signal II_f. The saturation properties of the radical are shown in the insert to Fig. 28 which indicates that it saturates at relatively high power. Compared to this radical, Signal I (EPR signal of P_{700}^+) saturates at somewhat lower power which could be the result of environmental differences between the two species.

D. Discussion

The most common inhibitory site on the oxidizing side of Photosystem II is at the oxygen evolving complex itself (e.g. [19]) and NH_2OH has a well-known inhibition at this site [33,155]. Fluorescence data indicate, however, that NH_2OH also produces an inhibition in PSII which is probably localized between Z, the physiological donor, and the oxidized reaction center pigment, P_{680} [156]. In the work reported here, we have used EPR to show that NH_2OH does block the flow of electrons from Z to P_{680} in a way which is completely reversible. In the absence of NH_2OH, Z, which can be identified with D_1 [74], the immediate electron donor to P_{680}^+ in a variety of chloroplast preparations [121], reduces P_{680}^+ in a reaction with a halftime $\leq$15 μs. Under these

conditions we observe the EPR signal of Z^{+}, produced after reaction of Z with P_{680}^{+}, but we are not able to follow the EPR signal of P_{680}^{+} because of the response time of our instrument. Upon addition of hydroxylamine, electron flow between Z and P_{680}^{+} is interrupted and P_{680}^{+} is reduced by back reaction with the reduced form of the primary acceptor, Q_A^{-}. This reaction is much slower compared to the reduction of P_{680}^{+} by Z [121] and we can follow it with our experimental apparatus.

Thus, we can explain the NH_2OH inhibition of PSII with the scheme shown in Fig. 29. According to that scheme, NH_2OH has two effects. In the first, NH_2OH interrupts the flow of electrons from the S-states to Z by extracting Mn [33,155] which results in the conversion of Signal II_{vf} to Signal II_f. In the second mode of inhibition, which appears to be unique to NH_2OH, the flow of electrons from Z to P_{680} is interrupted in a completely reversible manner. The mechanism of the second inhibition is not clear and it could be a direct effect on Z, for example formation of a Z-NH_2OH complex, or an effect on the membrane environment of Z. That P_{680}^{+} is rereduced by Q_A^{-} in the inhibited centers, however, implies that the chemical and not the redox properties of NH_2OH are responsible for this inhibition.

FIGURE 29.

A model for the inhibitory role of NH_2OH in Photosystem II. See text for details.

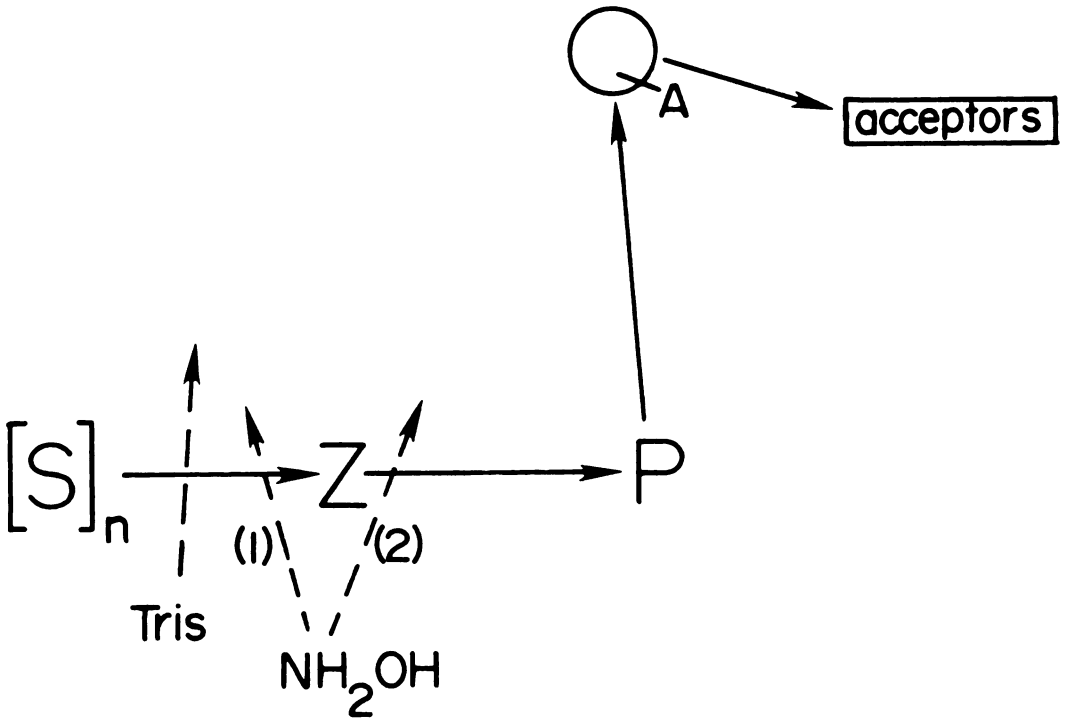
A
acceptors
[S]n
Z
P
(1)
(2)
Tris
NH2OH

CHAPTER VI.

INHIBITORY TREATMENTS OF OXYGEN EVOLUTION AND THEIR EFFECTS ON MANGANESE CONTENT, $Z^{+}_{\bullet}$ BEHAVIOR AND POLYPEPTIDE COMPOSITION.

A. Introduction

Signals II_{vf} and II_{f} are light-generated free radicals detected by EPR in chloroplast thylakoid membranes [67, 116]. Both signals arise from the same species, $Z^{+}_{\bullet}$, which is an intermediate electron carrier between the Photosystem II reaction center, P_{680}, and the oxygen evolving complex (OEC). Signal II_{vf} is the EPR signal of the radical $Z^{+}_{\bullet}$ observed in O_2-evolving chloroplasts and has a very fast decay (sub-msec) as the result of its reduction by the various S-states. Signal II_{f}, on the other hand, is the EPR signal of $Z^{+}_{\bullet}$ observed under conditions where oxygen evolving capacity has been inhibited by various treatments. One of the treatments used to uncouple the oxygen evolving complex from the rest of the photosynthetic chain is incubation with high concentration of Tris buffer [29-31]. Tris treatment releases functional manganese from the oxidizing side of Photosystem II by attacking the higher S-states, and under these conditions the electron flow from OEC to Z is

interrupted and the lifetime of the free radical is extended well into the ms time range. Under these conditions, the $Z^{+\bullet}$ free radical is referred to as Signal II_f. Upon addition of exogenous donors, the lifetime of $Z^{+\bullet}$ is decreased owing to a direct bimolecular reaction of the donor with $Z^{+\bullet}$ [36].

In addition to the change in the kinetic behavior of Z, tris-treatment also changes the power saturation properties of Signal II. Warden et al. [90] found that Signal II_{vf} could not be saturated at microwave powers up to 200 mW whereas Signal II_f was inhomogeneously broadened with saturation at ~25 mW. These findings were interpreted to indicate that II_{vf} was in the vicinity of a strongly relaxing species, probably Mn(II), associated with photosynthetic oxygen evolution. Another treatment which releases functional manganese from OEC is incubation with higher concentrations (~5 mM) of NH_2OH [32-35]. NH_2OH-induced Mn extraction occurs only from the lower S-states [155] and results in conversion of Signal II_{vf} to Signal II_f with properties similar to those observed upon tris-inhibition.

Treatment with various amines [38,39] has also been known to inhibit oxygen evolution activity, acting at the oxidizing side of PSII. Inhibition by ammonia and methylamine appears to be rather direct and does not result in the release of bound Mn that occurs with high concentrations of Tris buffer. Velthuys [40] and Frasch

and Cheniae [31] proposed that water binds to manganese in the OEC by a Lewis acid—Lewis base mechanism and that amines, being better Lewis bases, are able to compete with H_2O for binding sites (see also [9]). According to the model proposed by Velthuys [40], in the initial state S_1, no binding of NH_3occurs; in state S_2 the binding of ammonia is rapid (half-time about 0.5 s) and rapidly reversible; in state S_3 the binding is slower (half-time about 10 s) and slowly reversible. NH_3 bound to S_4 prevents the oxidation of water. Yocum and Babcock [157] have shown that the block at the S_2 or S_3 states of the oxygen evolving system by NH_3 is sufficient to induce Signal II_f, and more important, has enabled them to demonstrate that retention of Mn(II) in the OEC produces a condition whereby Signal II_f cannot be microwave power saturated.

Recently, Sandusky et al. [41], using PSII preparations, have shown that incubation with high concentrations of Tris buffer or NH_2OH releases two polypeptides which have been reported to be important for O_2-evolution, the 17 and the 23 KD [42,161,162]. In the same work [41], the authors have presented a series of other treatments (high salt, high pH, etc.) which inhibit O_2-evolution. A selective extraction of the above two polypeptides, but without releasing functional manganese, was possible by using the high salt (pH:6.0) treatment.

By monitoring the ESR properties of $Z^{+}_{\cdot}$, we have explored the role of manganese and of polypeptides, with molecular weights of 17 and 23 KD, in the O_2-evolving process. According to the results presented in this work, the 17 and 23 polypeptides seem to have a structural rather than a catalytic role in O_2 evolution activity. Removal of these polypeptides results in a condition whereby exogenous donors, such as benzidine, have ready access to components involved in the water splitting process.

B. Materials and Methods

Market spinach was used for preparing chloroplasts with high O_2 rates [163]. Leaves were kept dark at 4°C prior to use, then washed in distilled water and deveined under low light conditions. They were broken in a Waring blender for 12 s in a standard solution containing 0.4 M NaCl, 20 mM HEPES, 2 mM $MgCl_2$, 1 mM EDTA and 2 mg/ml BSA, pH adjusted to 7.5. The homogenate was then strained through 8 layers of cheesecloth and centrifuged for 2 min (5000 r.p.m., SS-34 Sorvall rotor) at about 4°C. The pellets were resuspended in a solution containing 0.15 M NaCl, 4 mM $MgCl_2$ and 20 mM HEPES, pH adjusted to 7.5, and then recentrifuged for 2 min (7500 r.p.m.) at about 4°C. The washed samples were resuspended in a minimal volume of SHN (0.4 M sucrose, 10 mM NaCl and 50 mM HEPES buffer) at pH 7.5. Chlorophyll concentrations

ranged between 3 and 5 mg chlorophyll per ml as determined by the Sun and Sauer method [94]. 20 μg/ml spinach ferredoxin and 5×10^{-4} M NADP, obtained from Sigma, were added to the final chloroplast suspension as an electron acceptor system. Hydroxylamine inactivation was carried out as described in [155].

Photosystem II oxygen evolving particles were prepared as described in Chapter V. A mixture of ferricyanide and ferrocyanide was used as an electron acceptor system in PSII particles. "High salt, low pH" inactivation was carried out by incubation of PSII particles in a solution containing 50 mM MES and 2 M NaCl, pH adjusted to 6.0, for 1 hr in the dark at 4°C. For "very low pH" inactivation PSII particles were incubated, for 1 hr in the dark at 4°C, in a solution containing 50 mM Succinate and 10 mM NaCl, pH adjusted to 4. "High salt, high pH" inactivation was carried out by incubation, under the same conditions, in a solution containing 50 mM CAPS buffer and 10 mM NaCl at pH ~10. All the above treatments were followed by a wash with SHN and final resuspension in a minimal volume of SHN (pH:7.5).

C. Results

It was shown previously that upon extraction of manganese from the oxidizing side of Photosystem II, with the use of Tris buffer, full Signal II_f magnitude is observed [116] (the ESR signal of $Z^{+\cdot}$, $Z^{+\cdot}/P_{680} = 1$ [92]).

The lifetime of the radical, $Z^{+}_{\cdot}$, is extended into the hundreds of ms time range in the absence of added reductants and is decreased upon addition of exogenous donors (e.g. ascorbate, benzidine) [36] or lipophilic anions (e.g. CCCP) [101] (see also Chapters II and IV). Another treatment which releases functional manganese from OEC is incubation with higher concentrations of NH_2OH [32-35]. We studied the behavior of Signal II after NH_2OH inactivation and found that full Signal II_f magnitude is observed only when the NH_2OH is removed carefully after the inhibitory treatment. It has been shown in Chapter V (see also Ref. [71]) that NH_2OH is able to inhibit between Z and P_{680}. In the present work we have avoided this complication by a washing procedure which removes NH_2OH once its inhibition at the OEC has gone to completion. When these precautions are taken the behavior of $Z^{+}_{\cdot}$ parallels that observed in tris-inhibited chloroplasts. Typical data are shown in Fig. 30. The major features can be summarized as follows: (a) $Z^{+}_{\cdot}$ formation in the ms range is stoichiometric with P_{680}; (b) the decay is monophasic and (c) exogenous donors are effective in accelerating its decay. In Fig. 31, we present data on the second order rate constants for benzidine and hydroquinone as donors. The rate constants observed, $k(BZ) = 1.1 \times 10^{6}\ \underline{M}^{-1}\ s^{-1}$ and $k(HQ) = 3.2 \times 10^{5}\ \underline{M}^{-1}\ s^{-1}$, are essentially the same as those observed in tris-inhibited chloroplasts [36].

FIGURE 30.

Kinetic transients of $Z^{+\cdot}$ at room temperature in NH_2OH extracted chloroplasts at pH 7.5; a) no further addition, b) 4 mM ascorbate and c) 50 μM benzidine, 4 mM ascorbate.

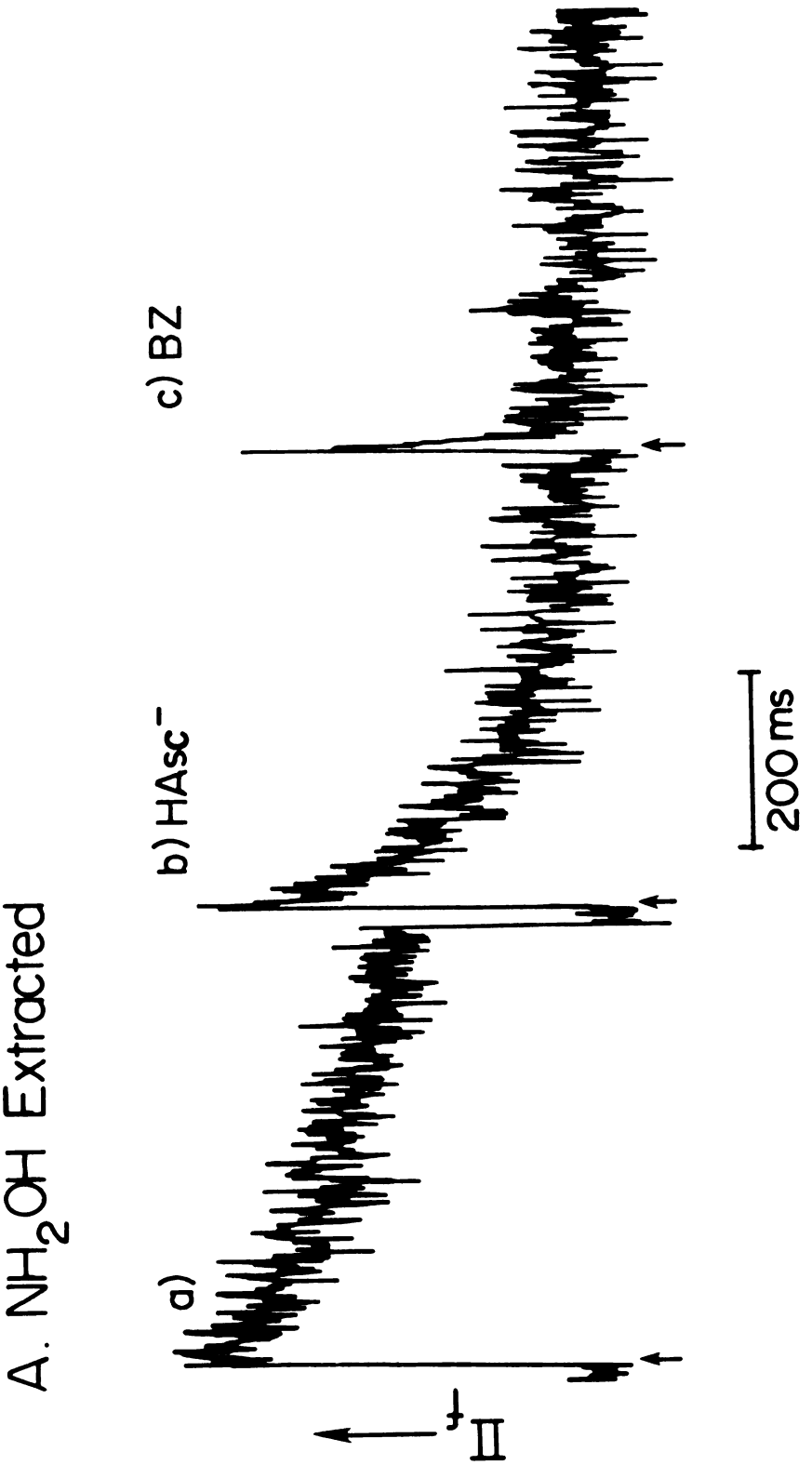
A. NH_2OH Extracted
a)
b) $HAsc^-$
c) BZ
II
200 ms

FIGURE 31.

Graphical determination of the second order rate constants for benzidine (---) and hydroquinone (——) donation to $Z^{+\cdot}$ in NH_2OH extracted chloroplasts.

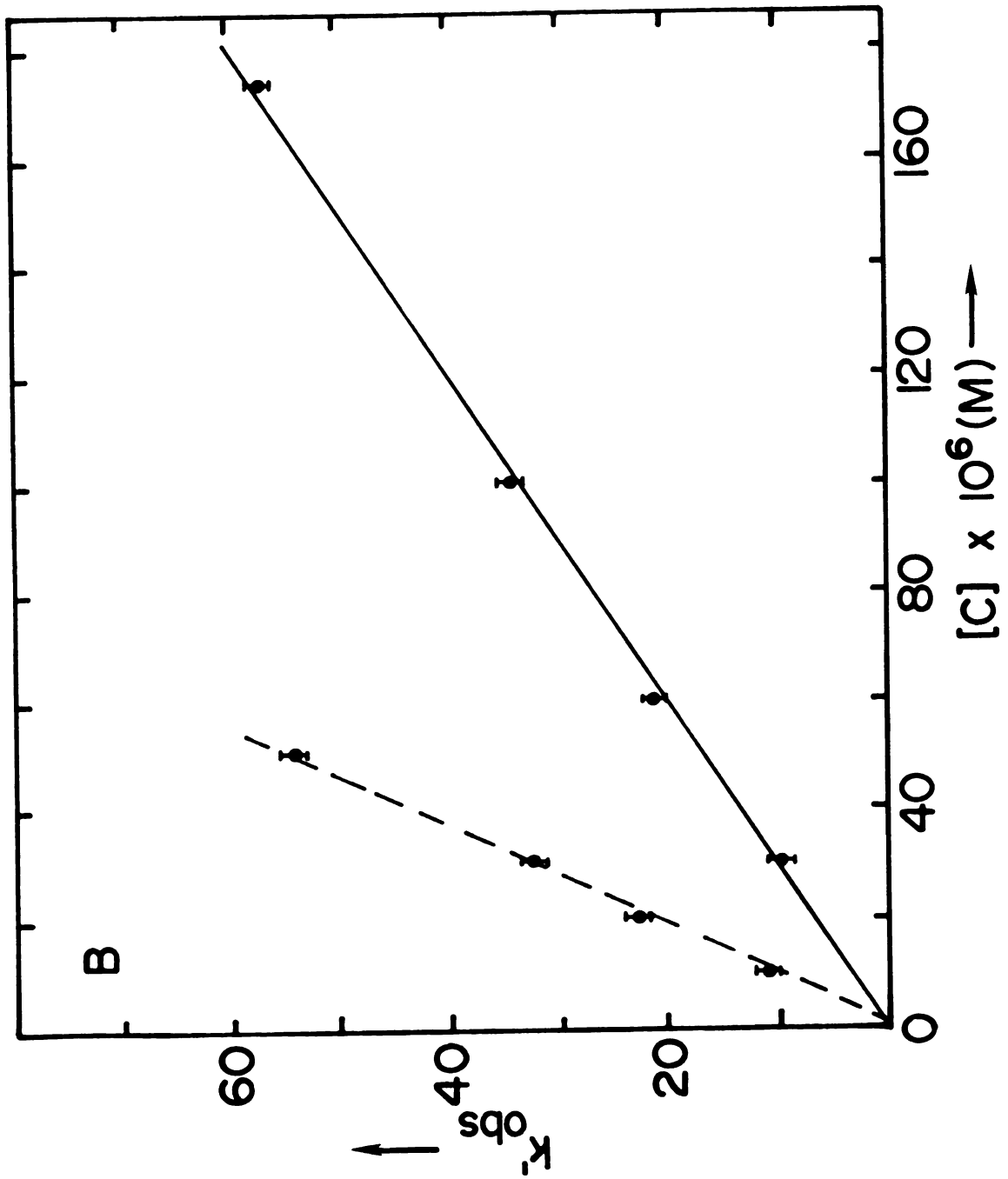
B
k'_{obs} ⟵
60
40
20
0
40
80
120
160
[C] x 10^6(M) ⟶

Yocum and Babcock [157] showed earlier that NH_3 inhibition of O_2 evolution retards the reduction of $Z^{+\cdot}$, but perturbs its microwave power saturation properties only slightly. Figure 32 shows $Z^{+\cdot}$ kinetic traces in NH_3 inhibited chloroplasts. Compared to the behavior of $Z^{+\cdot}$ in tris (under high concentration conditions) or NH_2OH extracted chloroplasts (see above), the behavior of $Z^{+\cdot}$ under these conditions is unusual. The amplitude of the signal in Fig. 32a accounts for only 0.3 $Z^{+\cdot}$ spins per PSII unit and the decay is biphasic. The rate constants for the two phases were determined to be 15 s^{-1} and 1.9 s^{-1} in separate, more highly resolved experiments. In Tris or NH_2OH inhibited chloroplasts, benzidine has been shown to be an effective donor to $Z^{+\cdot}$. In contrast, the data of Fig. 32c show that this reductant has little effect on the decay of $Z^{+\cdot}$ in the presence of NH_3. Figure 32b shows that Ca^{2+} addition accelerates the slow phase to the extent that the rereduction kinetics approach monophasic behavior. The last effect is only specific for Ca^{2+} and saturates at relatively low concentrations (~3 mM).

Sandusky et al. [41] have shown that incubation of PSII particles with high concentrations of Tris or higher concentrations of NH_2OH, releases the 17 and the 23 KD polypeptides (see also [161,162]). In the same work [41] the authors report a "high salt, low pH" treatment which results in extraction of the 17 and the 23 KD polypeptides

FIGURE 32.

Kinetic transients for Z^+ at room temperature in NH_3 (200 mM) treated chloroplasts at pH 7.5; a) no further addition, b) 5 mM $CaCl_2$ and c) 200 μM benzidine, 4 mM ascorbate. Time constant = 1 ms, 200 scans averaged at a rate of 0.25 Hz.

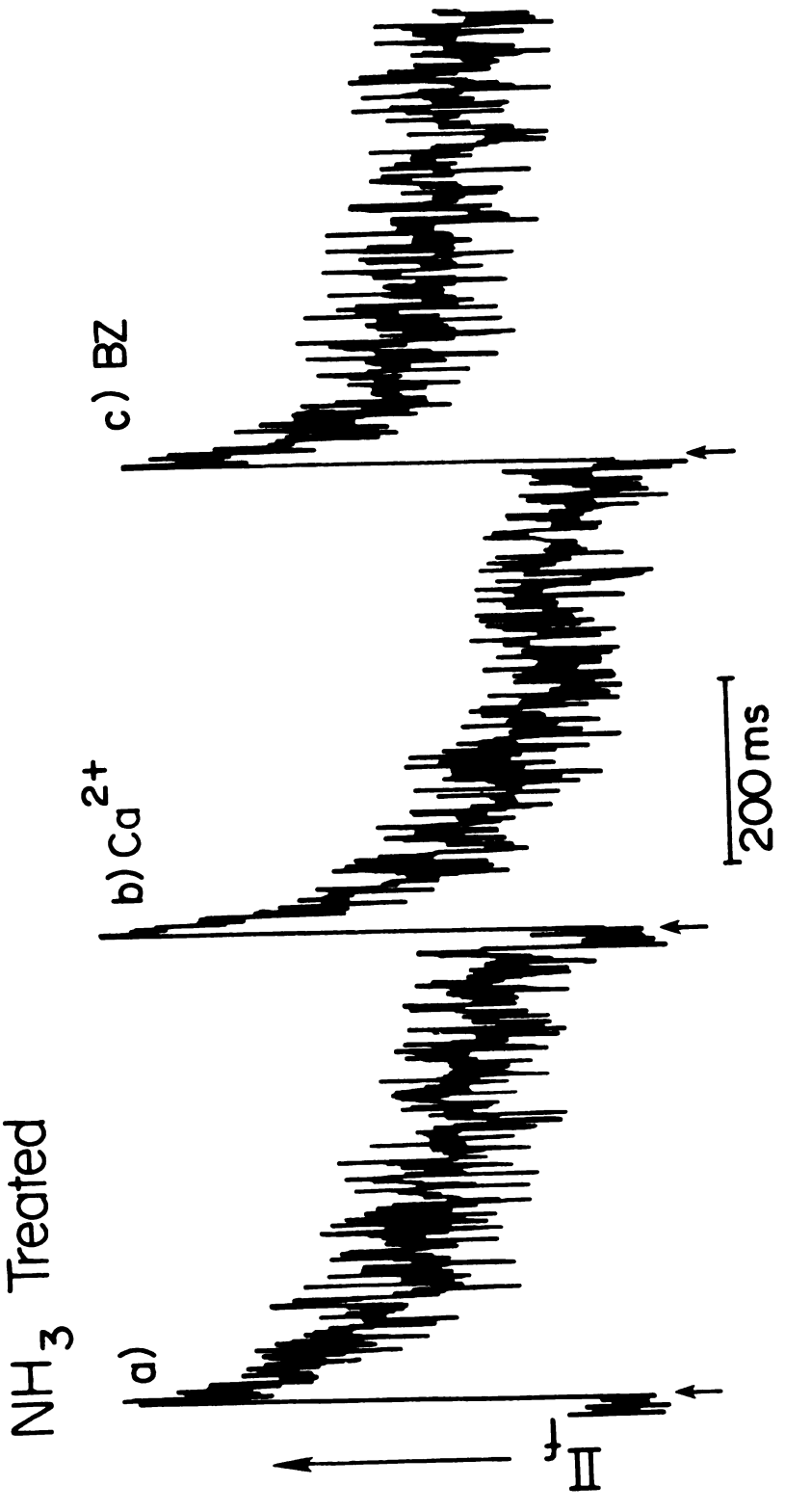
NH3 Treated
a)
II
b) Ca2+
c) BZ
200 ms

but, in contrast to Tris or NH_2OH inhibitions, does not release functional manganese. After the above treatment PSII particles are incapable of evolving O_2 and partial Signal II_f is observed. The characteristics of the EPR signal of $Z^{+\cdot}$ under these conditions are the following: a) High power saturation, as expected since no manganese was released; b) only ~0.3 $Z^{+\cdot}$ spins per PSII unit are observed; c) biphasic decay in the absence of any exogenous donor (Fig. 33a), and d) decay susceptible to exogenous donors (Fig. 33b). The decay of Signal II_f changed dramatically upon addition of benzidine (Figs. 33b and 34a-c) and titration with various concentrations of benzidine revealed an indirect rather than a direct reduction of $Z^{+\cdot}$ by the exogenous donors. Since manganese is in close interaction with Z, as shown by the power saturation properties of Signal II_f, it could very well serve as a donor to $Z^{+\cdot}$ and then be rereduced in a subsequent reaction with benzidine. To test this hypothesis we repeated the experiments of Fig. 33a and 33b but in the presence of NH_3. As shown in Fig. 33c,d even high concentration of benzidine has no effect on the decay time of Signal II_f in the presence of 200 mM NH_3. As shown in Fig. 34 the decay time of $Z^{+\cdot}$ depends on the dark time between flashes (t_d). At long t_d's the decay of $Z^{+\cdot}$ is accelerated upon addition of benzidine and the slow phase disappears (Fig. 34a-c). At short t_d's the effect of benzidine on the decay of the $Z^{+\cdot}$

FIGURE 33.

Kinetic transients for $Z^{+}_{\cdot}$ at room temperature in high salt (2 M NaCl, pH:6.0) treated PSII particles at pH 7.5. An equimolar mixture of ferricyanide and ferrocyanide (3 mM each) was used as an acceptor system. a) No further addition, b) 50 μM benzidine, c) 200 mM NH_3 and d) 200 mM NH_3 and 100 μM benzidine. Each kinetic trace is the average of 200 flashes. Time constant = 0.5 ms and the dark time between flashes t_d = 5 sec.

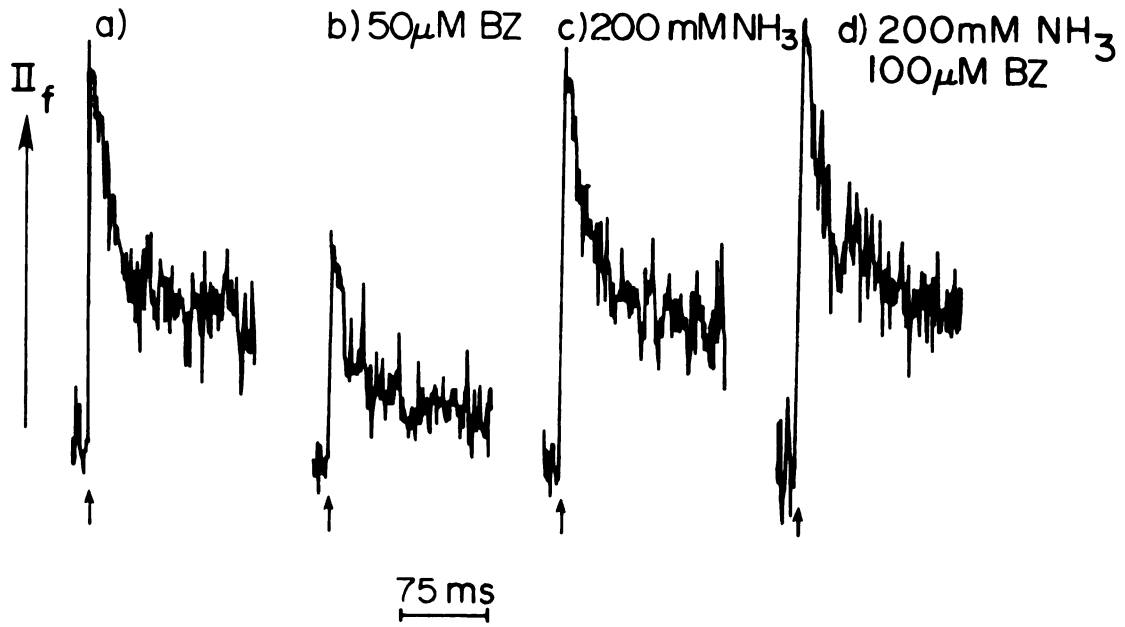
a)
b) 50μM BZ
c) 200 mM NH3
d) 200mM NH3
100μM BZ
If
75 ms

FIGURE 34.

Kinetic transients for $Z^{+}\cdot$ at room temperature in high salt (2 M NaCl, pH:6.0) treated PSII particles at pH 7.5. An equimolar mixture of ferricyanide and ferrocyanide (3 mM each) was used as an acceptor system. a) No further addition, t_d = 6 sec, b) 15 μM benzidine, t_d = 6 sec, c) 30 μM benzidine, t_d = 6 sec, d) no addition, t_d = 2 sec, e) 15 μM benzidine, t_d = 2 sec, and f) 30 μM benzidine, t_d = 2 sec. Each kinetic trace is the average of 250 flashes. Instrument time constant = 0.5 ms.

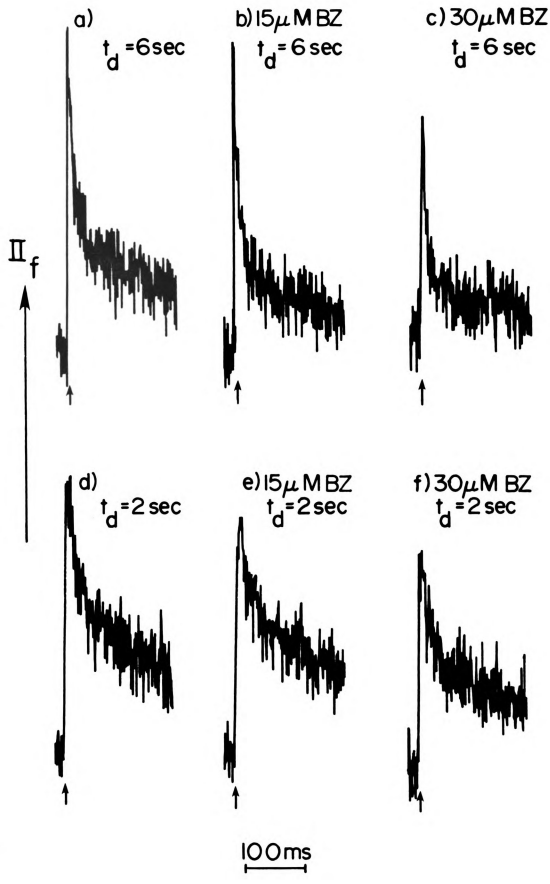
a)
t_d = 6 sec
b) 15 μM BZ
t_d = 6 sec
c) 30 μM BZ
t_d = 6 sec
Π_f
d)
t_d = 2 sec
e) 15 μM BZ
t_d = 2 sec
f) 30 μM BZ
t_d = 2 sec
100 ms

radical is less dramatic (Fig. 34d-f). Even in the presence of high concentrations of benzidine (Fig. 34f) the decay remains biphasic. Various other treatments have been used to inactivate O_2 evolution capacity and according to their effect on manganese content, $Z^{+}_{\cdot}$ behavior and polypeptide composition can be separated into three classes.

a) Class A:

i) Extraction with NH_2OH in the dark; ii) extraction with high concentration of Tris-buffer in the light; iii) treatment with high salt at pH:10. These treatments release functional manganese from PSII particles and also extract the 17, 23 and 33 KD polypeptides [41]. After these treatments we observe full Signal II_f magnitude and the radical saturates at low (~25 mW) microwave power levels. The lifetime of the radical, $Z^{+}_{\cdot}$, is extended well into the hundreds of ms time range and is decreased upon addition of exogenous reductants.

b) Class B:

Incubation with amines. This treatment releases neither manganese nor the 17 and 23 KD polypeptides. Although the system does not photooxidize water following these treatments we observe only partial Signal II_f ($Z^{+}_{\cdot}/P_{680} = 0.3$) upon flash excitation. The radical shows high (>100 mW) microwave power saturation properties and

follows a biphasic decay time course following illumination. Z^{+} under these conditions is not accessible to exogenous donors.

c) Class C:

i) High salt incubation at pH 6 and ii) incubation at low pH (~4). The above treatments remove the 17 and 23 KD polypeptides (pH:4.0 releases also the 33 KD, Ghanotakis, D.F. and Yocum, C.F., unpublished observations) but do not alter manganese content. Again, we observe only a fraction of Signal II_f and the species exhibits high (>100 mW) microwave power saturation properties. Z^{+} is apparently accessible to donors like benzidine although the process does not follow the simple first order dependence we observed above for Class A treatments. Rather it appears as if the donor reduces a membrane component, possibly Mn, which in turn reduces the radical (see Discussion).

D. Discussion

At high NH_3 concentration electron donation by water to Photosystem II is inhibited [38,39]. Velthuys [40,158] has proposed a model in which NH_3 binds to the S_2 and S_3 states but not to S_0 and S_1. According to this model, in a series of flashes Z^{+} is rereduced by the various S-states as follows (from Ref. 158):

$$S_0 + Z^{+\cdot} \xrightarrow{k_1} S_1 + Z \qquad (6.1)$$

$$S_1 + Z^{+\cdot} \xrightarrow{k_2} S_2 + Z$$

$$\downarrow 3\ s^{-1}\ NH_3$$

$$S_2(NH_3) \qquad (6.2)$$

$$S_2(NH_3) + Z^{+\cdot} \xrightarrow{k_3} S_3(NH_3) + Z$$

$$\downarrow 0.1 \text{ or } 1\ s^{-1}\ NH_3$$

$$S_3(NH_3)_2 \qquad (6.3)$$

$$S_3(NH_3) + Z^{+\cdot} \xrightarrow{k_4} S_4(NH_3) + Z \qquad (6.4)$$

$$S_3(NH_3)_2 + Z^{+\cdot} \xrightarrow{k_5} S_4(NH_3)_2 + Z \qquad (6.5)$$

As shown in the above model S_0 and S_1 do not bind NH_3, whereas S_2 and S_3 have the ability to bind one and two molecules of NH_3 respectively. Studying the oxygen yield in the presence of NH_4Cl, Delrieu [160] proposed that the turnover times $S_0 \rightarrow S_1$, $S_1 \rightarrow S_2$ and $S_2 \rightarrow S_3$ are accelerated in the presence of NH_3, but the $S_3 \rightarrow S_4 \rightarrow S_0$ reaction is slowed down significantly compared to the respective transition in O_2-evolving systems. From the data presented in references 67 and 160 we conclude that the reduction of $Z^{+\cdot}$ in reactions (6.1)-(6.3) is in the μsec region, and thus it is difficult to follow by our apparatus, whereas reduction by Eqs. (6.4) and (6.5) is extended into the ms time range and consequently detectable by EPR kinetic techniques. The above model would explain our kinetic results in the presence of NH_3

as follows: i) the fact that only 0.3 spins of $Z^{+\cdot}$ are observed in the presence of NH_3 could be explained by assuming that in a steady state experiment (series of 100-200 flashes) only 30% of $Z^{+\cdot}$ is rereduced by reactions (6.4) and (6.5). ii) The biphasic decay of Signal II_f would reflect the difference between k_4 and k_5. As shown in Fig. 32a the overall decay of $Z^{+\cdot}$ is a few hundreds of msec (~500 ms), in the absence of Ca^{2+}, which is in good agreement with the value reported in Ref. 160 for the transition $S_3 \rightarrow S_0$ (~300 ms). The fact that $Z^{+\cdot}$ is not accessible to exogenous reductants, like benzidine, could be due to the selectivity of the system in allowing only compounds of certain size and shape to enter the oxidizing side of PSII (see below).

In contrast to Tris or NH_2OH treatment which removes both, the 17 and the 23 KD polypeptides and functional manganese, high salt (pH:6.0) and low pH (~4.0) treatments remove the above two polypeptides without effecting manganese. Like NH_3-treatment, only partial signal is observed and the decay is biphasic. After the above treatments $Z^{+\cdot}$ is apparently accessible to donors like benzidine although the process does not follow the simple first order dependence observed for Tris or NH_2OH treatment. The fact that the benzidine effect disappears upon addition of NH_3 implies that some form of manganese could serve as an intermediate between $Z^{+\cdot}$ and the exogenous donor. Since manganese is in close

interaction with $Z^{+}_{\cdot}$, as shown by the power saturation properties of Signal II_f, we postulate that a set of modified S-states (let us call them M-states), which could probably reflect various oxidation states of a manganese complex, serves as a donor system to $Z^{+}_{\cdot}$. The partial Signal II_f observed, could be the result of a mechanism similar to that discussed above for NH_3 treatment; low M-states rereduce $Z^{+}_{\cdot}$ in very fast reactions, whereas rereduction of $Z^{+}_{\cdot}$ by the higher M-states is much slower. M-states, after the removal of the 17 and the 23 KD polypeptides, are accessible to benzidine which converts higher M-states to the lower ones, which in turn rereduce $Z^{+}_{\cdot}$. This model predicts that in the presence of benzidine the kinetic behavior of $Z^{+}_{\cdot}$, in a series of successive flashes will depend on the dark time between flashes (t_d). Long t_d's will allow benzidine to convert the higher M-states to the lower ones which are going to accelerate the decay of $Z^{+}_{\cdot}$; short t_d's will not allow such fast conversion and thus the benzidine effect will be less dramatic. Indeed, as shown in Fig. 34, variation of the time between flashes (t_d) changes the decay time of the $Z^{+}_{\cdot}$ radical. Longer times between flashes allow the conversion of higher M-states to the lower ones, which results in a faster reduction of $Z^{+}_{\cdot}$.

Another model which would explain our results in the presence of NH_3 or after extraction of the 17 and 23 KD

polypeptides (with high salt (pH:6.0) or low pH (~4.0) treatment) is the two parallel donor system (see Chapter I and Ref. 8) shown below:

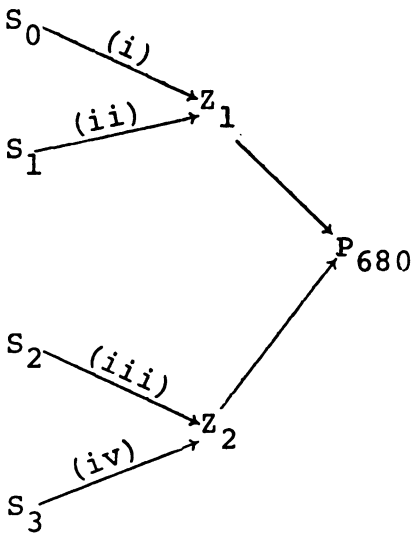

According to this model after photoexcitation P_{680}^{+} is rereduced by two competing donors, Z_1, of unknown identity (possibly manganese) and Z_2, the precursor to Signal II_{vf} in O_2-evolving chloroplasts and to Signal II_f in inhibited preparations. When both donors are functional only 0.3 spins of Z_2^{+} (or $Z^{+\cdot}$) are observed, whereas upon manganese extraction (with Tris or NH_2OH), Z_2 becomes the only donor to P_{680} and thus full Signal II_f is observed. If NH_3-treatment and polypeptide extraction disturb only reactions (iii) and (iv), the results of Figs. 32-34 would be explained by this model. This model would also explain the fact that Babcock et al. [67] observed no Signal II_{vf} for the transitions $S_0 \rightarrow S_1$ and $S_1 \rightarrow S_2$ (first two flashes), which

at that point was explained by proposing a very fast rereduction of Z^+ by states S_0 and S_1.

If we compare the treatments of the three classes presented above (A, B and C) in terms of the accessibility of the oxidizing side of PSII to exogenous donors, we conclude that the 17 and 23 KD polypeptides should have a structural role. When both polypeptides are there neither manganese (S-states) nor $Z^{+\cdot}$ is accessible to exogenous donors (Class B). When the polypeptides are extracted but without releasing manganese, exogenous donors react with manganese which in turn reacts with $Z^{+\cdot}$ (Class C). When both the polypeptides and manganese are extracted the system becomes wide open and exogenous donors react directly with $Z^{+\cdot}$ (Class A).

Recently, Radmer and Ollinger [159] proposed that the water binding site resides in a cleft which allows selectively the entrance of molecules with certain size and shape. Our data suggest that the 17 and 23 KD polypeptides are two possible structural units for building the H_2O binding site cleft. A possible arrangement of the oxidizing side of PSII is shown in Fig. 35.

The model presented above is mostly qualitative and a more complete kinetic as well as biochemical study is needed in order to unravel the details of H_2O oxidation. Such a study is currently in process (Ghanotakis, D.F., Yocum, C.F. and Babcock, G.T., unpublished observations).

FIGURE 35.

Model for polypeptide and manganese location in the oxidizing side of Photosystem II.

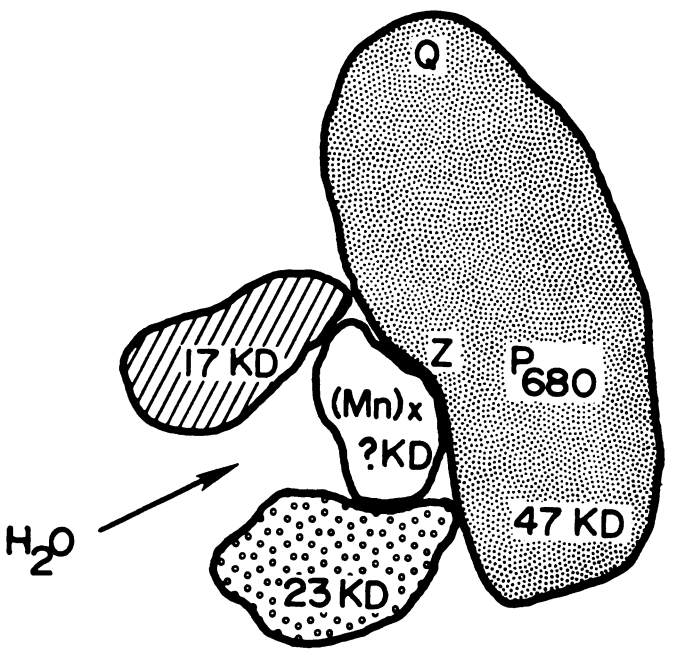
Q
17 KD
Z
P680
(Mn)x
?KD
47 KD
H2O
23 KD

LIST OF REFERENCES

LIST OF REFERENCES

1. Williams, W.P. (1975) in Primary Processes of Photosynthesis (Barber, J. ed) pp. 99-147, Elsevier, Amsterdam.

2. Sauer, K. (1978) Acc. Chem. Res. 11, 257.

3. Emerson, K. and Arnold, W. (1932) J. Gen. Physiol. 15, 391.

4. Döring, G., Renger, G., Vater, J. and Witt, H.T. (1969) Z. Naturforsch. Teil B. 24, 1139-1143.

5. Stiehl, H.H. and Witt, H.T. (1969) Z. Naturforsch. Teil B. 24, 1588.

6. Klimov, V.V., Klevanic, A.V., Shuvabv, V.A. and Kravsnovsky, A.A. (1977) FEBS Lett. 82, 183.

7. Bouges-Bocquet, B. (1973) Biochim. Biophys. Acta 314, 250.

8. Bouges-Bocquet, B. (1980) Biochim. Biophys. Acta 594, 85-103.

9. Ghanotakis, D.F., O'Malley, P.J., Babcock, G.T. and Yocum, C.F. (1983) Oxygen-Evolving System of Plant Photosynthesis, Academic Press, Japan, Inc., Tokyo, in press.

10. Träuble, H. (1977) in Structure of Biological Membranes (Abrahamson, S. and Paschar, J. ed) Plenum Press, London, New York, p. 509.

11. Wolff, C., Buchwald, H.E., Rüppel, H., Witt, K. and Witt, H.T. (1969) Z. Naturforsch. Teil. B 24, 1038.

12. Mitchell, P. (1966) Biol. Rev. 41, 445.

13. Joliot, P., Barbieri, G. and Chabaud, R. (1969) Photochem. Photobiol. 10, 309-329.

14. Kok, B., Forbush, B. and McGloin, M. (1970) Photochem. Photobiol. 11, 457-475.

15. Pirson, A. (1937) Z. Botan. 31, 193-267.

16. Kessler, E., Arthur, W. and Brugger, J.E. (1957) Arch. Biochem. Biophys. 71, 326-335.

17. Cheniae, G.M. and Martin, I.F. (1970) Biochim. Biophys. Acta 197, 219-239.

18. Blankenship, R.E., Babcock, G.T. and Sauer, K. (1975) Biochim. Biophys. Acta 387, 165-175.

19. Yocum, C.F., Yerkes, C.T., Blankenship, R.E., Sharp, R.R. and Babcock, G.T. (1981) Proc. Nat'l. Acad. Sci. USA 78, 7507-7511.

20. Dismukes, G.C. and Siderer, Y. (1981) Proc. Nat'l. Acad. Sci. USA 78, 274-278.

21. Fowler, C.F. (1977) Biochim. Biophys. Acta 459, 351-363.

22. Fowler, C.F. (1977) Biochim. Biophys. Acta 462, 414-421.

23. Saphon, S. and Crofts, A.R. (1977) Z. Naturforsch C: Biosci. 32C, 617-626.

24. Junge, W., Renger, G. and Aüslander, W. (1977) FEBS Lett. 79, 155-159.

25. Antonini, E. and Brunoni, M. (1971) in Hemoglobin and Myoglobin and their Reactions with Ligands, North-Holland Publ., Amsterdam.

26. Bucci, E. and Fronticelli, C. (1981) Methods in Enzymology 76, 523-533.

27. Katoh, S. and San Pietro, A. (1967) Arch. Biochem. Biophys. 122, 144-152.

28. Yamashita, T. and Butler, W.L. (1968) Plant Physiol. 43, 1978-1986.

29. Yamashita, T. and Butler, W.L. (1969) Plant Physiol. 44, 435-438.

30. Cheniae, G.M. and Martin, I.F. (1978) Biochim. Biophys. Acta 502, 321-344.

31. Frasch, W. and Cheniae, G.M. (1980) Plant Physiol. 65, 735-745.

32. Joliot, P. (1966) Biochim. Biophys. Acta 126, 587-590.

33. Cheniae, G.M. and Martin, I.F. (1971) Plant Physiol. 47, 568-575.

34. Ort, D.R. and Izawa, S. (1973) Plant Physiol. 52, 595-600.

35. Horton, P. and Croze, E. (1977) Biochim. Biophys. Acta 462, 86-101.

36. Yerkes, C.T. and Babcock, G.T. (1980) Biochim. Biophys. Acta 590, 360-372.

37. Cheniae, G.M. and Martin, I.F. (1971) Biochim. Biophys. Acta 253, 167-181.

38. Hind, G. and Whittingham, C.P. (1963) Biochim. Biophys. Acta 75, 194-202.

39. Izawa, S., Heath, R.L. and Hind, G. (1969) Biochim. Biophys. Acta 180, 389-399.

40. Velthuys, B.R. (1975) Biochim. Biophys. Acta 396, 392-401.

41. Sendusky, P.O., DeRoo, C.L.S., Hicks, D.B., Yocum, C.F., Ghanotakis, D.F. and Babcock, G.T. (1983) Oxygen-Evolving System in Plant Photosynthesis, Academic Press, Japan, Inc., Tokyo, in press.

42. Sayre, R. and Cheniae, G.M. (1982) Plant Physiol. 69, 1084-1095.

43. Butler, W.L. (1972) Biophys. J. 12, 851-857.

44. Haveman, J. and Mathis, P. (1976) Biochim. Biophys. Acta 440, 346-355.

45. Van Best, J.A. and Mathis, P. (1978) Biochim. Biophys. Acta 503, 178-188.

46. Conjeaud, H., Mathis, P. and Paillotin, G. (1979) Biochim. Biophys. Acta 546, 280-291.

47. Pulles, M.P.J., Van Gorkom, H.J. and Willemsen, J.G. (1976) Biochim. Biophys. Acta 449, 536-540.

48. Mathis, P. and Haveman, J. (1977) Biochim. Biophys. Acta 451, 167-181.

49. Renger, G. and Weiss, W. (1983) FEBS Lett. 722, 1-11.

50. Duysens, L.N.M. and Sweers, H.E. (1963) in Studies in Microalgae and Photosynthetic Bacteria (Japan Soc. Plant Physiologists, ed), pp. 353-372, University of Tokyo Press, Tokyo.

51. Butler, W.L., Visser, J.W.M. and Simons, H.L. (1973) Biochim. Biophys. Acta 325, 539.

52. Papageorgiou, G. (1975) in Bioenergetics of Photosynthesis (Govindjee, ed) , pp. 319-371, Academic Press, New York.

53. Lavorel, J. and Etienne, A.L. (1977) in Primary Processes of Photosynthesis (Barber, J., ed), pp. 203-268, Elsevier, Amsterdam.

54. Sonneveld, A., Rademaker, H. and Duysens, L.N.M. (1979) Biochim. Biophys. Acta 548, 536.

55. Amesz, J. and Van Gorkom, H.J. (1978) Ann. Rev. Plant Physiol. 29, 47-66.

56. Lavorel, J. (1975) in Bioenergetics of Photosynthesis (Govindjee, ed) pp. 225-314, Academic Press, New York.

57. Zankel, K.L. (1971) Biochim. Biophys. Acta 245, 373-385.

58. Barbieri, G., Delosme, R. and Joliot, P. (1970) Photochem. Photobiol. 12, 197-206.

59. Joliot, P., Joliot, A., Bouges-Bocquet, B. and Barbieri, G. (1971) Photochem. Photobiol. 14, 287-305.

60. Arnold, W. and Azzi, J. (1971) Photochem. Photobiol. 14, 233-240.

61. Arnold, W. and Azzi, J. (1971) in Biomembranes (Manson, L.A., ed), Vol. 2, pp. 189-191, Plenum, New York.

62. Babcock, G.T., Yerkes, C.T. and Buttner, W.J. (1981) Proc. 5th Int. Congr. on Photosynthesis, pp. 637-645, (Akoyunoglou, G., ed), Balaban International Services, Philadelphia.

63. Wydryzynski, T., Zumbulyadis, N., Schmidt, P.G., Gutowsky, H.S. and Govindjee (1976) Proc. Nat'l. Acad. Sci. USA 73, 1196.

64. Robinson, H.H., Sharp, R.R. and Yocum, C.F. (1980) Biochim. Biophys. Acta 593, 414-426.

65. Robinson, H.H., Sharp, R.R. and Yocum, C.F. (1980) Biochem. Biophys. Res. Commun. 93, 755-761.

66. Babcock, G.T. and Sauer, K. (1975) Biochim. Biophys. Acta 396, 48-62.

67. Babcock, G.T. Blankenship, R.E. and Sauer, K. (1976) FEBS Lett. 61, 286-289.

68. Malkin, R. and Bearden, A.J. (1975) Biochim. Biophys. Acta 396, 250-259.

69. Visser, J.W.M. (1975) Ph.D. Thesis, Leiden.

70. Van Gorkom, H.J., Tamminga, J.J. and Haveman, J. (1974) Biochim. Biophys. Acta 347, 417-438.

71. Ghanotakis, D.F. and Babcock, G.T. (1983) FEBS Lett. 153, 231-234.

72. Davis, M.S., Forman, A. and Fajer, J. (1979) Proc. Nat'l. Acad. Sci. USA 76, 4170-4179.

73. O'Malley, P.J. and Babcock, G.T. (1983) Proc. Nat'l. Acad. Sci. USA, submitted.

74. Boska, M., Sauer, K., Buttner, W. and Babcock, G.T. (1983) Biochim. Biophys. Acta 722, 327-330.

75. Rutherford, A.W., Paterson, D.R. and Mullet, J.E. (1981) Biochim. Biophys. Acta 635, 205-214.

76. Knaff, D.B. and Arnon, D.I. (1969) Proc. Nat'l. Acad. Sci. USA 63, 963.

77. Velthuys, B.R. (1980) Proc. 5th Int. Congr. on Photosynthesis, (Akoyunoglou, G., ed), Balaban International Services, Philadelphia.

78. Commoner, B., Heise, J.J. and Townsend, J. (1956) Proc. Nat'l. Acad. Sci. USA 42, 710.

79. Sogo, P.B., Pon, N.G. and Calvin, M. (1957) Proc. Nat'l. Acad. Sci. USA 43, 387.

80. Beinert, H. and Kok, B. (1964) Biochim. Biophys. Acta 88, 278.

81. Kohl, D.H. (1972) in Biological Applications of ESR (Schwartz, H., ed), p. 213, John Wiley and Sons, New York.

82. Kohl, D.H., Townsend, J. Commoner, B., Crespi, H.L., Dougherty, R.C. and Katz, J. (1965) Nature 206, 1105.

83. Kohl, D.H. and Wood, P.M. (1969) Plant Physiol. 44, 1439.

84. Kohl, D.H., Wright, J.R. and Weissman, M. (1964) Biochim. Biophys. Acta 180, 536.

85. Hales, B.J. and Gupta, A.D. (1981) Biochim. Biophys. Acta 637, 303-311.

86. Esser, A.F. (1974) Photochem. Photobiol. 20, 167-172.

87. O'Malley, P.J. and Babcock, G.T., unpublished data.

88. Berthold, D.A., Babcock, G.T. and Yocum, C.F. (1981) FEBS Lett. 134, 232-234.

89. Babcock, G.T. and Sauer, K. (1975) Biochim. Biophys. Acta 375, 339.

90. Warden, J.T., Blankenship, R.E. and Sauer, K. (1976) Biochim. Biophys. Acta 423, 462-478.

91. Babcock, G.T. and Sauer, K. (1975) Biochim. Biophys. Acta 376, 315-328.

92. Babcock, G.T., Ghanotakis, D.F., Ke, B. and Diner, B.A. (1983) Biochim. Biophys. Acta, in press.

93. Babcock, G.T. and Sauer, K. (1973) Biochim. Biophys. Acta 325, 483-503.

94. Sun, A.S.K. and Sauer, K. (1971) Biochim. Biophys. Acta 234, 483.

95. Diner, B.A. and Sollman, F.A. (1980) Eur. J. Biochem. 110, 521-526.

96. Vernon, L.P. and Shaw, E.R. (1971) Methods Enzymol. 23, 277-289.

97. Klimov, V.V., Dolan, E., Shaw, E.R. and Ke, B. (1980) Proc. Nat'l. Acad. Sci. USA 77, 7227-7231.

98. Poole, C.P. (1967) Electron Spin Resonance, pp. 404-410, Interscience Publishers, New York.

99. Yerkes, C.T. (1981) Ph.D. Dissertation, Michigan State University.

100. Diner, B.A. and Bowes, J.M. (1981) Proc. 5th Int. Congr. on Photosynthesis, (Akoyunoglou, G., ed), Balaban International Services, Philadelphia, pp. 875-883.

101. Ghanotakis, D.F., Yerkes, C.T. and Babcock, G.T. (1982) Biochim. Biophys. Acta 682, 21-31.

102. Yerkes, C.T. and Babcock, G.T. (1981) Biochim. Biophys. Acta 634, 19-29.

103. Van Gorkom, H.J. (1974) Biochim. Biophys. Acta 347, 439-442.

104. Evans, M.C.W., Diner, B.A. and Nugent, J.H.A. (1982) Biochim. Biophys. Acta 682, 97-105.

105. Renger, G. and Reuter, R. (1981) Photobiochem. Photobiophys. 3, 317-325.

106. Velthuys, B.R. and Amesz, J. (1974) Biochim. Biophys. Acta 333, 85-94.

107. Itoh, S. (1978) Plant Cell Physiol. 19, 149-166.

108. Itoh, S. (1978) Biochim. Biophys. Acta 504, 324-340.

109. Overbeak, J.T.G. (1950) in Colloid Science (Kruyt, H.R., ed), Vol. I, pp. 115-193, Elsevier, Amsterdam.

110. Adamson, A.W. (1960) Physical Chemistry of Surfaces Academic Press, New York.

111. Ikegami, I. and Katoh, S. (1973) Plant Cell Physiol. 14, 829-836.

112. Visser, J.W.M., Riggersberg, C.P. and Gast, P. (1977) Biochim. Biophys. Acta 460, 36-45.

113. Bearden, A.J. and Malkin, R. (1973) Biochim. Biophys. Acta 325, 266-274.

114. Bowes, J.M., Crofts, A.R. and Itoh, S. (1979) Biochim. Biophys. Acta 547, 320-335.

115. Velthuys, B.R. and Kok, B. (1978) in Proc. IV Int. Congr. Photosynthesis, (Hall, D., ed), pp. 397-405, The Biochemical Society, London.

116. Babcock, G.T. and Sauer, K. (1975) Biochim. Biophys. Acta 376, 329-344.

117. Clark, W.M. (1960) Oxidation-Reduction Potentials of Organic Systems, The Williams and Wilkins Co., Baltimore, MD, p. 264.

118. Freifelder, D. (1982) Physical Chemistry for Students of Biology and Chemistry, Science Books International, Inc., Boston, MA, p. 469.

119. Levine, S. and Bell, G.M. (1965) J. Colloid Sci. 20, 695-727.

120. Itoh, S. and Nishimura, M. (1977) Biochim. Biophys. Acta 460, 381-392.

121. Mathis, P. and Paillotin, G. (1981) Biochem. of Plants 8, 97-161.

122. Rutherford, A.W., Mullet, J.E., Paterson, D.R., Robinson, H.H., Arntzen, C.J. and Crofts, A.R. (1981) Proc. 5th Int'l. Congr. on Photosynthesis, (Akoyunoglou, G., ed), Balaban International Services, Philadelphia.

123. Nugent, J.H.A., Diner, B.A. and Evans, M.C.W. (1981) FEBS Lett. 124, 241-244.

124. Hales, B.J. and Case, E.E. (1981) Biochim. Biophys. Acta 637, 291-302.

125. Blankenship, R.E., Babcock, G.T., Warden, J.T. and Sauer, K. (1975) FEBS Lett. 51, 287-293.

126. Reinman, S. and Mathis, P. (1981) Biochim. Biophys. Acta 635, 249-258.

127. Eckert, H.J. and Renger, G. (1980) Photochem. Photobiol. 31, 501-511.

128. Bowes, J.M., Crofts, A.R. and Itoh, S. (1979) Biochim. Biophys. Acta 547, 336-346.

129. Hong, Y.-Q., Förster, V. and Junge, W. (1981) FEBS Lett. 132, 247-251.

130. Velthuys, B.R. (1980) FEBS Lett. 115, 167-170.

131. Radmer, R. and Cheniae, G.M. (1977) in Bioenergetics of Photosynthesis (Barber, J., ed), pp. 301-348, Elsevier, Amsterdam.

132. Izawa, S. (1980) Methods Enzymol. 69, 413-434.

133. Joliot, P., Hoffnung, M. and Chabaud, R. (1966) J. Chim. Phys. 63, 1423-1441.

134. Kimimura, M., Katoh, S., Ikegami, I. and Takamiya, A. (1971) Biochim. Biophys. Acta 234, 92-102.

135. Renger, G. (1972) Biochim. Biophys. Acta 256, 428-439.

136. Renger, G., Bouges-Bocquet, B. and Delosme, R. (1973) Biochim. Biophys. Acta 292, 796-807.

137. Renger, G. (1972) Eur. J. Biochem. 27, 259-269.

138. Crofts, A.R. and Wood, D.M. (1978) Curr. Topics in Bioenerg. 7, 175-244.

139. Renger, G. and Eckert, H.J. (1981) Biochim. Biophys. Acta 638, 161-171.

140. Vater, J. (1973) Biochim. Biophys. Acta 292, 786-795.

141. Homan, P.H. (1973) Eur. J. Biochem. 33, 247-252.

142. Itoh, S. (1979) Biochim. Biophys. Acta 548, 579-595.

143. Renger, G. (1972) FEBS Lett. 23, 321-324.

144. Karlish, S.J.D., Shavit, N. and Avron, M. (1969) Eur. J. Biochem. 9, 291-298.

145. Lozier, R.H. and Butler, W.L. (1973) Photochem. Photobiol. 17, 133-137.

146. Babcock, G.T. and Sauer, K. (1973) Biochim. Biophys. Acta 325, 504-519.

147. Velthuys, B.R. and Visser, J.W.M. (1975) FEBS Lett. 55, 109-112.

148. Cramer, W.A. and Whitmarsh, J. (1977) Ann. Rev. Plant Physiol. 28, 133-172.

149. Yamashita, K., Konishi, K., Itoh, M. and Shibata, K. (1969) Biochim. Biophys. Acta 172, 511-524.

150. Itoh, M., Yamashita, K., Konishi, K. and Shibata, K. (1969) Biochim. Biophys. Acta 180, 509-519.

151. Velthuys, B.R. (1981) FEBS Lett. 126, 272-276.

152. Homan, P.M. (1972) Biochim. Biophys. Acta 256, 336-344.

153. Homan, P.M. (1971) Biochim. Biophys. Acta 245, 129-143.

154. Lingane, J.J. (1945) J. Am. Chem. Soc. 67, 1916-1922.

155. Sharp, R.R. and Yocum, C.F. (1981) Biochim. Biophys. Acta 635, 90-104.

156. Den Haan, G.A., Gorter de Vries, H. and Duysens, L.N.M. (1976) Biochim. Biophys. Acta 430, 265-281.

157. Yocum, C.F. and Babcock, G.T. (1981) FEBS Lett. 130, 99-102.

158. Velthuys, B.R. (1976) Ph.D. Dissertation, Leiden.

159. Radmer, R. and Ollinger, O. (1983) FEBS Lett. 152, 39-43.

160. Delrieu, M.J. (1975) Biochim. Biophys. Acta 440, 176-188.

161. Akerlund, H.E., Jansson, C. and Anderson, B. (1982) Biochim. Biophys. Acta 681, 1-10.

162. Yamamoto, Y., Shimara, S. and Nishimura, M. (1983) FEBS Lett. 151, 49-53.

163. Robinson, H.H. and Yocum, C.F. (1980) Biochim. Biophys. Acta 590, 97-106.